# A STUDY OF FORESTED WETLAND SOIL COLOR AND BIOGEOCHEMISTRY IN THE REGION OF NORTHERN VIRGINIA: IMPLICATIONS FOR WETLAND ECOLOGY AND MANAGEMENT

by

Stephanie Ann Schmidt
A Dissertation
Submitted to the
Graduate Faculty
of
George Mason University
in Partial Fulfillment of
The Requirements for the Degree
of
Doctor of Philosophy
Environmental Science and Public Policy

Committee:

Dr. Changwoo Ahn, Dissertation Director

Dr. Daniel Sklarew, Committee Member

Dr. Younsung Kim, Committee Member

Dr. Diego Valderrama, Committee Member

Dr. A. Alonso Aguirre, Department Chairperson

Dr. Donna M. Fox, Associate Dean Office of Student Affairs & Special Programs, College of Science

Dr. Fernando R. Miralles-Wilhelm, Dean, College of Science

Date: 5/6/2022

Spring Semester 2022
George Mason University
Fairfax, VA

# A Study of Forested Wetland Soil Color and Biogeochemistry in the Region of Northern Virginia: Implications for Wetland Ecology and Management

A Dissertation submitted in partial fulfillment of the requirements for the degree of Doctor of Philosophy at George Mason University

by

Stephanie Ann Schmidt
Bachelor of Science
Michigan State University, 2015
Bachelor of Science
Michigan State University, 2015
Bachelor of Arts
Michigan State University, 2015

Director: Changwoo Ahn, Professor, Graduate Program Director
Department of Environmental Science and Public Policy, George Mason University

Spring Semester 2022
George Mason University
Fairfax, VA

## DEDICATION

I dedicate this dissertation to my advisor, Dr. Changwoo Ahn, whose strong will and guidance have been instrumental in my achievements as a PhD student.

## ACKNOWLEDGMENTS

I am thankful to my friends and family who have encouraged and supported my pursuit of research. To my parents, Ray and Shelly, thank you for never doubting me as I have navigated the despair and joy of being a PhD student over the past six years.

I am incredibly grateful to my committee chair, Dr. Changwoo Ahn, whom I met during my first semester at Mason in 2016 and found immediate direction from. Dr. Ahn, I will never forget the many hours we met over Zoom and face-to-face to work on my manuscripts, nor will I forget the life lessons you taught me along the way. I am likewise overwhelmed with gratitude for my committee members, Dr. Dann Sklarew, Dr. Younsung Kim, and Dr. Diego Valderrama, who have shown nothing but faith in me. Dr. Dann, thank you for bringing me to Mason in the first place; I will be forever grateful for the encouragement you gave me as I considered what I wanted to accomplish here at the start of my PhD. Dr. Kim, thank you for supporting my growth as a student/teacher, and I am truly touched by your interest in my post-grad success. Dr. Valderrama, thank you for being there for me in the eleventh hour; your kindness and sincerity in supporting me will not be forgotten. Additionally, I am grateful to Dr. Julia Nord, who provided me with the foundations in soil science necessary to fuel my academic interest in soils.

I would like to thank several undergraduate and graduate students who significantly aided in my physical and mental wellbeing in addition to my research progress; thank you to Jesse Wong (2018), Natalya Moody (2019), Katie Ledford (2018–2020), Katrina Napora (2021), Aysan Yazdanpanah (2021–2022), and Alex Murphy (2021–2022).

I would like to thank the University's Provost Office, the Environmental Science and Policy Department, and the Cosmos Club Foundation for supporting my research.

Finally, I am grateful for being able to publish peer-reviewed articles in *Wetlands Ecology and Management* (Ch. 2), *Communications in Soil Science and Plant Analysis* (Ch. 3), *Science of the Total Environment* (Ch. 4), and *Journal of Environmental Management* (Ch. 5); thank you to Dr. Ahn, the journal editors, and peer reviewers.

TABLE OF CONTENTS

## LIST OF TABLES

## LIST OF FIGURES

## LIST OF EQUATIONS

## LIST OF ABBREVIATIONS

| | |
|---|---|
| Algonkian Regional Park | ARP |
| Banshee Reeks Nature Reserve | BR |
| Bulk density | $D_b$ |
| Calculated [color variables] | C |
| Chroma index | CI |
| Chroma [Munsell color space] | $C_M$ |
| Gravimetric soil moisture | GSM |
| Hue / Value / Chroma [color space] | HVC |
| Impervious surface cover | ISC |
| International Commission on Illumination | CIE |
| Julie J Metz–Neabsco Creek Wetland Bank | JJM |
| Mason Neck Wildlife Refuge | MN |
| Measured [color variables] | M |
| Mobile phone camera | MPC |
| Munsell Soil Color Chart | MSCC |
| National Technical Committee for Hydric Soils | NTCHS |
| Principal Component Analysis | PCA |
| Redoximorphic features | RMFs |
| Soil organic carbon | SOC |
| Soil organic matter | SOM |
| Seasonal high-water table | SHWT |
| [Soil] Total carbon | TC |
| US Army Corps of Engineer | USACE |
| US Department of Agriculture–Natural Resource Conservation Service | USDA–NRCS |
| US Environmental Protection Agency | US EPA |
| US Fish and Wildlife Service | USFWS |
| Web Soil Survey | WSS |
| Watershed Index Online | WSIO |

## ABSTRACT

A STUDY OF FORESTED WETLAND SOIL COLOR AND BIOGEOCHEMISTRY IN THE REGION OF NORTHERN VIRGINIA: IMPLICATIONS FOR WETLAND ECOLOGY AND MANAGEMENT

Stephanie Ann Schmidt, Ph.D.

George Mason University, 2022

Dissertation Director: Dr. Changwoo Ahn

Hydro-physicochemical (HP) settings and soil color attributes including redoximorphic features (RMFs) were assessed at four forested wetlands in Northern Virginia, USA, to identify whether four simply measurable HP attributes—inundation/saturation frequency, bulk density, soil moisture, and percent sand—can provide an explanatory framework for characterizing and classifying soil color attributes related to hydric soil field indicators. Study plots (n = 16) were grouped by site for initial characterizations and comparisons of HP (n = 4) and color attributes (n = 11); each attribute was additionally characterized and compared between three HP-based clusters formulated through k-means clustering analysis. Whereas only one HP attribute (inundation/saturation frequency) significantly differed between sites, all HP attributes but percent sand differed between HP-based clusters ($p < 0.05$), with PCA Dimensions 1 and 2 explaining over 80% of variability in plot HP attributes. Moreover, more sets of

color attributes were significantly different when plots were grouped by HP-based cluster (n = 5: frequency of concentrations, non-matrix color count, hue, chroma, and depth to concentrations) compared to by site (n = 3: value, frequency of depleted matrices, depth to depletions) ($p < 0.10$). Simply measurable HP attributes are thus closely associated with certain soil RMF and color characteristics beyond site identity, potentially serving as a suite of measurements that can be adopted to assess and monitor RMFs indicative of wetland soils.

Soil color patterns are essential to understand hydrologic regime and biogeochemical processes in wetland ecosystems. The Munsell Soil Color Chart (MSCC) has been traditionally and predominantly used to identify and quantify hydric soil field indicators, but several simple, low-cost alternatives have become recently available to compare their efficacy in complementing the MSCC in soil color assessment. An intensive literature review on studies utilizing different methods was conducted to identify and quantify hydric soil colors and associated patterns; these include 1) the MSCC, 2) the Nix Color Sensor (Nix), 3) mobile phone camera (MPC) and medium-end digital camera photography, and 4) colorimetry and spectrometry. A review of these methods elucidates their respective strengths and weaknesses and highlights the importance of considering study-specific attributes in determining which method to choose for field studies of hydric soil colors. Redoximorphic features (RMFs) require methods capable of capturing small and heterogeneous soil surfaces and features such that the MSCC and digital photography are the most appropriate methods; on the other hand, the Nix provides rapid assessment of soil color that does not necessitate rigorous training to overcome biases that might come about in more subjective methods such as the MSCC. Overall, all alternative methods reviewed have their own merits and capacity to complement measurements made by the MSCC.

While the MSCC is the most frequently used, well-established field method for reading soil color, the Nix is an inexpensive, app-based alternative that can complement or potentially substitute for the MSCC. In this study, soils were collected and their colors were measured from four forested sites across Northern Virginia, USA using both the MSCC and Nix. For each observed color, 3 MSCC variables and 15 Nix variables were collected in the field; a methodology was established to use these *measured* (M) variables to derive 9 Nix *calculated* (C) variables. A stepwise correlation identified Nix variables most suitable for relating the Nix to each of the MSCC attributes: hue (H), value (V), and chroma ($C_M$). Ultimately, H, V, and $C_M$ were deemed to be best represented by $H_{RGB}$ calculated from the RGB color space ($\rho = 0.56$), L from the CIE–Lab color space ($\rho = 0.73$), and $\hat{z} = Z/(X+Y+Z)$ from the XYZ color space ($\rho = -0.80$), respectively ($p < 0.001$). The corresponding explanatory powers of final Nix variables (i.e., $H_{RGB}$, L, and $\hat{z}$) for H, V, and $C_M$ were 26%, 54%, and 62%, respectively ($p < 0.01$). Significant differences in $\hat{z}$ between soils identified as hydric and nonhydric, but lack of nonoverlapping ranges, indicate a potential for the Nix to complement the MSCC in assessing wetland soil color in an accessible and reproducible manner, including hydric soil identifications for wetland delineation practices. Further study with more data over various types of soils is necessary to establish stronger relationships between the Nix and MSCC. Nonetheless, the method of characterizing soil color variables from the two field methods presented in the study can serve as a template for future studies or environmental education programs desiring to use the Nix as a complement to the MSCC.

Forested wetland soils within the Piedmont and Coastal Plain physiographic provinces of Northern Virginia (NOVA) were investigated to determine the utility of the Nix for predicting carbon contents (TC) and stocks (TC stocks) from on-site color measurements. Both the Nix color variables (n = 15) and carbon contents significantly differed between sites, with redder soils (higher $a$ and $h$) at Piedmont sites, and higher TC at sites with darker soils (lower values of $L$, or lightness; $p < 0.05$). Nix–carbon correlation analysis revealed strong relationships between $L$ (lightness), $X$ (a virtual spectral variable), $R$ (additive red), and $K_K$ (black) and log-transformed TC (Ln[TC]; |r| = 0.70; $p < 0.01$ for all). Simple linear regressions were conducted to identify how well these four final Nix variables could predict soil carbon. Using all color measurements, about 50% of Ln(TC) variability could be explained by $L$, $X$, $R$, or $K_K$ ($p < 0.01$), yet with higher predictive power obtained for Coastal Plain soils ($0.55 < R^2 < 0.65$; $p < 0.01$). Regression model strength was maximized between Ln(TC) and the four final Nix variables using simple linear regressions when color measurements observed at a specific depth were first averaged ($0.66 < R^2 < 0.70$; $p < 0.01$). While further study is warranted to investigate Nix applicability within various soil settings, these results demonstrate potential for the Nix and its soil color measurements to assist with rapid field-based assessments of soil carbon in forested wetlands.

Finally, a case study is presented and discussed that highlights the applications of the Nix in monitoring and assessing soil colors for wetland ecology and land management. Within an Ecological Sustainability undergraduate class at George Mason University, we designed and executed a class project in which students investigated soil colors across campus green sites using the Nix. Students were given direction on measurement steps and techniques, including at which depths to collect colors, through a Standard Operating Procedure (SOP) made to be adaptable to various locations and/or soil types. Not only were students able to collect, store, and share soil color data for various locations across campus more rapidly than possible using the MSCC, but they also gained an understanding and appreciation for soil ecology and the importance of color as an indicator. With continued refinement and adaptation to intended use, the SOP herein presented has the potential to aid land/watershed planning by providing data on soil colors that can be tracked over time and may identify wetland areas, while also encouraging citizen science endeavors in soil ecology that can engage and connect communities to their belowground soils.

# CHAPTER ONE:
# INTRODUCTION

## **Background**

From natural areas to urban city centers, soils are at the heart of ecological sustainability: they provide a substrate necessary for plant growth, nutrient cycling, water purification, carbon sequestration, and food production, among many other functions. Be it urban soils covered in lawns, forest soils littered with leaves, or wetland soils periodically inundated or saturated, soil services are inexorably linked with soil structural and functional properties like bulk density, soil texture, and soil organic matter (Adhikari and Hartemink 2016). While soil properties influence their surrounding environs, so too are they are influenced by their surroundings: climate change, flora and fauna, and human management, use, and/or alteration of watersheds—whether directly or indirectly—can adjust the soilscape, thus affecting the geospatial distribution and intensity of soil services on a human time scale (Brady and Weil 2008).

Landcover changes within a watershed have particularly watershed-wide impacts on the distribution of wetland soils—i.e., *hydric soils*—and their functions across a landscape. Formed through periods of saturation, flooding, and/or ponding that are long enough during the growing season to provide anaerobic conditions necessary for hydrophytic plant growth and reproduction (Federal Register 1994; USDA–NRCS 2018), hydric soils are an essential component of the ecosystem services wetlands provide.

Though often viewed as an "in-between" of terrestrial soils and deepwater aquatic soils (National Research Council 1995), hydric soils provide a unique medium that encourages water storage during flooding, high rates of carbon sequestration, and nitrogen and phosphorus removal from waterways. Such ecosystem services are inextricably linked to the biologically mediated cycling of nutrients like carbon and nitrogen that defines wetland biogeochemistry (Reddy 2008).

Because of these important ecosystem services, wetland conservation and restoration are imminent concerns in regions like the metropolitan D.C. area where over 70% of historic wetlands have been lost to agriculture and urban development (Fretwell et al. 1996; US EPA 2021). To reverse such losses in wetland coverage and ecosystem services, a federal "no net loss" policy endorsed by President George H.W. Bush in 1987 expanded a joint USACE and EPA permitting program in which private landowners or businesses were required to obtain a permit before destroying a wetland or draining/dredging hydric soils; under the 1987 policy, only "unavoidable" wetland losses were to be permitted, and such permits required compensatory mitigation of wetland acreage and functions in a separate location (Votteler and Muir 1996; Blumm 2018; Heller 2019). In conjunction with protecting ecosystem services of remaining wetlands, the policy of compensatory mitigation encouraged the development of monitoring protocols and indicators—increasingly focused on hydric soil properties due to their inherent relationship to wetland biogeochemical processes and related functions—to determine if natural, disturbed, constructed, and/or restored wetlands were developing and/or sustaining desirable wetland ecosystem functions (Stolt et al. 2000; National

Research Council 2001; Cole et al. 2001; Campbell et al. 2002; Lindig-Cisneros et al. 2003; Ehrenfeld 2005; Dewey et al. 2006; Ballantine and Schneider 2009; Hossler and Bouchard 2010; Wolf et al. 2011; Dee and Ahn 2012; Ahn and Peralta 2012; Peralta et al. 2013). While the national wetland policy has had some success, the inherently political practices of permitting wetland destruction and deciding placement of mitigation wetlands renders an inherently vulnerable mosaic of regional wetlands. Such vulnerability may be best reversed in such areas through improved education and outreach, and begins with better mapping of hydric soils, understanding their propensity to form in diverse geomorphic and hydro-physicochemical settings, and identifying changes to soil properties within an urban landscape.

When monitoring and assessing ecosystems across a landscape through soil properties, soil color has become an important tool for farmers, ecologists, land managers, and laypeople alike. Wetland delineation, monitoring, and management often rely on the observation of soil colors that are inherently connected to the presence of hydric soils, as outlined in the USDA–NRCS field manual for identifying hydric soils (USDA–NRCS 2018). Fluctuating water tables of wetlands encourage dynamic reduction–oxidation ("redox") potentials that affect iron (Fe) and manganese (Mn) chemistry; in soils where Fe and/or Mn are relatively abundant, soil colors and patterns called redoximorphic features (RMFs) form as microbially-mediated redox reactions reduce, translocate, and/or oxidize Fe and Mn. In contrast to upland soils, the reducing conditions present in hydric soils can reduce ferric iron ($Fe^{3+}$) to ferrous iron ($Fe^{2+}$), a mobile, blueish-green ion that can accumulate to form reduced Fe matrices under temporary periods of saturation. $Fe^{2+}$ can be fully leached out of soil horizons during extended periods of soil saturation as water moves down the soil profile, leaving iron-free soils with an uncoated light gray color (Simonson and Boersma 1972; Richardson and Hole 1979); conversely, exposure to air as oxygen becomes reintroduced into soils will reoxidize $Fe^{2+}$ and create mottled patterns of iron oxide concentrations that contrast the iron-depleted soil grains (Daniels et al. 1961).

To provide wetland scientists and managers with a standardized method to identify hydric soil presence, hydric soil field indicators rely on thresholds of color using the Munsell Soil Color Chart (MSCC), created by A.H. Munsell in 1905 and used in soil surveys since the 1930s (Simonson 1993). Through the MSCC, color is parsed into attributes of hue, value (lightness), and chroma (color purity or richness), where depleted and/or reduced matrices are identified as having low-chroma ($\leq 2$) and high-value ($\geq 4$) colors; redox concentrations are judged by their hue, value, and chroma contrast to soil matrix colors; and organic-rich soils common in wetlands are identified as having low-chroma ($\leq 2$) and low-value ($\leq 4$) colors. While soil colors do not directly relate to duration of saturation and reduction without calibration to soil texture, pH, redox potentials, and historic rainfall and water table levels (He et al. 2003; Vepraskas 2015), the underlying processes responsible for hydric soil colors are inherently connected to the frequency, duration, and intensity of soil saturation as well as soil organic matter (SOM) and carbon sequestration; thus, soil color variables like chroma and value are useful indicators of soil and ecosystem functions.

The current convention of recording and analyzing soil color through the MSCC has proven to be useful for identifying hydric soils but has several shortcomings including the dependence on user perception and judgment; time required for making judgments; and training to overcome biases that may limit accessibility for non-scientists. Given these shortcomings, a subset of soil studies concerned with soil color have focused on field alternatives to the MSCC, including handheld colorimetry and spectrophotometry, mobile phone cameras, and higher-end digital photography, further discussed in Chapter 3. A promising alternative that has shown utility and reproducibility in measuring soil colors is the Nix Color Sensor (Nix), which may provide citizen scientists the capacity to participate in the identification of hydric soils to complement the use of MSCC by soil scientists and wetland managers. While the Nix has been shown to accurately measure soil colors with strong interchangeability with the MSCC (Stiglitz et al. 2016a), research endeavors have not included hydric soils in datasets, nor have they focused on measuring colors with the Nix in the field; filling this research gap is the focus of Chapter 4.

Beyond use of the Nix to complement the MSCC in monitoring color patterns indicative of hydric soils per the USDA–NRCS field indicators, a quantitative sensor that measures continuous variables of color—e,g, the Nix—has the potential to overcome the discrete nature of MSCC variables that can be correlated to other continuous variables related to wetland function. Most pertinent to urbanizing areas that are increasingly developing climate action plans and strategies to mitigate and/or reduce greenhouse gas emissions is the function of carbon sequestration and carbon storage, the monitoring of which require significant resources and lab-based methodologies. Wetlands are highly touted for their carbon storage potential due to their high productivity and the biogeochemically reduced conditions in wetland soils that slow decomposition of organic matter; it has been documented that, despite occupying less than 10% of the earth's land surface, wetlands host 20–30% of the world's soil carbon stores  (Lal 2004; Mitsch and Gosselink 2015; Nahlik and Fennessy 2016). Monitoring of soil total carbon (TC) and TC stocks is useful in predicting sequestration rates; furthermore, carbon contents and stocks have been previously linked to soil color variables in various geographic regions (Wills et al. 2007; Moritsuka et al. 2014; Pretorius et al. 2017; Stiglitz et al. 2017a; Mikhailova et al. 2017). Thus, assessing the usefulness of the Nix to provide estimates or predictions of soil carbon content and/or stocks from soil color variables is the focus on Chapter 5.

Along with their connections to ecosystem functions, the connections between soil colors and their hydrologic, geomorphic, and physiographic settings complicates the universality of inferences made from soil colors. Heterogeneity in landscape geology, geomorphology, physiography, and overall soil properties can also impact hydric soil functioning and should be studied to provide context to a study investigating soil colors and wetland functions (Axt and Walbridge 1999; Wang et al. 2017; Ledford et al. 2022). For example, wetlands in the Piedmont and Coastal Plain physiographic provinces found in the D.C. metropolitan region have distinct distribution patterns, hydrologic regimes, and soil series that may impact correlations between wetland functions and soil colors (Fretwell 1996; Heath 1984). Thus, investigations on relationships between hydric soil colors and ecosystem functions using the MSCC and/or alternatives like the Nix should furthermore identify the potential roles that outside forces play in soil colors and their patterns. Chapter 2 sets the stage for linking observed colors and features of color patterns in wetland areas to distinct hydrologic settings that are easily classified and put colors in context, independent of spatial proximity or separation; furthermore, Chapter 5 investigates whether relationship strength between soil colors and TC depends on physiographic province.

## Research Goals and Setting

Focused on the urban region of Northern Virginia within the metropolitan D.C. area, the goal of this study was to investigate four forested wetlands within the Piedmont and Coastal Plain physiographic provinces to characterize site soil properties, hydro-physicochemical settings, and carbon contents. The bi-directional link between soil hydro-physicochemical setting and observed soil colors and features was investigated to put color patterns in context and assess the potential for classifying soil colors into *hydricity classes* rather than binary hydric versus non-hydric (Chapter 2). Furthermore, based on the theoretical applicability of the Nix to measuring soil colors (Chapter 3) and provide information useful to indicate wetland carbon storage, this research aimed to assess the relationships between Nix color variables and MSCC color variables for soil colors within each site (Chapter 4), and determine the usefulness of Nix color measurements to estimate soil carbon contents and/or stocks valuable for local planning and management (Chapter 5). Finally, to provide a beta-test for deployment of the Nix in soil education and outreach, a reflection on the success of using the Nix in a semester-long undergraduate research investigation of soil colors in 2021 and 2022 is provided in Chapter 6.

## CHAPTER TWO:
## CHARACTERIZATION OF REDOXIMORPHIC FEATURES OF FORESTED WETLAND SOILS BY SIMPLE HYDRO-PHYSICOCHEMICAL ATTRIBUTES IN NORTHERN VIRGINIA, USA

### Introduction

The establishment of various national policies to conserve wetland functions—notably, the United States (US) "no net loss" policy of 1990 (Page and Wilcher 1990)—has led to a suite of monitoring protocols for identifying, monitoring, constructing, and conserving wetland sites (Berkowitz 2012; Tiner 2017). A subset of such protocols is specifically focused on *hydric soils*, defined by the US Department of Agriculture–Natural Resources Conservation Service (USDA–NRCS) as "soil[s] that formed under conditions of saturation, flooding, or ponding long enough during the growing season to develop anaerobic conditions in the upper part" (Federal Register 1994; USDA–NRCS 2018).

Unseen in upland environments, colors and color patterns called *redoximorphic features* (RMFs) materialize in such anaerobic soil environments due to microbially-mediated redox reactions that reduce, translocate, and oxidize soil iron (Fe) and manganese (Mn), and are thus inherently useful in establishing and utilizing field indicators of hydric soil presence. Using the Munsell Soil Color Chart (MSCC) to characterize soil *hues*, *values*, and *chromas*, observers can identify three key RMF types

(Figure 1) relevant to the hydric soil field indicators published by the USDA–NRCS: (1) redox depletions, or low-chroma [≤ 2] and high-value [≤ 4] areas where Fe–Mn oxides have been removed; (2) reduced matrices, or blue, green, or gray low-chroma areas containing reduced aqueous iron ($Fe^{2+}$); and redox concentrations, or orange, red, or brown accumulations of Fe–Mn oxides (Daniels and Gamble 1967; Simonson and Boersma 1972; Moore 1974, p. 19; Guthrie and Hajek 1979; Richardson and Hole 1979; Franzmeier et al. 1983; Evans and Franzmeier 1988; Vepraskas 2015; USDA–NRCS 2018). Beyond soil color observations, visual measurement of ferrous iron can be possible using a α,α'-dipyridyl dye reagent, often utilized for in-situ soil observation for RMFs at the profile scale (Berkowitz et al. 2017).

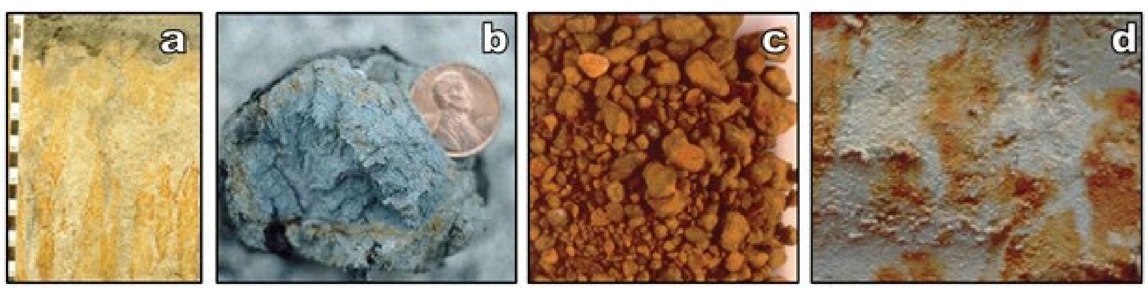


**Figure 1.** Examples of redoximorphic features including (**a**) redox depletions, (**b**) reduced matrix; and two types of redox concretions, (**c**) Fe nodules and (**d**) Fe masses (USDA–NRCS 2018)

As the underlying processes responsible for RMF formation are inexorably linked to the frequency, duration, and intensity of soil saturation and reduction, RMF characterizations can be used as signals of past and present wetland development. For example, high-chroma Fe concentrations have been correlated to seasonal high-water table (SHWT) depths, and low-chroma depleted/reduced matrices have been correlated to saturation durations (Veneman et al. 1998; Jacobs et al. 2002). Contemporary hydric soil research has sought to clarify and quantify the complex relationships between RMF development and environmental conditions, allowing links between field observations of RMFs and longer-term site hydrology and wetland ecosystem development (Megonigal et al. 1993; He et al. 2003; Vepraskas et al. 2006; Vepraskas and Caldwell 2008). In particular, the USDA–NRCS manual of field indicators for hydric soils is the official procedural guide for identifying if soil morphological features legally indicate the presence of a hydric soil, where indicators are differentiated between sandy soils and loamy/clayey soils (USDA–NRCS 2018).

While this binary classification of soils as *hydric* or *nonhydric* required for regulatory decision-making has been informed by research confirming the link between reducing conditions and the presence of specific color patterns by depth, thickness, abundance, and contrast, it has arguably suppressed classification systems that could classify the diverse visual cues of soil biogeochemistry into *hydricity* classes. Furthermore, the capacity to not only apply field indicators precisely and confidently, but also to appropriately generalize observed color patterns at a plot throughout the wetland site, relies on technical understanding and/or training that may not be intuitive for land and watershed managers, citizen scientists, or general ecologists who are not well-versed in the indicator details or relationships between soil biogeochemistry and water—

landscape processes. A more simplified framework may enhance the capacity for these stakeholders to participate in hydric soil assessment.

Linking classes of color characteristics to hydricity and determining how such categories of hydricity should be informed are key to developing such a framework. Individual hydrologic variables are often inadequate for simply relating RMFs to hydrology, as a combination of various hydrological and soil physicochemical attributes like soil texture, pH, redox potentials, and historic rainfall and water table levels influence RMF formation (Genthner et al. 1998; Jacobs et al. 2002; He et al. 2003; Vepraskas 2015); however, multiple indicators of hydrologic and soil physicochemical settings may be apt for the genesis of RMF color classes. Certain hydro-physicochemical (HP) soil attributes are not only ubiquitously and simply measured for various applications of soil and ecological research (Bestelmeyer et al. 2009; Kachergis et al. 2011), but also hold evidenced relationships to wetland development, including RMFs. In particular, soil texture and moisture relate to redox potential (Megonigal et al. 1993) and wetland functions like denitrification (Palta et al. 2016); soil moisture, despite its variability that may be unrelated to water table depth, has been linked to wetland vegetation prevalence index (Bollman et al. 2012) and RMF abundance (Raymond et al. 2013); wetland surface inundation and bulk density can reflect wetland hydrology and influence wetland development (Campbell et al. 2002; Palta et al. 2017); and lower bulk densities are known to encourage water infiltration necessary for producing reducing conditions and/or relate to soil organic matter contents that can be increased by the slowed decomposition of reduced soils (Adams 1973; Martens and Frankenberger Jr. 1992; Ehrich 2010).

HP attributes have previously provided the basis for distinguishing "soil condition groups," or HP-based clusters of study areas (Schoenholtz et al. 2000; Dee and Ahn 2012; Ahn and Peralta 2012; Peralta et al. 2013), but relevance for soil RMF and color attributes was not addressed. Studies that have previously distinguished patterns of RMFs have not employed simply measurable HP attributes as a basis for such classifications (Wheeler et al. 1999; Pruitt 2001). Investigating the use of such HP attributes for classifying and characterizing RMFs may highlight the method's capacity to unleash additional information about the development of soil colors and patterns that could be challenging to uncover using the USDA–NRCS procedures.

The goal of this study was to determine if simply measurable and accessible hydro-physicochemical attributes—inundation/saturation frequency, gravimetric soil moisture, bulk density, and soil texture as percent sand—can serve as the genesis for classifying and characterizing soil color and RMF attributes for identifying both hydric and future potential hydric soils. Toward this aim, we assessed the efficacy of using HP-based clusters, in comparison to site identity, in classifying RMF color patterns in four forested wetlands of Northern Virginia, USA by (1) analyzing and comparing plot-scale HP and soil color / RMF attributes between wetland sites to identify the capacity for site identity to distinguish classes of color and RMF patterns; and, in contrast, (2) analyzing and comparing HP and soil color / RMF attributes between HP-based clusters of study plots.

# Materials and Methods

## Study area

To investigate forested wetlands at a regional scale, field research was conducted from spring 2018 to fall 2019 at four freshwater wetlands within the Coastal Plain and Piedmont physiographic provinces of Northern Virginia, USA. Average temperatures were 13.5˚C (-13.9˚C to 35.0˚C) in 2018 and 14.0˚C (-18.9˚C to 37.8˚C) in 2019; total precipitation was 169.5 cm in 2018 and 103.7 cm in 2019, with 2018 being the wettest year of the decade by 50-plus cm (Menne et al. 2012). Sites within the Coastal Plain physiographic province include Elizabeth Hartwell – Mason Neck Wildlife Refuge (MN) in Fairfax County and Julie J. Metz – Neabsco Creek Wetland Bank (JJM) in Prince William County; sites within the Piedmont physiographic province include Banshee Reeks Nature Preserve (BR) and Algonkian Regional Park (ARP) in Loudoun County (Figure 2). While Coastal Plains soils are generally sandier than Piedmont soils (Markewich et al. 1990), all investigated soils would be classified as *loamy/clayey* rather than *sandy* per hydric soil field indicators (USDA–NRCS 2018; USDA–NRCS Soil Survey Staff 2020).

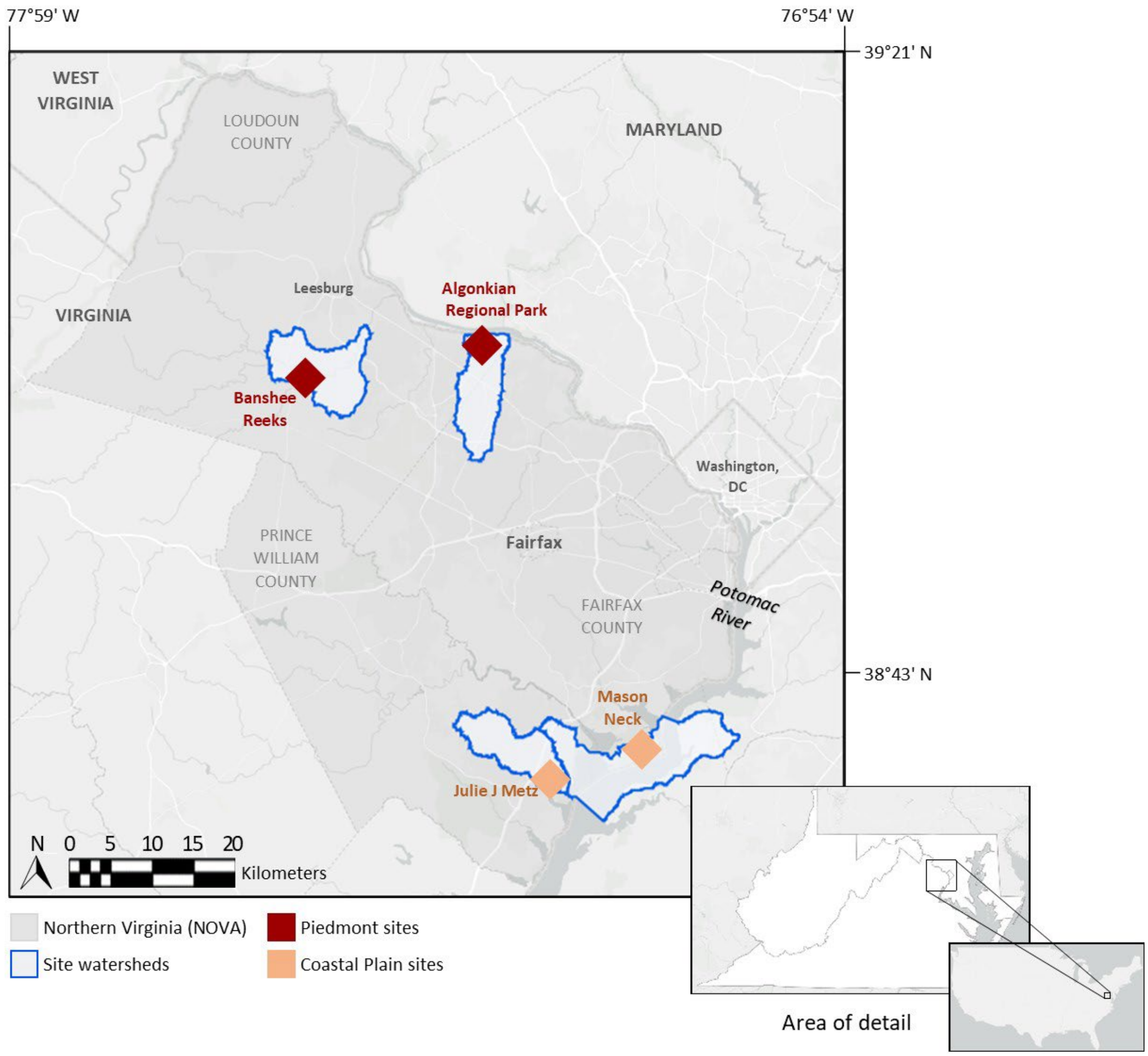


**Figure 2.** Regional map displaying the four study sites, their subwatersheds, and their physiographic province in Northern Virginia, USA

MN (38°38'38" N, 77°09'57" W) includes a hardwood forest and forested wetland with rolling microtopography consisting of high points (hummocks) and low points (hollows) with precipitation being the main hydrologic input. The occasionally to frequently saturated hollows are mapped as the hydric Gunston silt loams; the rarely saturated hummocks are mapped as the nonhydric Matapeake silt loams and Mattapex loams (Table 1; Ahn et al. 2009; USDA–NRCS Soil Survey Staff 2020). JJM (38°36'23" N, 77°16'38" W) lies adjacent to Neabsco Creek, a tributary of the Potomac River, and has sustained wetland hydrology since its construction as a mitigation wetland in 1994 (Environmental Laboratory 1987). The wetland contains occasionally, frequently, and permanently flooded soils mapped as the hydric Featherstone mucky silty loam and Hatboro–Codorus Complex (Table 1) influenced by groundwater recharge, precipitation, and stream surface flow (USDA–NRCS Soil Survey Staff 2020).

In the Piedmont, BR (39°1'31" N, 77°35'30" W) includes occasionally to frequently saturated forested areas mapped as the hydric Albano silt loam plus the nonhydric Codorus and Manassas silt loams (Table 1; USDA–NRCS Soil Survey Staff 2020). Floodplains and riparian zones are influenced by subsurface flow from Goose Creek, precipitation, and surface runoff from tributaries. ARP (39°3'28" N, 77°21'51" W) includes riparian forests and freshwater forested and emergent wetlands influenced by overland flow from the Potomac River, a groundwater connection with nearby emergent wetlands, and precipitation. Mapped soil series include Rowland silt loams and Lindside silt loams (Table 1); while neither is hydric, ARP was observed to be capable of supporting wetland vegetation before sampling began (USDA–NRCS Soil Survey Staff 2020).

Per site, four 1 x 1 m randomly selected plots were chosen to represent local wetland heterogeneity (n = 16) using ESRI ArcGIS software. Nonhydric plots within sites were included to increase variability in HP attributes and provide results applicable to sites not yet identified to be wetlands. Randomly chosen plots were modified if necessary to ensure accessibility and maintain ≥ 200 m between plots (Chi et al. 2018).

**Table 1.** Site description summaries for the four study sites (USDA–NRCS Soil Survey Staff 2020; US EPA 2021)

| | **Algonkian Regional Park (ARP)** | **Banshee Reeks (BR)** | **Julie J. Metz – Neabsco Creek (JJM)** | **Mason Neck (MN)** |
|---|---|---|---|---|
| **Watershed Name** | Sugarland Run | Big Branch – Goose Creek | Neabsco Creek | Occoquan Bay – Potomac River |
| **% Impervious Surface** [1] | 26.2% | 0.7% | 24.9% | 0.1% |
| **Physiographic province** | Piedmont | Piedmont | Coastal Plain | Coastal Plain |
| **Geologic Age** | Upper Triassic | Upper Triassic | Quaternary | Quaternary |
| **Parent Material** | alluvium (sandstone) | Alluvium (sandstone, shale) over residuum | alluvium, marine deposits | Fluviomarine deposits (sedimentary gravel, sand) |
| **Geomorphology** | Drainageways, floodplains, terraces | Drainageways, floodplains | Terraces, floodplains | Fluviomarine terraces, interfluves, drainageways |
| **Nonhydric soil series** | Linside silt loam<br>Huntington silt loam | Leedsville cobbly silt loam<br>Oatlands gravelly silt loam<br>Manassas silt loam | Dumfries sandy loam Lunt loam | Gunston silt loam<br>Matapeake silt loam<br>Mattapex loam |
| **Hydric soil series** | Kinkora–Delanco complex<br>Huntington silt loam | Codorus silt loam<br>Albano silt loam<br>Hatboro silt loam | Featherstone mucky silt loam<br>Hatboro–Codorus silt loam | Elbert, Elkton silt loams |
| **Major Vegetation communities** | Black walnut and oak forested floodplains; freshwater forested and emergent wetlands | Hardwood forests, riparian wetlands, and Mountain–Piedmont basic seepage swamp | Forested, scrub, and emergent wetlands | Hardwood oak–hickory forest, palustrine forested wetlands |

[a] %ISC = Percent impervious surface cover in the watershed; sourced from the Watershed Index Online (WSIO) (US EPA 2021)

**Field methods**

To capture seasonal variations in soil color, soil profile characterizations and color measurements were obtained at each plot during spring (February–March), summer (May–July), and fall (September–October) of 2018 and 2019, yielding 96 profiles overall. Per visit, soil was collected from each plot using a 10-cm diameter soil auger (AMS) to a depth of roughly 60 cm, with subsequent profiles spaced ≥ 10 cm apart to avoid disturbed areas. Soil surface inundation/saturation down to 30 cm was also visually assessed and recorded per visit.

Augered soil peds were repeatedly broken into smaller pieces up to ~4 cm in diameter to ensure internal colors were identified, including redox depletions (matrix or nonmatrix), concentrations, reduced matrices, and gley colors. For each unique color observed (n = 374), the MSCC was used to determine color *hue*, *value*, and *chroma*. Conventional methods of soil profiling per the MSCC were employed, including wetting soils before color judgments and noting RMF abundance (as a percentage), size, and location (i.e., depth from surface [cm] and horizon); Schmidt and Ahn (2019) provides further discussion of the MSCC methodology. To assess HP attributes, soils were collected at three subplots per plot (n = 48) between March and August 2020, approximately 50 cm from soil profile locations. A PVC pipe with handcrafted jigsaw teeth (radius = 3.8 cm) was used to remove soil cores with minimal disturbance for lab processing.

**Lab processing and calculations**

Soil cores were massed ($M_{s+w}$) and placed in a drying oven at 98 °C for 3 to 6 days until a constant dry mass ($M_s$) was achieved. Calculations based on wet and dry masses and total core volumes ($V_T$, calculated as $\pi \cdot 3.8^2 \cdot 10$ cm$^3$) include soil bulk density ($D_b$, g·cm$^{-3}$), equal to $M_s / V_T$, and (2) gravimetric soil moisture (*GSM, %*), equal to $100 \cdot (M_{s+w} - M_s) / M_s$. Additionally, inundation/saturation frequencies were calculated per plot by summing binary observations of surface inundation and/or saturation across the study period and dividing by the number of plot visits (6). Soil texture for the top 30 cm was represented by percent sand, obtained from the Web Soil Survey (WSS) using plot GPS coordinates (USDA–NRCS Soil Survey Staff 2020).

Given within-site heterogeneity and sufficient spatial separation, plots were treated as independent samples for soil HP and color attributes, which were obtained by profile then summarized by plot before statistical analyses. Soil RMF and color attributes (henceforth collectively termed *color attributes*) were summarized for the top 60 cm of each plot; organic (O) horizons were excluded, as no plots met hydric field indicators relating to O horizon thickness. To prepare data for statistical analysis, each color was defined to be one of the following: (1) non-RMF matrix, (2) concentration, (3) depleted matrix, (4) non-matrix depletion, (5) reduced matrix, or (6) non-matrix reduction. Color hues, values, and chromas were reduced to three single measurements per plot by averaging only matrix colors for the A horizon. Eight additional color attributes deemed relevant to RMF characterization and hydric soil field indicators were calculated from non-averaged field data, including attributes defined at the individual color level (n =

374; e.g., contrast) or profile level (n = 96; e.g., depth to depletions) (USDA–NRCS 2018). Metrics relied on either non-matrix RMF colors (e.g., contrast), or both matrix and non-matrix RMF colors (e.g., depth to depletions). Overall, 11 color attributes were prepared for statistical analysis per plot: (1) *hue*, (2) *value*, (3) *chroma*, and RMF attributes including (4) *contrast*; (5) *non-matrix color count* (e.g., relative contribution of RMFs to all horizon colors, independent of abundance); *frequencies of* (6) *concentrations*, (7) *depleted matrices*, (8) *reduced matrices*, and (9) *gley colors*; and *depths to* (10) *depletions* and (11) *concentrations*. Contrast was converted to a numerical attribute where prominent = 3, distinct = 2, faint = 1, and n/a = 0. Hue was converted to a numerical attribute by equating 10YR with 10; hues from MSCC pages were set to be smaller (redder) or larger (yellower) than 10 in steps of 2.5.

In addition to preparation for statistical analyses, each site's color observations were systematically simplified and summarized for general characterization. Using the aforementioned categories of color observations (n = 6), profile observations were pooled by plot to judge reproducibility of specific horizon matrix and non-matrix RMF observations; if deviations in a specific color occurred between visits (where value/chroma pairs differed by at most 1/1), ranges for hues were recorded, and half-points were awarded to reports of values and chromas. If deviations across visits altered the categorization of a color—e.g., the non-RMF matrix color 7.5YR 4/3 later being as a RMF matrix color 7.5YR 4/2—colors were not combined and instead reported for both relevant categories. Site color summaries were similarly obtained from plot color summaries and summarized by two depth intervals, 0–30 cm and 30–60 cm. Differences among plot colors where value/chroma pairs differed drastically were both retained and reported; where value/chroma deviations differed by at most 1/1, half-points were awarded to reports of values and/or chromas. RMFs with the highest chroma (concentrations) and lowest value (reduced matrices and depletions) were noted as typical site colors, with ranges in hues reported and half-points awarded for similar value/chroma pairs (difference of at most 1/1). For example, if plot visits to BR rendered matrix observations within the top 30 cm of 7.5 YR 5/4, 7.5YR 6/5, 10YR 5/5, and 7.5YR 4/3 at each plot, the maximum difference of 1/1 for the first three colors would yield a reporting of "7.5YR – 10YR 5.5/4.5", and 7.5YR 4/3 would be reported as its own color.

**Statistical analysis**

Principal component analysis (PCA) and k-means clustering were conducted in R 4.0.0 software (R Core Team 2013) to group study plots with the PCA being run using plot-scale HP attributes (Jolliffe and Cadima 2016). One JJM plot was removed after outlier analysis; hence, 15 plots were analyzed. The optimal number of clusters was determined using a combination of the silhouette and elbow methods in R, from which clusters of plots were grouped—herein called HP-based clusters—and described in terms of HP and color attributes using descriptive statistics (Marutho et al. 2018).

Both HP attributes (n = 4: inundation/saturation frequency [field-based], GSM and $D_b$ [lab-based], and percent sand [WSS-based]) and color attributes (n = 11) were summarized and compared between study plots initially grouped by (1) sites and subsequently grouped by (2) HP-based clusters. To assess variability in hydro-physicochemistry within each site, HP attributes were averaged as medians and compared between sites; HP attributes were analogously summarized and compared between HP-based clusters to assess the efficacy of the k-means clustering analysis to produce hydro-physicochemically distinct groups of plots. Color attributes were also averaged as medians and compared between sites and between HP-based clusters. Descriptive assessments of the resulting color classes created by the two grouping variables, site and HP-based cluster, were conducted to comment on the efficacy of using HP-based clusters, in comparison to site identity, in classifying RMF color patterns. For all analyses, nonparametric Kruskal–Wallis and post-hoc Dunn's tests were conducted for comparisons, and $\alpha$ was set to 0.05 to determine significance (marginal significances, where $\alpha = 0.10$, were also noted).

## Results

### Hydro-physicochemical attributes by site

The initial comparison of HP attributes between sites indicated high intra-site (e.g., plot) heterogeneity. Sites were similar in their distribution of HP attributes, specifically for GSM and percent sand ($p > 0.10$); nonetheless, $D_b$ was significantly higher at BR than all other sites ($p < 0.05$) due to the inclusion of two plots—BR2 and BR4—with soils that had bulk densities above 1.5 $g \cdot cm^{-3}$, exhibited no surface inundation/saturation, and were consistently perceived to be relatively dry at depths below 30 cm during the augering process. A weakly significant difference in inundation/saturation frequency between sites ($0.05 < p < 0.10$) was highlighted through the contrast between the poor drainage of all JJM plots—inundated at all 6 site visits—and other sites which included more variability, e.g. MN, which included both poorly-drained areas with inundation/saturation frequencies over 50% (MN hollows, MN2 and MN4) and well-drained areas with 0% inundation/saturation (MN hummocks, MN1 and MN3) (USDA–NRCS Soil Survey Staff 2020). GSM differed between MN hummocks (33.8% and 24.9%) and hollows (60.9% and 52.9%), highlighting the relationship between the ephemeral soil water content and surface inundation/saturation (Table 2).

**Table 2.** Comparisons of hydro-physicochemical attributes between sites, summarized by medians and ranges*

| | ARP | BR | JJM | MN |
|---|---|---|---|---|
| *Inundation/Saturation Frequency (%)* * | 83 (83 – 100) [ab] | 50 (0 – 100) [a] | 100 (100 – 100) [b] | 50 (0 – 100) [a] |
| *GSM (%)* | 43.9 (40.3 – 48.2) | 28.8 (24.7 – 46.0) | 56.7 (13.7 – 88.2) | 43.3 (24.9 – 60.8) |
| BD ($g \cdot cm^{-3}$) | 1.2 (1.2 – 1.4) | 1.3 (1.2 – 1.8) | 1.1 (0.7 – 1.5) | 1.2 (1.0 – 1.3) |
| *Sand (%)* | 19.3 (11.3 – 27.3) | 32.1 (27.4 – 35.3) | 30.1 (27.1 – 30.1) | 24.7 (11.8 – 40) |

* Differences are significant at $p < 0.05$ (Kruskal-Wallis)
[a, ab, b] Groups followed by the same letter are not significantly different ($\alpha = 0.05$) (Dunn's test)

## Characterizing and comparing soil color attributes by site

Characterizations and comparisons of color attributes at ARP, BR, JJM, and MN highlighted large variability in color patterns within and between sites, with the determination that both hydric and nonhydric soils were present at each site. Out of all study plots, 8 were deemed hydric—ARP3, ARP4, BR3, JJM1, JJM3, JJM4, MN2, and MN4—while 8 were deemed nonhydric—ARP1, ARP2, BR1, BR2, BR4, JJM2, MN1, and MN3 (USDA–NRCS Soil Survey Staff 2020).

Table 3 summarizes typical observed colors within wetland sites, including matrix colors and observed redoximorphic features. Redox concentrations were present within both 0–30 cm and 30–60 depth intervals at all sites; in particular, red (5R) concentrations were observed at ARP, BR, and JJM. Concentrations were generally more abundant between 30 and 60 cm than between 0 and 30 cm. Below 30 cm, plots with less abundant concentrations, like MN hollows, tended to have a greater extent of redox depletions. While all sites had depleted matrices, ARP plots near an emergent wetland's edge had colors below 30 cm that were identified as either depleted or reduced matrices depending on season and year. Finally, all sites had reduced matrices and gley colors; reduced matrices were most abundant at JJM and MN, while gley colors were most abundant at BR (Table 4).

**Table 3.** Predominant soil color and redoximorphic ("redox") features at each site, including concentrations, depletions, and reduced matrices, for (a) the top 30 cm (0-30 cm, Horizon A) and (b) bottom 30 cm (30-60 cm, Horizon B) [a]

| Site | Hydric Soil Indicators | Depth (cm)[1] | Non-RMF Matrix Colors[1] | Redox Concentrations | | | Redox Depletions (including depleted matrices) | | | Reduced Matrices |
|---|---|---|---|---|---|---|---|---|---|---|
| | # plots / % of 6 visits | | | *Color* | *Contrast* | *Abundance (%)* | *Color* | *Contrast* | *Abundance (%)* | *Color* |
| ARP | 2 /<br>50 to 100% | 0–30 | 7.5–10 YR 3.5/3<br>7.5–10 YR 4/4 | 7.5YR 4.5/8<br>10R 3/3 | P,D | 0 – 25<br>0 – 5 | 7.5–10 YR 4.5/1.5 | D, P | 0 – 15 | N 4/0 |
| | | 30–60 | 7.5–10 YR 4.5/3<br>7.5–10 YR 4/4 | 2.5–7.5 YR 4/8 | | 10 – 40 | 10YR 4/1 | D | 20 – 50 | N 5/0 |
| BR | 2 /<br>25 to 100% | 0–30 | 2.5–10 YR 5.5/4.5<br>7.5 YR 4/3 | 2.5–10 YR 4/8<br>10R 3.5/3 | P | 0 – 25 | 0N 5/0<br>2.5–10 YR 4/1.5 | Matrix | 0, 70<br>0, 70 | 5–10 GY 4.5/1 |
| | | 30–60 | 5–7.5 YR 5/3.5 | 5–10 YR 5/8<br>2.5YR 2.5/5 | P<br>P | 15 – 30<br>0 – 10 | 7.5–10 YR 4.5/1<br>7.5YR 8/1 | Matrix<br>P | 45 – 60<br>10 – 50 | 5–10 GY 4.5/1<br>N 4.5/0 |
| JJM | 3 /<br>75 to 100% | 0–30 | 2.5Y–10YR 3/4 | 2.5–7.5 YR 6/8 | P | 10 – 30<br>5 – 15 | 2.5Y–10YR 3.5/2 | P, Matrix | 5 – 65 | - |
| | | 30–60 | 7.5–10 YR 3.5/4 | 5–10 YR 5/8<br>2.5–5 YR 3.5/6<br>10R 3/6 | P<br>D | 5 – 35<br>5 – 35<br>0 – 5 | 10YR 4.5/1.5 | P, Matrix | 5 – 65 | 5GY 6/2 |
| MN | 2 /<br>75 to 100% | 0–30 | 2.5Y–2.5YR 5.5/4.5<br>7.5–10 YR 4.5/2.5<br>10YR 6/6 | 2.5Y–10YR 6/5<br>7.5–10 YR 5.5/8 | D<br>P | 5 – 10<br>10 – 35 | 2.5Y 8/1.5<br>5–10 YR 4.5/1.5 | P | 5 – 30 | N 5.5/0 |
| | | 30–60 | 2.5Y–10YR 5.5/5.5<br>10YR 4/4 | 2.5Y–5YR 5.5/8<br>2.5–10 YR 4/6 | P<br>P | 5 – 25<br>5 – 25 | 2.5Y–10YR 5.5/1.5<br>N 5.5/1 | Matrix | 0, 50 – 75<br>0, 60 | N 5.5/0 |

[a] Redox concentrations include all types of concentrations; depletions include all colors independent of size identified where value ≥ 4 and chroma ≤ 2; and reduced matrices refer to matrices (>50% of ped) which are reduced when present in at least one plot (see Figure 1)

At ARP, two plots, ARP3 and ARP4, met the indicators for hydric soils for 50% of the site visits, notably in the spring and summer of 2018 when precipitation was ample. Plots tended to have matrix hues of 7.5YR and 10YR; commonly observed value/chroma pairs were 3/4, 4/4, and 4/3. All plots, particularly those closer to the emergent wetland (ARP3 and ARP4), contained distinct to prominent concentrations, most frequently the orange-red color 7.5YR 4/8. Depletions, but not depleted matrices, were found at ARP2, ARP3, and ARP4, and were most common in the B horizons of ARP3 and ARP4. Finally, ARP4 consistently had reduced matrices (N 4/0 and N 5/0) for 50–75% of site visits.

At BR, only one plot, BR3, was officially classified as hydric. While BR1 and BR4 matrix colors were not low-chroma, the hydric BR3 as well as BR2 contained low-chroma colors including 10YR 2/1, 10GY 4(5)/1, 5GY 5/1, and N 4(5)/0. All plots but BR2 had distinct to prominent red and orange redox concentrations. While BR4 was extremely dry at each visit to a depth of >30 cm, high-value iron depletions, identified as 7.5YR 8/1, were observed in the Bt horizon.

Three of the JJM plots—JJM1, JJM3, and JJM4—were classified as hydric. Like ARP and BR, JJM plots exhibited matrix hues of 7.5YR, 10YR, and 2.5Y. JJM2 and JJM4 included low-chroma matrices in both the A and B horizons. All plots included red- to yellow- colored redox concentrations, with prominence increasing with depth. Depletions were common among JJM2, JJM3, and JJM4 with colors like 10YR 4/1, 10YR 4/2, and 10YR 5/1. JJM1 had a uniformly reduced matrix beginning near 0 cm (observed as 5GY 6/2) and was the only plot to be fully reduced and/or depleted down to 60 cm.

Finally, MN showed similar patterns between the two hydric plots, MN2 and MN4, which showed low-chroma matrix colors including 10YR 5/2. Depletions and concentrations occurred more prominently and with greater abundance in the hollows. The hummocks (MN1 and MN3) did not include low-chroma matrix colors and tended to have matrices with more yellowish hues including 2.5Y. Gley colors were found at all plots but in higher abundance at the hollows. MN2 tended to have more purplish-blue gley colors than MN4, at which neutrally colored soils were observed but were identified to be depleted rather than reduced matrices.

Overall, MSCC value ($p < 0.05$), depleted matrix frequency ($p < 0.05$), and depth to depletions ($p < 0.10$) differed between sites (Table 4), indicating that site identity is useful for informing 2 *(3)* color attributes when $\alpha = 0.05$ *($\alpha = 0.10$)*. While neither hue nor chroma differed between sites, median value was highest at MN (5.1) compared to ARP (4.0; $p < 0.05$). Similarly, depleted matrices were most abundant at JJM (67%) and least abundant at ARP (0%; $p < 0.05$). Differences in value were highlighted between Piedmont and Coastal Plain soils, particularly for the comparison of ARP (Piedmont) and MN (Coastal Plain) soils.

**Table 4.** Medians and ranges for RMF and soil color attributes compared between sites, including measured MSCC color aspects and RMF characteristics

| Color attributes | ARP | BR | JJM | MN |
|---|---|---|---|---|
| *Hue* [d] | 7.0 – 7.5YR (6.6 – 7.7) | 10.1 – 10YR (7.7 – 11.5) | 8.4 – 7.5YR (6.1 – 11.0) | 8.7 – 7.5YR (6.2 – 11.0) |
| *Value* * | 4.0 (3.6 – 4.1) [a] | 4.5 (3.3 – 4.7) [ab] | 4.2 (3.7 – 4.4) [ab] | 5.1 (5.0 – 5.8) [b] |
| *Chroma* | 3.5 (3.3 – 3.8) | 4.2 (3.6 – 5.5) | 3.9 (3 – 5) | 3.7 (1.7 – 4.3) |
| *Contrast* | 1.1 (0.2 – 1.5) | 1.6 (0.0 – 2.1) | 2.0 (0.7 – 2.3) | 0.8 (0.7 – 1.6) |
| *Non-matrix colors (%)* | 49 (22 – 63) | 65 (0 – 79) | 79 (29 – 85) | 38 (30 – 66) |
| *Concentrations, frequency (%)* | 24 (21 – 40) | 42 (0 – 45) | 51 (14 – 56) | 14 (12 – 47) |
| *Depleted Matrix, frequency (%)* * | 0 (0 – 0) [a] | 25 (0 – 67) [ab] | 9 (0 – 29) [ab] | 67 (50 – 100) [b] |
| *Reduced Matrix frequency (%)* | 14 (8 – 25) | 10 (0 – 28) | 9 (0 – 12) | 19 (14 – 26) |
| *Gley colors, frequency (%)* | 8 (0 – 14) | 7 (0 – 32) | 0 (0 – 7) | 13 (5 – 16) |
| *Depth to Depletions (cm)* + | 33 (7 – 60) [a] | 47 (14 – 60) [a] | 14 (3 – 60) [a] | 9 (8 – 21) [a] |
| *Depth to Concentrations (cm)* | 18 (7 – 60) | 18 (11 – 60) | 7 (3 – 20) | 30 (11 – 36) |

+, * Attributes are marginally (+; $0.05 < p < 0.10$) or significantly (*; $p < 0.05$) different between clusters
a, ab, b, bc, c For attributes with noted differences: groups followed by the same letter are not significantly different ($\alpha = 0.10$)
d Hue is presented both numerically (10YR = 10) and as the nearest alphanumeric hue per the Munsell Soil Color Chart (MSCC)

## Characterizing and comparing plot hydro-physicochemistry and soil colors by HP-based cluster

As an alternative to comparing plots by site, the HP-based cluster analysis identified three distinct clusters of study plots using inundation/saturation frequency, GSM, $D_b$, and percent sand. Dimensions 1 and 2 of the PCA explained 81.1% (50.0% and 31.1% for dimensions 1 and 2, respectively) of the total variability in HP attributes (Figure 3). GSM had a strong and positive relationship with Dimension 1 ($p < 0.01$). Inundation/saturation frequency similarly plotted positively along Dimension 1, but with a more positive loading along Dimension 2. $D_b$ plotted negatively along Dimension 1 and positively along Dimension 2. Finally, percent sand plotted negatively along both

Dimensions 1 and 2. Given the strong positive link to GSM and inundation/saturation frequency, Dimension 1 can be associated with overall water content within soil; conversely, given the negative link to percent sand, positive link to $D_b$, and positive link to inundation, Dimension 2 can be related to soil drainage as influenced by physicochemistry including texture, bulk density, and highlighted through the resulting aboveground flooding (Figure 3).

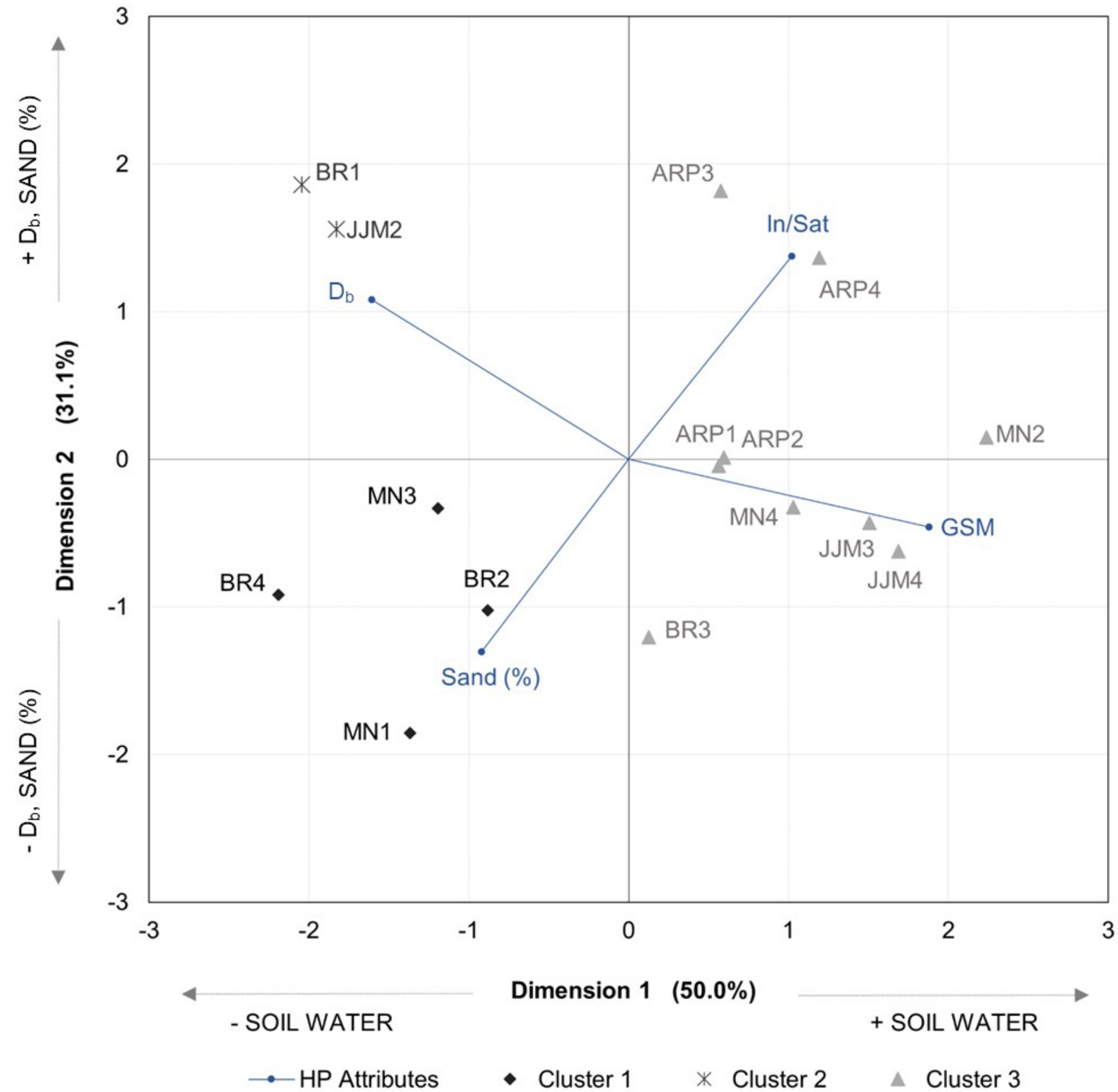


**Figure 3.** Principal Component Analysis (PCA) of plots based on the following hydro-physicochemical attributes: (1) bulk density (BD), (2) inundation/saturation frequency ("In / Sat"), (3) gravimetric soil moisture (GSM), and (4) percent sand

The optimal number of HP-based clusters was identified to be three (between/total sum of squares = 64.6%), and k-means cluster analysis resulted in clusters comprising 4, 2, and 9 plots, respectively (Figure 3; Table 5). Cluster 1 included BR2, BR4, and MN hummocks (MN1 and MN3); cluster 2 included BR1 and JJM2, which were both relatively rocky below the epipedons; finally, cluster 3 included all plots at ARP, JJM3 and JJM4, BR3, and MN hollows (MN2 and MN4). All plots identified to be hydric belonged to the third cluster of 9 plots (with the exception of JJM1, which was not included in the cluster analysis).

Except percent sand, all HP attributes differed significantly between clusters ($p < 0.05$; Table 5). Depicted in Figure 3, cluster 1 plots shared negative loadings on both Dimension 1 and Dimension 2, plotting in the opposite direction of inundation/saturation frequency. Similarly, cluster 2 plots shared negative loadings on Dimension 1, but had positive loadings on Dimension 2 and plotted in a similar (opposite) direction as $D_b$ (GSM). In accordance with their negative loadings on Dimension 1, clusters 1 and 2 were characterized by relatively low soil moistures in comparison to cluster 3, which plotted in the positive direction on Dimension 1 ($p < 0.05$). Cluster 1 had higher GSM than cluster 2 but was composed solely of plots with 0% inundation/saturation over the study period and contained relatively high sand percentages. Highest soil moistures and lowest bulk densities—and thus high Dimension 1 loadings—belonged to soils in cluster 3 ($p < 0.05$; Table 5). Despite having similar inundation/saturation frequencies as cluster 3, cluster 2 soils were characterized by higher bulk densities and lower GSM ($p < 0.05$) due to the abundance of rocks and gravel below the epipedons, rendering negative loadings for Dimension 1.

**Table 5.** Comparisons of hydro-physicochemical (HP) and soil color attributes, noted by medians and ranges, between three clusters created from k-means clustering on the principal component dimensions (between/total sum of squares = 64.6%)

| | **Cluster 1 (n = 4)** | **Cluster 2 (n = 2)** | **Cluster 3 (n = 9)** |
|---|---|---|---|
| | BR2, BR4, MN1, MN3 | BR1, JJM2 | ARP1, ARP2, ARP3, ARP4, BR3, MN2, MN4, JJM3, JJM4 |
| HP attributes | | | |
| *Inundation/Saturation Frequency (%)* $^{**}$ | 0 (0 – 0) $^{a}$ | 100 (100 – 100) | 83 (50 – 100) $^{b}$ |
| *GSM (%)* $^{**}$ | 28.7 (24.7 – 33.8) $^{a}$ | 19.4 (13.7 – 25.0) $^{a}$ | 48.2 (40.3 – 60.8) $^{b}$ |
| *BD* ($g \cdot cm^{-3}$) $^{*}$ | 1.3 (1.2 – 1.4) $^{a}$ | 1.6 (1.5 – 1.8) $^{b}$ | 1.2 (1.0 – 1.4) $^{a}$ |
| *Sand (%)* | 31.4 (21.2 – 40) $^{a}$ | 28.0 (27.1 – 28.9) $^{a}$ | 27.3 (11.3 – 35.3) $^{a}$ |
| Color attributes | | | |
| *Hue* $^{d, +}$ | 10.1 – 10YR (7.6 – 21.0) | 9.3 – 10YR (7.2 – 11.5) | 6.9 – 7.5YR (6.1 – 10.3) |
| *Value* | 4.9 (3.3 – 5.8) | 4.6 (4.4 – 4.7) | 4.0 (3.6 – 5.1) |
| *Chroma* $^{+}$ | 4.5 (3.6 – 5.5) | 3.5 (3.4 – 3.6) | 3.6 (1.7 – 4.4) |
| *Contrast* | 0.8 (0 – 1.3) | 1.9 (1.8 – 1.9) | 1.4 (0.2 – 2.1) |
| *Non-matrix colors (%)* $^{*}$ | 38 (0 – 58) $^{a}$ | 80 (79 – 81) $^{b}$ | 61 (22 – 77) $^{ab}$ |
| *Concentrations, frequency (%)* $^{*}$ | 13 (0 – 40) $^{a}$ | 50 (45 – 56) $^{c}$ | 25 (14 – 56) $^{bc}$ |
| *Depleted Matrix, frequency (%)* | 6 (0 – 8) | 9 (0 – 19) | 0 (0 – 59) |
| *Reduced Matrix, frequency (%)* | 7 (0 – 26) | 17 (13 – 21) | 17 (0 – 29) |
| *Gley colors, frequency (%)* | 5 (0 – 11) | 5 (0 – 10) | 13 (0 – 32) |
| *Depth to Depletions (cm)* | 40 (7 – 60) | 18 (3 – 34) | 14 (7 – 60) |
| *Depth to Concentrations (cm)* $^{+}$ | 30 (23 – 60) $^{a}$ | 8 (3 – 12) $^{b}$ | 13 (7 – 60) $^{ab}$ |

$^{+, *}$ Attributes are marginally ($^{+}$; $0.05 < p < 0.10$) or significantly (*; $p < 0.05$) different between clusters
$^{a, ab, b, bc, c}$ Groups followed by the same letter are not significantly different ($\alpha = 0.05$)
$^{d}$ Hue is presented both numerically (10YR = 10) and as the nearest alphanumeric hue per the MSCC

At the α = 0.05 (*α = 0.10*) level, clusters strongly differed for two (*five*) color attributes—concentration frequency and non-matrix color count (*plus hue, chroma, and depth to concentrations*)—as opposed to the two (*three*) attributes when grouped by site—value and depleted matrix frequency (*plus depth to depletions)* (Table 4; Table 5). Notably, while value and depletion frequencies and depths were most distinct between sites, concentration frequencies and depths were most distinct between HP clusters. Furthermore, HP-based clusters of plots could be distinguished by soil chroma ($p < 0.10$) and non-matrix color counts ($p < 0.05$), which was not the case when classified by site (Table 4; Figure 3; Table 5). Cluster 1 was characterized by lowest frequencies ($p < 0.05$) and greatest depths to concentrations ($p < 0.10$), plus lower counts of non-matrix colors ($p < 0.05$) than cluster 2. Cluster 1 had the lowest median frequency of all RMFs combined ($p < 0.10$), corroborating the HP characterization of cluster 1 with low GSM and low inundation/saturation frequency, i.e., conditions that are less likely to encourage hydric soil development. Cluster 1 also had the highest median chroma, albeit to an insignificant degree, as it consists of plots that generally showed homogeneously-colored soil matrices. Cluster 3 did not significantly differ from clusters 1 or 2 in characterizations of chromas or concentrations but exhibited the lowest minimum chroma of the clusters (< 2).

## Discussion

### Hydro-physicochemical classifications for study plots

This study supports conclusions of previous research that the combination of soil attributes can aid in the creation of wetland indicators (Dee and Ahn 2012; Ahn and Peralta 2012; Peralta et al. 2013). The analysis highlighted that study plots within four spatially separated wetland areas can occupy substantially different combinations of these attributes, rationalizing analysis techniques to reduce attribute variability into fewer dimensions and highlight similarities between plots with cluster analysis. The PCA provided justification for k-means clustering analysis using the four HP attributes by indicating the distinct role each variable played in explaining variability in plot loadings on Dimensions 1 and 2. As similarly observed with physicochemical attributes assessed by Wolf et al. (2011), Figure 3 nonetheless highlights the interconnectedness of the four HP attributes; for example, GSM shared a negative relationship with bulk density, and percent sand plotted opposite to inundation/saturation frequency, indicating a strong negative correlation that is likely related to the role of soil texture in water infiltration (Jackson et al. 2014). Such interconnectedness does not imply redundancy, as the 4-variable PCA was more capable of explaining HP variability and providing distinct clusters of plots than a 3-variable PCA. In assessing a site for hydric soil development and/or future potential, using the combination of HP attributes can more effectively characterize soil conditions compared to site identity.

**Soil color and RMF attributes by site**

While distinct characterizations of 5 color and RMF attributes were better derived from HP-based clusters, three color attributes—value, depleted matrix frequencies, and depth to depletions—were still solidly characterized by geographic site location (Table 4; Table 5), a factor that is characterized by homogenous geomorphology and historic large-scale hydrology that are known to influence hydric soil formation (Veneman et al. 1998; Fiedler and Sommer 2004; Li et al. 2018). The disparities in color and RMF attributes distinguished by either site identity or HP-based clusters highlight the relevance of both landscape and plot-specific HP attributes in influencing RMF and color attributes, where site identity is more capable of classifying indicators of more long-term or permanent saturation and reduction conditions like depleted matrices and high values that form only with longer (e.g., ≥ 21 days) periods of reduction (Schelling 1960; Franzmeier et al. 1983; Vepraskas et al. 2004; Vepraskas and Vaughan 2016). Conversely, attributes related to high-chroma colors and concentrations are likely to be more variable across a wetland site due to variability in HP attributes: although SHWT has also been correlated to concentration depth (Genthner et al. 1998), Fe concentrations can form depth near the topsoil with little relation to water table depth when surface soil inundation/saturation and limited oxygen diffusion produces temporary reducing conditions (Dorau et al. 2020).

Our results also highlighted the importance of physiography when characterizing RMFs and relating them to hydrology. Higher color values observed in the Coastal Plain compared to the Piedmont may be the result of finer-textured soils with better drainage but may also be related to problematic hydric soils of the Culpeper Triassic Basin, which have developed red colors due to the reddish-brown shales of the parent material and can sustain anerobic environments without high quantities of low-chroma, high-value depletions (Elless et al. 1996). A focus on the factor of physiography, specifically with inclusion of problematic hydric soils, is warranted to better discern potential differences in HP attributes as influenced by these factors.

**Soil color and RMF attributes by HP clusters**

The distinct characterizations of 5 color and RMF attributes by HP-based clusters not only linked hydro-physicochemistry to RMFs, but also provided a classification of plot-level soil ecosystems via both hydro-physicochemistry and soil colors. The nonhydric cluster 1 plots—most homogenously colored and hosting the lowest frequency of RMFs—were matched to observed HP settings unlikely to support hydric soils, indicating that the cluster analysis was aligned with a core tenet of hydric soil science, i.e., that nonhydric plots do not exhibit substantial RMFs. Also in accordance with well-documented relationships between hydrology and soil biogeochemistry, cluster 3 soil environments—showing high soil moistures and high inundation/saturation frequencies—encouraged reducing conditions that produced less concentrations but generally frequencies reduced matrices and depletions within the top 30 cm. Coinciding with having the highest GSM, cluster 3 represents plots where surface $D_b$ is relatively low and permeability is relatively high, such that soil inundation aboveground also coincides with high soil moisture (Table 5; $p < 0.05$). Such plots are most common in wetlands which are occasionally to frequently flooded, as was included in this study;

semipermanently ponded wetlands with mineral soils may exhibit different combinations of HP attributes that yield a distinct cluster of RMF characteristics not exhibited in Figure 3.

The usefulness of this analysis methodology is underscored through focusing on unexpected connections that can serve as the basis for scientific questions, hypotheses, and hypothesis testing. In particular, unexpected combinations of HP attributes and their links to observed RMFs were observed in cluster 2: while the nonhydric cluster 2 plots exhibited relatively low soil moistures ($p < 0.05$) and lower maximum frequencies of reductions and/or depletions in comparison to cluster 3, they had highest frequencies of inundation/saturation (Table 5). Both BR1 and JJM2 were characterized by higher bulk densities than cluster 3 plots (Table 5; $p < 0.05$), likely due to the abundance of cobbles and rocks below the epipedon, a feature that was not present above 60 cm at other plots. The epipedons of BR1 and JJM2 may have similar water holding capacities to other study plots that encourage surface inundation/saturation, the coarser textures below may promote oxygen diffusion that lowers moisture and limits the long-term potential for reducing conditions to be present (Davis 1995; Jackson et al. 2014), allowing concentrations to predominate (Table 5). Over time, soil forming processes may encourage further development of wetland conditions, identified through monitorable increases in reduction and depletion frequencies.

Furthermore, the plotting of nonhydric ARP1 and ARP2 with otherwise hydric plots in cluster 3 provides more variability in several color attribute indicative of hydric soils—e.g., depleted matrix frequency (0% for ARP plots; Table 4)—within cluster 3 and indicates the importance of historic land use, a factor that might outweigh HP setting and produce unexpected HP-based RMF characterizations. A previous work (Schmidt and Ahn 2021a) illustrated that, compared to the other study sites, ARP tended to deviate from generally observed patterns linking hydrology and soil biogeochemistry. While the forested floodplains of ARP currently exhibit HP attributes that would indicate a high level of *hydricity*—with ARP1 and ARP2 hosting relatively low bulk densities and high GSM compared to other nonhydric plots—these plots occur on land that was nonforested farmland as late as 1957 (Loudoun County Office of Mapping and Geographic Information 2021). Such inconsistencies may explain why cluster 3 did not display significantly higher frequencies of depleted or reduced matrices than cluster 2 (Table 5; $p > 0.10$). Similarly young floodplains that experience increased flooding due to changing precipitation patterns—as seen in 2018—may not yet host the biogeochemical maturity required to show RMFs necessary for being classified as hydric but provide a proper setting for wetland functions to develop over time.

**Implication and recommendations for further study**

Linking patterns of color attributes, like chroma and concentration frequency, to plot hydro-physicochemistry has the potential to transform color indicators into accessible field estimations of soil biogeochemistry; watershed managers or planners without sufficient experience with hydric soil field indicators can rely on site history and HP attributes to characterize, assess, and track soil colors and thus hydric soil presence and/or development. This approach can be beneficial for approaching conservation planning that should view each site of interest, such as a community park or blue-green infrastructure, as a matrix of heterogeneous HP settings; furthermore, it is particularly timely as climate, landcover patterns, and stormwater management can alter hydrologic regimes, inducing more intense and frequent flooding events and modifying water flow paths and hydrologic sinks (Wissmar et al. 2004; O'Driscoll et al. 2010). Changes in flooding patterns may encourage the onset of redoximorphic feature formation that are not substantial enough to yet qualify as indicators of hydric soils. In areas prone to flooding, monitoring HP attributes and soil colors can provide a characterization of such areas that may not yet host hydric soils but nonetheless indicate the potential for hydric soil development.

The conclusions of this study are drawn from a pertinent set of sampling sites and sound statistical analyses; nonetheless, sampling and analysis constraints provide opportunities for methodological refinement. The exploratory PCA and cluster analysis provided novel insights, but a large-scale regression and/or systems model may further demonstrate the value in a multivariate link between hydro-physicochemical setting and RMF characterizations. Various environmental factors such as seasonality were not integrated into the analyses, as HP attributes like inundation/saturation frequency were evaluated at a plot- rather than profile- scale to reflect longer-term HP settings; however, as color attributes plus other included HP attributes like GSM are dynamic across seasons, an inclusion of season as a blocking variable may provide more nuanced insights if investigated. The 4 HP and 11 color attributes used within the analyses were capable of distinguishing color attributes by site and HP-based cluster, but modifications to attributes may be pertinent. For example, an analysis that retains finer details of color observations within each soil horizon—e.g., inclusion of color thicknesses as an attribute and horizons/depths as a covariate—may elucidate more sensitive patterns in color characterizations. With respect to HP attributes, a semiquantitative measure of percent sand derived from the soil texture triangle may be more accurate than Web Soil Survey data (i.e., percent sand), which was deemed sufficient for this study given the limited range in textures studied (from loam, least sandy, to loam, most sandy) that would not have been differentiated by reliance on hydric soil indicators' distinction of *loamy/clayey* versus *sandy* soils. Additional physicochemical attributes, such as reaction to α,α’-dipyridyl dye—an indicator of reducing conditions (Berkowitz et al. 2017)—are appropriate to include; this study did not rely on the dye as an HP attribute due to its binary nature (positive/negative reaction) in contrast to the other HP attributes.

Overall, the inclusion of a greater number and diversity of HP settings, such as permanently flooded wetland areas and sandier soils, could have aided in the power of the Kruskal–Wallis comparisons by elucidating additional clusters with distinct patterns of color and RMF attributes. Several hydric field indicators rely on *depths to depleted matrices* that are as little as 10 cm—e.g., F3, "Depleted Matrix"—which was only observed for one plot with a depth of 3 cm to a depleted matrix (USDA–NRCS 2018). It is recommended that our approach be utilized for a larger study area to more fully flesh out HP attributes and HP-based clusters of terrestrial plots which may or may not be wetlands, allowing the resulting RMF characteristics to indicate their hydric soil status on a multi-class categorical scale including hydric, potentially hydric, or stable upland.

## Conclusions

Our investigation has indicated that plot-specific HP attributes—e.g., seasonally observed frequencies of inundation/saturation, bulk density, soil moisture, and soil texture—can serve as the basis for classifying and distinguishing soil color characteristics that differ from those indicated through larger-scale wetland site alone. Hue, chroma, depth to concentrations, frequencies of concentrations, and number of non-matrix colors were distinguished through HP attributes, highlighting the applicability for HP-based clusters to indicate RMF characteristics related to shorter periods of soil reduction. Conversely, value, frequency of depleted matrices, and depth to depletions were distinguished through site identity, indicating the utility of landscape and site characteristics to inform RMF characteristics related to longer periods of soil reduction. While measures of the individual 11 color attributes used in this study cannot substitute for indicators of hydric soils, the capacity to characterize and distinguish RMFs and soil colors from HP attributes highlights the latter's suitability as a mechanism for identifying wetland functions and potential for future development. Furthermore, this approach highlights that the combination of information from multiple soil color measures can together depict a wetland setting capable of being explained through hydro-physicochemistry. Future research focused on a wider range of HP attributes in more field sites is warranted to further demonstrate the efficacy of a suite of simple HP attributes to be used in assessing, tracking, and indicating wetland soil development consequential to changing environmental conditions.

## CHAPTER THREE:
## A COMPARATIVE REVIEW OF METHODS OF USING SOIL COLORS AND THEIR PATTERNS FOR WETLAND ECOLOGY AND MANAGEMENT

### Introduction

In the United States, almost 50% of palustrine and estuarine wetlands of the 18th century were lost by the 1970s; the Commonwealth of Virginia had lost 42% of its colonial wetlands by 1980, which have continued to be converted for agriculture, industry, urban development, and recreation (Fretwell et al. 1996). The rate of wetland loss has decreased from 185,000 hectares per year between 1950 and 1970 to 13,800 acres per year between 2004 and 2009 (Dahl 1990, 2000, 2006, 2011) (check for update) due to an influx of wetland laws and regulations that required mitigation of the loss of wetlands through compensatory actions, allowing newly created wetlands to make up for the loss (Page and Wilcher 1990). Compensatory wetland mitigation guidelines require wetland delineation and monitoring in such a way that natural wetland locations could be identified, and ecosystem development in created wetlands could be tracked to aid the mitigation of lost wetland functions.

Wetland delineation produced a workforce trained in rapid determination of wetland presence and boundaries based on three key features of wetlands: hydrology, hydrophytic vegetation (i.e., wetland plants), and hydric soil (i.e., wetland soils). Wetland delineation primarily focused on hydrophytic vegetation in the 1970s and 1980s; vegetation has remained the most commonly used attribute to evaluate the success of wetland mitigation through the 21st century (Spieles 2005; Dewey et al. 2006). This single indicator approach is a weak measure of wetland performance (National Research Council 2001); vegetative characteristics of created wetlands are more powerful in predicting ecosystem function when combined with soil and hydrologic characteristics (Ehrenfeld 2005; Dewey et al. 2006; Ballantine and Schneider 2009; Hossler and Bouchard 2010; Wolf et al. 2011; Dee and Ahn 2012; Ahn and Peralta 2012; Peralta et al. 2013). Furthermore, the failure of mitigation wetlands to develop maturity in their structures and functions is often attributable to the lack of development in soil properties, such that proper identification and diagnosis of wetland development necessitates an understanding of soil properties (Stolt et al. 2000; Cole et al. 2001; Campbell et al. 2002; Craft et al. 2002; Lindig-Cisneros et al. 2003; Hossler and Bouchard 2010). By 1994, wetland delineation methods used by United States Army Corps of Engineers (USACE), Department of Agriculture–Natural Resource Conservation Service (USDA–NRCS), and Fish and Wildlife Service (USFWS) had expanded to include a focus on hydric soils.

Hydric soils are legally defined as "soil[s] that formed under conditions of saturation, flooding, or ponding long enough during the growing season to develop anaerobic conditions in the upper part" (Federal Register 1994; USDA–NRCS 2018). In anaerobic and chemically reduced wetland soils, organic matter accumulation and oxidation-reduction (redox) reactions with manganese, iron, and sulfate produce unique soil morphologies—in particular, soil color patterns—that are not found in upland soils. The inclusion of hydric soil criteria into wetland delineation and monitoring practices thus allows for hydrologically-driven soil color properties to inform decisions concerning wetland existence, development, and/or hydrologic regime changes. In the last twenty years, criteria related to hydric soils have become an essential component in properly delineating wetlands and assessing ecosystem development. USACE performance standards for mitigation wetlands have mirrored the national prioritization of hydric soil criteria; the agency currently necessitates that entire wetland restoration or creation areas annually meet the Hydric Soil Technical Standard developed by the National Technical Committee for Hydric Soils (NTCHS) (U.S. Army Corps of Engineers 2018). The Technical Standard guides landowners and managers in identifying and delineating hydric soils through hydric soil field indicators, which consist of soil pedon descriptions that necessitate specific patterns of soil colors resulting from biogeochemical processes in reduced soils.

Hydric soil field indicators rely on the Munsell Soil Color Chart (MSCC) created by A.H. Munsell to standardize color determinations through three observations: (1) hue, or relative attributions of red, yellow, green, blue, and purple; (2) value, or lightness; and (3) chroma, or color richness with respect to a neutral tone (Munsell 1905). The Munsell Hue, Value, and Chroma (HVC) color space is an asymmetric cylindrical color space where a difference of two units of chroma is perceptually analogous to a one-unit difference of value (Barrett 2002; Hunt and Pointer 2011). To create the MSCC, the color space was parsed into 1500 discrete color chips to resonate with perceivable differences between colors (Figure 4) (Torrent and Barrón 1993).

(a)

(b)

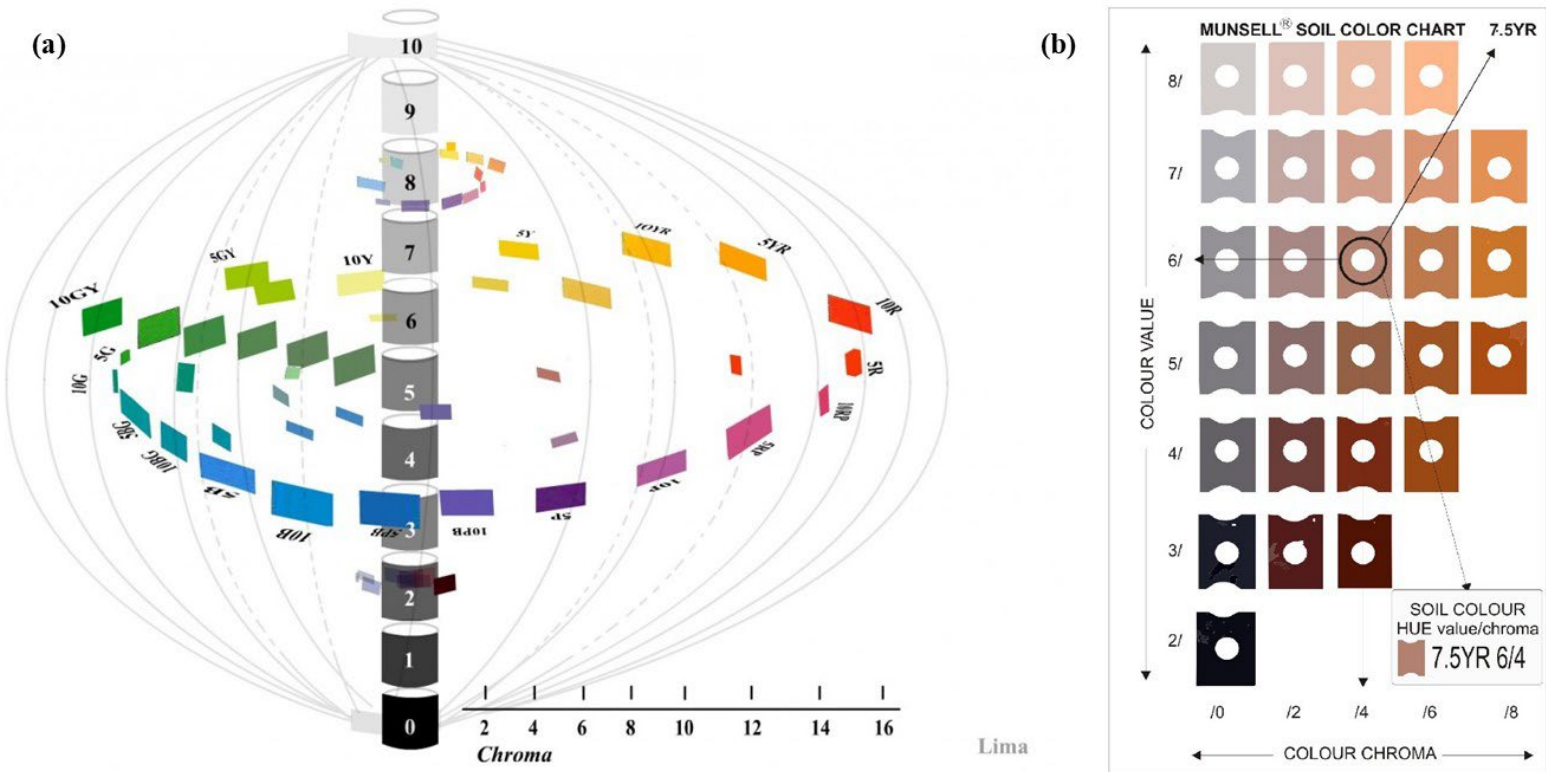


**Figure 4. (a)** The Munsell color space in polar coordinates (Lima 2014) **(b)** A page from the Munsell Soil Color Chart (MSCC) illustrating a hue (page), value (vertical axis), and chroma (horizontal axis) for a given color chip (Silva et al. 2013)

The presence of certain Munsell colors are fool-proof indicators of hydric soils when identified in the field: certain colors and associated patterns are only present when extended saturation events, leading to anaerobic conditions, instigate redox reactions that affect soil morphology (USDA–NRCS 2018). In particular, hydrologically driven changes in soil color due to redox reactions with iron and/or manganese have been noted in a plethora of publications (Daniels et al. 1961, 1971; Daniels and Gamble 1967; Simonson and Boersma 1972; Moore 1974; Schwertmann and Fanning 1976; Guthrie and Hajek 1979; Richardson and Hole 1979; Franzmeier et al. 1983; Evans and Franzmeier 1986).

Soil color is influenced by a variety of factors including length and periodicity of saturation and reducing conditions, organic matter, parent material, and iron and manganese concentrations and oxidation states (Daniels et al. 1961; Schwertmann 1993). Common iron oxides like hematite and goethite have MSCC hues ranging from 10YR to 5R (Schwertmann and Lentze 1966; Schwertmann 1993), which are normally uniformly distributed within non-hydric soil peds to create a uniform reddish hue. During anaerobiosis, iron oxide (ferric, $Fe^{3+}$) is reduced to ferrous iron ($Fe^{2+}$), a mobile, blueish-green ion that can be translocated within the soil profile through water movement and immobilized upon exposure to air (Daniels et al. 1961). Additionally, under extended periods of reducing conditions, ferrous iron can be fully leached out such that iron-free soils are left with an uncoated gray color (Simonson and Boersma 1972; Richardson and Hole 1979). Hydrologically-driven redox reactions with iron thus result in three characteristic color patterns, or redoximorphic features (RMFs), that are included in the hydric soil indicators (Figure 1): (a) redox depletions, formed under long periods of saturation as dissolved iron is translocated out of or within the soil profile, leaving areas or entire matrices with a gray color; (b) reduced matrices, in which sufficient amounts of ferrous iron color the soil blueish-green under shorter periods of saturation and anaerobic conditions; and (c) redox concentrations, formed as fluctuating water tables trap previously mobilized ferrous iron such that orange, red, or brown iron oxides accumulate in situ (Vepraskas 2015). The umbrella term redoximorphic features is often discussed using various terms including red, gray, and/or gley mottles; iron nodules; and iron concretions (Schlichting and Schwertmann 1973; Bouma et al. 1990; Veneman et al. 1998; Vepraskas et al. 2018). Because the term "mottle" may relate to any color change regardless of its relationship to oxidation-reduction reactions, RMFs is the preferred terminology (Vepraskas, 2018).

All three parameters of the Munsell soil color space are used for the identification of redoximorphic features, as all three are informative of iron cycling and hydrology within wetland soils. Gley colors are indicated through blue and green hues; a chroma $\leq 2$ and value $\geq 4$ indicate the absence of iron and thus reducing conditions; and, depending on a soil's matrix color, mottles of prominent differences in chroma and value—each necessitating a difference of at least 2 from the matrix chroma and value—can indicate the presence of RMFs (USDA–NRCS 2018).

Unlike vegetative properties, soil color is more sensitively to correlate with wetland hydrology (Vepraskas et al. 2004) and can provide inference on waterlogging duration and soil drainage (Evans and Franzmeier 1986; Blavet et al. 2000; Chaplot et al.

2000; Malone et al. 2018). The presence of a hydric soil indicator automatically qualifies a given soil as hydric (USDA–NRCS 2018) such that an accurate identification of all colors present in a soil pedon is essential for determining if a field site undergoes biogeochemical processes related to wetland ecosystem functions; thus, the observation of soil color using the MSCC has become a convention in any wetland study and/or delineation.

A suite of wetland research publications have focused on wetland ecosystem dynamics as examined through soil color patterns, as color is not only an accessible measurement to make, but also related to various physical, chemical, and geologic properties of soil beyond water fluctuations including soil texture (in particular, clay content), percent moisture, and concentrations of carbon, iron, nitrogen, phosphorus, manganese, and iron (Barron and Torrent 1986; Evans and Franzmeier 1988; Viscarra Rossel et al. 2008; O'Donnell et al. 2010; Summers et al. 2011; Liles et al. 2013; Moritsuka et al. 2014; Moonrungsee et al. 2015; Jien et al. 2016; Aquino et al. 2016). Identification of hydric soil indicators provides direct insight into site hydrology and soil biogeochemistry such that methodology drives results of ecosystem assessments and management decisions; thus, an investigation of methods by which soil color can be accurately determined in the field is particularly consequential.

The goal of this review is to identify, summarize, and compare methods that are currently available and simple-to-use for soil color assessment in the field of wetland delineation, mitigation, and monitoring to diagnose and/or explain wetland ecosystem processes and functional development. Specific objectives of this review include:

1) To describe each documented method of soil color determination and identify key conventions or procedural considerations related to hydric soil morphologic measurements; and
2) To compare each methods' strengths and weaknesses with respect to serving as a field-ready rapid measurement tool for soil color properties used in the practice of wetland delineation and ecological monitoring.

## Methods

Peer-reviewed journal articles were thoroughly examined for studies exploring hydric soil color patterns or explaining the relationship between soil color and hydrology, topography, vegetation, and/or attributes of biogeochemistry in wetlands. The George Mason University ProQuest library search was initially used with the following Boolean search strategies: a) ((wetland AND soil AND color) OR ("hydric soil" AND color)); b) ((redoximorphic features AND wetland AND color) or (redoximorphic feature AND wetland AND color)); c) (("soil color" AND chroma AND wetland) OR ("soil color" AND chroma AND hydric); as well as other similar strategies that included the search terms "wetland", "hydric soil", "soil color", "chroma", and "redoximorphic features". A "snowball" method was also used to review references included in relevant papers in an iterative manner. The final scope of the review includes 96 papers dated between 1960 and 2018. Several methods of color determination were included in the final review, screened by their use in studies focused on wetland soils and/or the relationship between soil color and hydrology. Additionally, methods were chosen by popularity, capacity for rapid in-situ soil color determination, cost accommodations, and accessibility as related to use and data analysis.

## Results and Discussion

Table 6 describes the results of the methodology review for hydric soil color assessment. We focused our review on four major ways to study soil colors in wetlands: the MSCC that is most abundantly used by researchers; Nix Color Sensor; mobile phone camera (MPC) and digital photography that are rather recently available and easy-to-use; and colorimetric and spectrometric techniques that have been traditionally used for color studies. The description of each chosen method is as follows:

**Table 6.** Color measurement methodology/tool assessed, associated cost, quantity of citing references, and relevance of such methods for examining or assessing RMFs

| Color determination Method | Cost | Citing References | Successful Use with Wetland RMFs |
|---|---|---|---|
| Munsell Soil Color Chart | $205 | 70 | Yes |
| In conjunction with Color Indices | - | 8 | Yes |
| Nix Color Sensor | $349 | 3 | No |
| Mobile Phone Camera | $30 + | 5 | No |
| Digital Photography | $150+ | 2 | Yes |
| Handheld Colorimeter / Spectrometer | Varies; > $1,000 | 8 | Yes |

## Munsell soil color chart (MSCC)

Of the literatures included in the review that involves wetland soil colors, approximately 80% utilized the MSCC to determine colors of wetland soil matrices and/or redoximorphic features. The MSCC became the codified standard for soil science in the 1950s (Pendleton and Nickerson 1951); by 1970, several articles investigating properties of wetland soils and/or iron cycling in soils utilized the MSCC (Daniels et al. 1961; Schwertmann and Lentze 1966; Daniels and Gamble 1967). Although methodology for identifying and recording RMFs using the MSCC was introduced in 1994 (Federal Register 1994), wetland soil color patterns, particularly low chroma (≤ 2) and iron and/or manganese concentrations, had already been identified and defined as important features of hydric soils (Torrent et al. 1983; Evans and Franzmeier 1988). In addition to describing matrix and RMF colors within soil horizons, morphological characterizations have conventionally included four pieces of information regarding RMFs: (1) types, i.e. concentration, depletion, or reduced matrix; (2) quantities, expressed as percentages; (3) sizes; and (4) color contrast, determined by differences in value and chroma from the matrix color (Johnston et al. 1995; Vepraskas 2000; Vepraskas et al. 2004; Schoeneberger et al. 2012).

Most articles have focused on a relationship between the nature of hydric soil color and a feature of wetlands, such as soil texture (Jien et al. 2016), topography (Vogel and Märker 2011), redox potential (Fiedler and Sommer 2004), and water table fluctuations, both long term and short term (Simonson and Boersma 1972; Franzmeier et al. 1983; Guertal and Hall 1990; Mokma and Cremeens 1991; Mokma and Sprecher 1994; Vepraskas et al. 2004; Morgan and Stolt 2004). When examining soil morphology using the MSCC, the conventional method of soil sampling begins with digging a soil pit, usually greater than 1 $m^3$ (Tassinari et al. 2002; Vepraskas et al. 2004). While some studies have identified soil colors and redoximorphic features to a certain horizon depth such as B or C (Franzmeier et al. 1983; Malone et al. 2018), others have sampled soils to the depth of 30 cm used in the definition of wetlands and in which the greatest biogeochemical activity occurs (Wolf et al. 2011; Ahn and Peralta 2012; USDA–NRCS 2018). Simple characterization of soils based on hue, value, and chroma at various horizons and/or depths has elucidated the relationship between soil drainage class and depth to low chroma colors (Guertal and Hall 1990). Additionally, seven types of hydric indicators characterized by distinct coloring patterns using the MSCC were predictable with given durations of water saturation when geology was treated as a random effect

(Tassinari et al. 2002). The relationship between wetland hydrology and presence of low-chroma depletions was determined for Ultisols in North Carolina by Daniels et al. (1971). More recently, abundance of RMFs was determined to be predictable based on site-specific parameters, with saturation length related to depth, as well as percentage, of redox depletions and concentrations (He et al. 2003; Vepraskas et al. 2004). Nonetheless, various authors have noted a disconnect between hydric soil indicators, as identified by soil color, and vegetative and hydrological properties of a known wetland (Berkowitz et al. 2014); other factors that may hinder the use of hydric soil indicators using the MSCC include low organic matter content, high iron concentrations, and high-chroma minerals. In such problem hydric soils, the use of MSCC for soil color determination may not be a robust tool to elucidate the presence of hydric soils (Rabenhorst and Parikh 2000).

Several papers identified the value in calculating color indices from Munsell Soil Color components which are defined as functions of Munsell hue, value, and chroma (HVC) data (Evans and Franzmeier 1988; Thompson and Bell 1996; Jien et al. 2004). For indices which have included hue, numerical assignments have been made to each discrete hue to transform them to quantitative data (Mokma and Cremeens 1991). Evans and Franzmeier (1988) created a chroma index (CI), calculated as the sum of RMF abundances multiplied by their respective chromas; matrix color and percentage are also included in the sum. CI has been found significantly correlated with both saturation time and reduction time (Jien et al. 2004). Other indices have focused on wet and dry values and chromas and omit RMFs in their equations; despite an exclusion of mottles, such indices are useful for evaluating depleted matrices corresponding to long-term conditions of reduction (Evans and Franzmeier 1988; Van Huyssteen et al. 1997). Given their the relatively simple linear nature of the color index functions, indices can be used in conjunction with the MSCC to provide rapid assessment and prediction of soil properties related to its color patterns.

**Nix color sensor (Nix)**

The Nix Color Sensor (Nix) (www.nixsensor.com) has not yet been used to determine hydric soil colors for wetland delineation purposes; however, the sensor has been deployed in a research endeavor that has recently yielded four relevant publications (Stiglitz et al. 2016a,b, 2017a,b). Though manufactured with interior design in mind, the Nix has shown its usefulness and relative accuracy within the food industry (Hodgen 2016; Holman et al. 2018, 2019; Holman and Hopkins 2019).

The diamond-shaped device has a 1.5 cm diameter aperture with a highly consistent light-emitting diode (LED) light source that can isolate samples from ambient light when surface contact is made. The Nix connects to both Android and Apple products using Bluetooth; immediate scan results can be saved and exported to obtain compiled sample color data that includes sample ID, time, and data for various color spaces (Figure 5); these include the CIE XYZ space of the International Commission on Illumination (CIE), where *Y* is luminance and *X* and *Z* are virtual components of the primary spectra; CIE L*a*b*, a rectangular-based space where *L** is luminosity and relates to CIE *Y* and Munsell *V*, and *a** and *b** relate to chromaticity akin to a red (+*a**) to green (-*a**) scale, and a blue (+*b**) to yellow (-*b**) scale; CIE L*c*h, which is similar to Munsell HVC as a cylindrical coordinate space with luminosity ($L^*$), chroma ($C^*$), and hue ($h$); RGB, a cube-shaped space consisting of additive mixtures of red ($R$), green ($G$), and blue ($B$); and CMYK, or the subtractive cyan ($C$), magenta ($M$), yellow ($Y$), and black ($K$) color percentages used in additive printing color spaces (Viscarra Rossel et al. 2006). Additional information regarding these color spaces is provided in Ibraheem et al. (2012). With homogenized soil samples, the Nix was comparable to and/or better than a more expensive colorimeter method (Stiglitz et al. 2016a). Further research may be necessary to elucidate the usefulness of the Nix in rapid determination and assessment of soil color and RMFs in wetlands.

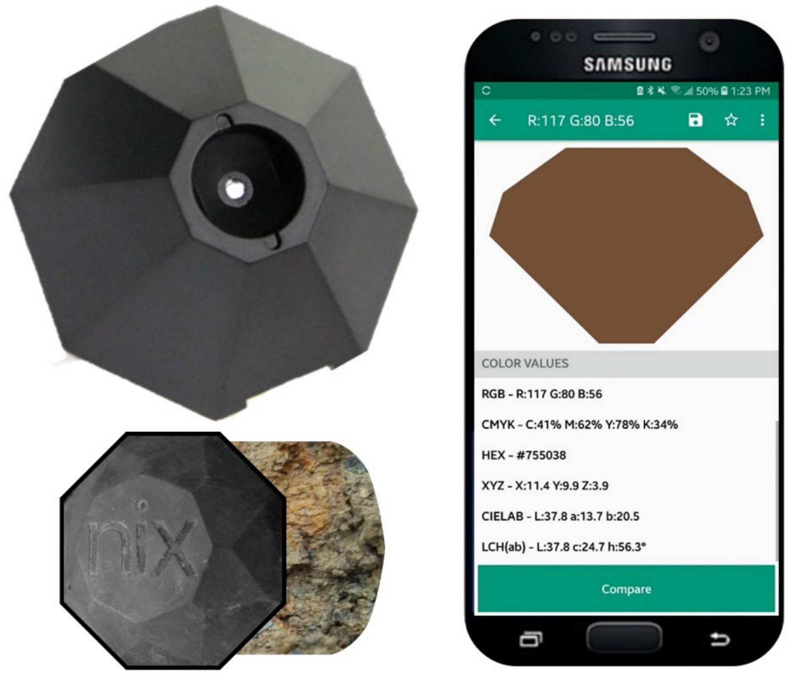


**Figure 5.** The Nix Color Sensor and Nix Pro app on a Samsung Galaxy smartphone, where the ~1.5 cm aperture on the bottom part of the device scans and records/displays the color of the surface underneath it (e.g., soil)

### Mobile phone camera (MPCs) and digital photography

Mobile smartphones have become ubiquitous in the past two decades, equipping users with internet-enabled computers that can double as calculators, cameras, and a variety of sensors that can record location and movement, weather conditions, and other data provided through a variety of software applications (Teacher et al. 2013). The structuring of environmental field education and/or research around mobile phone use has enhanced citizen science as well as academic research via improved efficiency, accessibility, and flexibility in the field and laboratory. Users can simultaneously record

GPS coordinates, audio, and notes; additionally, mobile phones can be programmed with algorithms to complete tasks such as image analysis (Aitkenhead et al. 2014). Mobile phone cameras (MPCs) serve as a particularly useful feature in environmental science monitoring and management. MPCs have greatly improved in quality over time; newer models such as the Apple iPhone 8 (www.apple.com/iphone) and Samsung Galaxy S8 (www.samsung.com/global/galaxy/) can compete with image quality from low- to medium-end through their high-quality lenses, sensors, and resolutions of up to 12 megapixels. MPCs provide color data via the RGB color model in which colors are formed as linear combinations of red, green, and blue. RGB outputs are device-dependent, such that hardware and software differences between mobile phones can result in different colors for identical RGB data (Ibraheem et al. 2012).

Five studies have relied on mobile phone cameras (MPCs) to study soil colors; however, none have focused specifically on hydric soils and RMFs (Gómez-Robledo et al. 2013; Moonrungsee et al. 2015; Han et al. 2016; Aitkenhead et al. 2016a; Fan et al. 2017). There is great potential for MPCs to accurately capture the signatures of hydric soil colors based on promising establishment of applications, procedures, analyses, and results by previous researchers studying non-hydric soils. Studies have focused on the reproducibility and accuracy of MPCs when compared to the MSCC using colorimeters, spectrophotometers, and spectroradiometers as measurers of objectively accurate data (Gómez-Robledo et al. 2013; Moritsuka et al. 2014; Han et al. 2016; Fan et al. 2017). Except for Aitkenhead et al. (2016a, 2016b), all studies measured soil color using MPCs in indoor laboratories to control camera stability, soil moisture, lighting conditions, soil particle sizes, soil surface smoothness, and focal length, i.e., distance between MPC and soil (Moonrungsee et al. 2015). Consistency in illumination intensity is known to significantly affect color read by MPCs; mobile phones have the tendency to overestimate soil darkness even under controlled light (Fan et al. 2017). The employment of dark rooms and standardized light sources as well as calibration cards such as reference white or gray color cards allow for the minimization of error and has rendered color measurements that agree with MSCC determinations (Gómez-Robledo et al. 2013; Moritsuka et al. 2014; Fan et al. 2017).

In the field, many conditions affecting image turnout such that brightness and shadowing cannot be systematically controlled in the same manner as they can in the lab. Aitkenhead et al. (2016a, 2016b) demonstrated the vastly different colors that can result within images taken of the same outdoor location under different lighting conditions. Nonetheless, efforts to ensure appropriate weather conditions, consistent angles of photographing, soil smoothness that does not smudge soil color, and the use of color correction cards can enhance reproducibility in the field (Viscarra Rossel et al. 2009; Aitkenhead et al. 2016b).

In the Wetland Ecology and Management graduate course at George Mason University, an educational field trip to explore hydric soil colors at a palustrine forested wetland at the Elizabeth Hartwell Mason Neck National Wildlife Refuge (Lorton, VA) highlighted the practicality of MPCs in aiding student understanding as well as elucidating visible patterns in wetland soils. Hummocks and hollows differed greatly in their soil properties as affected by their geomorphology, hydrologic regimes, and thus biogeochemical cycling (Ahn et al. 2009). Despite differences in MPC quality between students, visible color features were identifiable and qualitative comparisons could be made between the hummocks and hollow soils using pictures taken with MPCs (personal communication).

Two publications have relied non-MPC photography to identify wetland soil colors via the use of medium-end camera devices designed for capturing photographs. Although more common before the rise of MPCs, medium-end cameras are still useful for controlling and modifying lighting, aperture, shutter speed, image size, and photograph stability (O'Donnell et al. 2010). Usually more customizable and standardizable than mobile phone cameras, medium-end digital cameras can be successfully implemented to capture and identify RMFs in soil profiles. Work by O'Donnell et al. (2010) stands out as the best example of accurately describing hydric soil morphology through imagery. From images of in-tact soil cores, a 20 $cm^2$ area was randomly taken from each horizon, then classified as a) high value, b) low chroma, c) high chroma, d) matrix, and e) low value/chroma. Using an identical lighting environment for each image, they sought to standardize the delineation of RMFs when an adequate area of the soil profile was photographed and digitized (O'Donnell et al. 2010). Unlike spectroscopy, the procedure was capable of explicitly tracing colors to particular RMFs. More rigorous procedures could enhance soil color description by removing the subsampling schema and including an entire soil profile in image analysis. Unlike MPCs, medium-end photography and analyses have not been used to rapidly assess soil colors as procedures required lengthy set-up and analysis processes, the latter of which could not be done on the camera device itself; nonetheless, they offer improved accuracy and precision.

**Colorimetry and spectrophotometry**

Soon after the MSCC was released by the U.S. Soil Survey (Rice 1941) and incorporated into the soil classification system (Pendleton and Nickerson 1951), a more objective approach was sought after by scientists. Spectrophotometers were identified as color quantifiers in which soil color data could be obtained from an absorbance spectrum. As early as 1966, spectrophotometers were shown to be accurate soil color measurement instruments (Shields et al. 1966). Recently, more sophisticated instrumentation such as Vis–NIR spectroscopy have corroborated these results (Viscarra Rossel et al. 2009). Colorimeters record trichromatic data rather than parsing light into an absorption or reflectance spectrum like spectrophotometers; the Nix is a sort of handheld colorimeter. Most colorimeters and spectrophotometers allow for the conversion between color spaces, including CIE–L*a*b* as well as the Munsell HVC. Colorimeters often cost less than spectrometers, and more handheld, field-accessible colorimeters are on the market.

Eight studies of our review used either colorimeters or spectrophotometers to measure soil color in the field and/or the lab. Colorimeters and spectrophotometers have been most successful when soils are first homogenized (Rabenhorst and Parikh 2000), lack redoximorphic features (Campos and Demattê 2004; Gómez-Robledo et al. 2013; Moonrungsee et al. 2015; Stiglitz et al. 2016a), or when used to measure additional data beyond soil color—for example, chemical makeup of minerals (Aquino et al. 2016).

Spectrometry and colorimetry are proven to be reproducible and accurate methods of soil color determination (Moritsuka et al. 2014; Stiglitz et al. 2016a), but often require sample homogenization to reduce sensitivity to particle size (Han et al. 2016). Controlled laboratory experiments with soil samples using colorimetry can successfully determine soil particle colors in reduced environments to elucidate the propensity to form depleted matrices (Rabenhorst and Parikh 2000).

While most commonly used in the lab, colorimetry and spectrometry can be deployed in the field using handheld instruments which work similarly to their desktop counterparts. Viscarra Rossel et al. (2009) relied on a handheld spectrophotometer to measure absorption spectra of soils in various horizons; from the spectra, Munsell HVC were determined. As spectra and thus color determinations are affected by soil surface heterogeneity, the use of handheld colorimeters or spectrophotometers necessitates procedures to overcome surface heterogeneity while preserving in-situ soil properties such as RMFs (Viscarra Rossel et al. 2009).

**Strengths and weaknesses of each method**

***Munsell Soil Color Chart (MSCC).***

While the Munsell Color Space and accompanying chart provide a systematic approach to soil color, hence their reliability for hydric field indicators, scientists have identified several key shortcomings. First, the variability in manufacturing procedures, as well as the aging, of Munsell Soil color charts can render inconsistencies between two charts (Rabenhorst et al. 2015). Beyond charts themselves, environmental factors affect human perception of soil color and soil color chips. Natural lighting, affected by day of time and weather, plays a significant role in matching soil to color chips (Sánchez-Marañón et al. 2011). All color measurements—including hydric soil field identification—are to be done in sunny conditions, but such a standard cannot always be met when soil sites are visited on cloudy days or where canopy cover creates a shaded ground cover. Although field guides call for a measurement of soil color when soil is moist but not wet, differences in the moisture content of soil in the field cannot always be controlled and can lead to discrepancies in color interpretations, as moisture affects the way light is reflected off a surface. Overly wet or dry soils may be perceived to be a different color than the 'moist' soil prescribed to be sampled by USDA protocol (Torrent and Barrón 1993).

Arguably the largest shortcoming is the human dimension of current color determination conventions. In addition to psychological biases introduced when humans discriminate between colors, anatomical and physiological systems which process light—e.g., photoreceptors—are different between individuals, such distinct colors can be perceived from different people from a single light source (Webster and Mollon 1997; Neitz et al. 2002; Elliot 2015). Particularly relevant to identifying the color of redoximorphic features is the significant effect that backgrounds colors have on the perception of an object in focus (Werner and Walraven 1982). While NRCS scientists are specially trained to understand and denote soil color, it is likely that individuals would need to be personally trained to overcome consistent biases.

Even if the system of soil color determination through the MSCC could be perfected, it is nonetheless problematic for statistics. Creative transformations are necessary to form statistically based conclusions from a choice of 1500 discrete Munsell colors which are descriptive but nonetheless semiquantitative (Odeh and McBratney 2005; Viscarra Rossel et al. 2009; Kirillova et al. 2015). Color indices are successful in transforming MSCC color codes into meaningful indicator values that can represent waterlogging duration, soil drainage, and duration and frequency of saturation (Thompson and Bell 1996) (Thompson and Bell 1996).

***Nix Color Sensor (Nix).***

The Nix is a relatively new tool that has yet to be included in codified color determination procedures, which would require more research and deployment to formulate best practices related to soil color determination. Nonetheless, while the MSCC requires training to overcome personal biases, the Nix removes human perception, thus being more accessible to citizens and students who are not familiar with soil color and use of the MSCC. Data analysis is more accessible and efficient using the Nix than the MSCC. Although transformations of MSCC data have been created to transform qualitative and discrete data into continuous variables, the Nix stores colors in multiple color spaces on continuous scales including RGB, CIE–XYZ and L*a*b*, CMYK, and Munsell HVC (Nix Sensor Ltd. 2022). Information stored within data is less likely to be degraded in quality when transformations do not need to be conducted such that the multiple color spaces provided by the Nix are advantageous for statistical analysis

(Aitkenhead et al. 2016a). Overall, the Nix provides immediate and replicable results that can provide results comparable to the MSCC (Stiglitz et al. 2016a).

While MSCC measurements are dependent on light scattering related to soil surface texture, human vision can compensate for patterns of shadows such that soil surface heterogeneity is not detrimental to color determination. However, the Nix may be subject to measurement issues arising from soil surface heterogeneity and light scattering (personal observation); heterogeneous soil surface color determination needs to be further explored with this method. Additionally, RMFs of size smaller than the 1.5 cm diameter will likely be homogenized with surrounding soil color such that the Nix is unsuitable for accurate RMF identification and quantification when features are too small to cover the entire light source. The MSCC only requires that RMFs be detectable to the human eye such that they can span millimeters and still be measured.

***Mobile phone camera (MPC) and digital photography.***

The greatest strength of photography and associated analyses is the capacity to simultaneously analyze an entire soil profile, pedon, or horizon rather than subsampling to determine colors at specified locations. While the MSCC and Nix require to scan—either visually or with an instrument—a soil profile in a piecemeal fashion, one photograph can be taken to identify all colors present in a profile. Depending on the quality of the MPC or medium-end camera, close-up images are also possible to provide the same or better resolution provided by human eyesight and the Nix at close range.

Photography may not render efficient image analysis given the need for computer software and lengthy procedures (O'Donnell et al. 2010). However, MPC images can be immediately transferred to phone applications that can extract color data from a predetermined set of pixels in an image or an entire image (Han et al. 2016). Such extraction requires an understanding of MPC programming to produce an application that uses an appropriate algorithm and can store data sets for analysis. Unlike the Nix, MPCs provide colorimetric data in the RGB space, permutations of which do not fulfill all possible Munsell colors; however, when using digital images, the RGB space is more accessible and convenient than CIE L*a*b* (Ibraheem et al. 2012; Aitkenhead et al. 2016a). Programs and websites are available for free to convert RGB and CIE L*a*b* data to Munsell hue ($H$), value ($V$), and chroma ($C_M$) (HVC), such that color space conversions, though undesirable in terms of data integrity, can likely be solved (Moritsuka et al. 2014; Stiglitz et al. 2016a; Aitkenhead et al. 2016a). Several works have utilized self-produced transformation equations to support color space transformations, including non-linear transformations to convert CIE XYZ to and from Munsell HVC and CIE XYZ to and from RGB, as well as independent correlations between the three components of the Munsell chart to independent components of various color spaces including RGB and CIE L*a*b* (Viscarra Rossel et al. 2006). Additionally, polynomic process transformations can convert RGB values into Munsell HVC or CIE L*a*b* (Gómez-Robledo et al. 2013). Conversion tables and programs that have been used include the Munsell Conversion program and its associated data table which can transform Munsell HVC to CIE XYZ, L*a*b*, and RGB (Van Aken 2006); BabelColor

Gamut (www.babelcolor.com), which provides transformations from Munsell HVC to RGB; and Pipette software (www.sttmedia.com/pipette) which can convert RGB to CMYK (Stiglitz et al. 2016a).

Although the Nix and photography methods both remove subjectivity from the visual assessment required when using the MSCC, cameras do not have the ability to remove environmental variability, such as lighting conditions, that can be controlled using the Nix. However, the use of color correction cards as well as appropriate image analysis procedures (O’Donnell et al. 2010) can correct these weaknesses. Additionally, using standardized conditions and/or a color correction card, the preservation of profile colors through maintaining heterogeneous surfaces present in undisturbed soil cores can be photographed in such a way that image analysis can normalize color brightness, as well as shadows and/or highlights (O’Donnell et al. 2010).

***Colorimetry and spectrometry.***

When used in the field, handheld colorimeters and spectrophotometers can greatly aid rapid assessment of soil color with objectivity and reproducibility. However, out of all the methods assessed in this review, colorimeters and spectrophotometers are the least affordable (Table 6), usually costing over $1,000. Similar to the Nix, the instruments must make contact with the soil surface. Issues of soil heterogeneity affect their accuracy; measured soil spectra and/or tristimulus color data occur for a set area dependent on the instrument’s aperture such that soil features smaller than the aperture may be diluted (Barrett 2002), and measurement of soil color on an undisturbed soil ped will face issues of light scattering from uneven surfaces. Thus, almost all studies that utilized colorimeters and spectrophotometers did not use field-ready handheld instruments and instead measured soil color in the lab. Lab-based methods allow for soil particle homogenization through air drying, sieving, and grinding to < 2 mm or <50 μm which smooths soil surfaces, reduces noise from light scattering, and simplifies the complexity of soil heterogeneity (Gómez-Robledo et al. 2013; Moritsuka et al. 2014; Stiglitz et al. 2016a; Fan et al. 2017). Furthermore, lab methods allow for more controlled contact between smoothed sample surfaces and instrumentation, positively influencing reproducibility (Moritsuka et al. 2014). While reproducibility is higher in homogenized samples, heterogeneity is essential for identifying and quantifying RMFs in wetland soils. Thus, future research should focus on the capacity for field colorimetry and spectrometry to identify soil color on heterogeneous soil surfaces.

**Thoughts for wetlands soil applications**

Table 7 highlights the key takeaways for each comparable method discussed. For each variable of interest, each method was given a score from 1 to 3, with 3 being most desirable and 1 being least desirable. Given the largely objective nature, capacity to control external variables, and potential for rapid scanning of an entire soil pedon with 1) photography and 2) handheld colorimeters or spectrophotometers, the ratings for these two alternatives are the highest. However, as these are the most expensive options, a score with greater weight given to cost may lead to the Nix color sensor becoming the most desirable. Each method has strengths and weaknesses that should be considered to reflect the goal of a given study; for example, redox concentrations are likely to have non-uniform shapes and sizes such that the Nix color sensor, as well as handheld colorimeters, may be too large to accurately capture the feature's color, but may be appropriately used to identify low chroma soil matrix colors often found in consistently inundated wetland areas.

**Table 7.** Advantages and disadvantages of each soil color measurement method. On a scale from 1 to 3, higher scores indicate greater suitability for the respective factors

| Factor | Munsell Soil Color Chart | Nix Color Sensor | Mobile Phone Camera | Digital Photography | Handheld Colorimeter / Spectrometer |
|---|---|---|---|---|---|
| Cost Effectiveness | 3 | 3 | 3 | 2 | 1 |
| Reproducibility in variable lighting / texture | 1.5 | 2.5 | 2 | 2.5 | 2.5 |
| Outdoor Suitability | 3 | 2 | 2 | 1.5 | 2 |
| Speed of determination | 2 | 2.5 | 2.5 | 2 | 3 |
| Statistical Analysis | 1.5 | 3 | 2 | 2 | 3 |
| Calibration possible | 1 | 1 | 2 | 3 | 3 |
| Capacity to measure small features | 2.5 | 1.5 | 3 | 3 | 2 |
| Potential for RMF rapid assessment | 2 | 2 | 3 | 3 | 2.5 |
| Total Score | 16.5 | 17.5 | 19.5 | 19 | 19 |

Overall, the Nix sensor, MPCs, and digital photography were determined to be suitable replacements for the MSCC. Not only is subjectivity removed, but, given appropriate procedures such as color correction cards, issues with lighting can be handled. Nonetheless, the role of soil texture, shadows, and their effects on photography cannot be ignored. Although Fan et al. (2017) highlighted the effect of texture, or roughness, on light reflection, such soil properties are necessary to preserve when determining soil color of in-tact redoximorphic features. The most promising solution is the use of color correction cards and appropriate photographic angles to remove shadowing when relying on outdoor photography.

Many methods of color analysis, such as photographic processing, necessitate more time than is afforded in the field and require controlled environments. When rapid field assessment is desired for wetland identification procedures necessary for landowners, soil scientists, and wetland managers, such methods are thus inappropriate. While mobile phone cameras and the Nix may be suitable for rapid assessments, neither has been used to measure colors of redoximorphic features or hydric soils. Additionally, except for the work of O'Donnell et al. (2010) where soil peds were broken along structural voids before photographs were taken, studies have not maintained in-situ structural, textural, and color properties of soil when describing and quantifying RMFs using methods beyond the MSCC. For the use of alternatives that are easy-to-use, cost-effective, rapid, replicable and reproducible to the MSCC for identifying and quantifying hydric soil indicators in the field more studies and the documentation of their outcomes are necessary, further assessing each method's accountability for soil heterogeneity, roughness, size and irregularity of RMF shapes, and variable lighting conditions.

## **Conclusion**

We have reviewed methods that are easy-to-use, affordable, and field-friendly to study wetland soil colors and their patterns applicable to wetland delineation and ecological monitoring. Several low-cost methods of wetland soil color determination have been identified as tools which can complement the conventional use of the MSCC.

However, not all are suitable in the field, or require modifications to procedures such as color correction cards and/or post-field data correction to account for the effect of uncontrollable environmental variables. Considerations specific to a given study or purpose should be made to determine which method is most appropriate to use. Future research is warranted to further examine the efficiency and efficacy of MPCs, the Nix, medium-end digital photography, and handheld colorimeters and spectrophotometers to complement data achieved by the MSCC.

# CHAPTER FOUR:
# ANALYSIS OF SOIL COLOR VARIABLES AND THEIR RELATIONSHIPS BETWEEN TWO FIELD-BASED METHODS AND ITS POTENTIAL APPLICATION FOR WETLAND SOILS

## Introduction

Color's prominence in human observation of the environment has rendered soil color an accessible and readily apparent indicator of the structural and functional properties of soils. Soil colors are reflective of, and thus serve as indicators for, organic matter content, productivity, mineralogy, and hydrologic conditions, among others (Evans and Franzmeier 1988; Guertal and Hall 1990; Schwertmann 1993; Ketterings and Bigham 2000; Sánchez-Marañón et al. 2011; Ibáñez-Asensio et al. 2013; Moritsuka et al. 2014; Vepraskas 2015; Moonrungsee et al. 2015; Pretorius et al. 2017; Malone et al. 2018). Because of its link to such ecosystem attributes, soil color has been incorporated into assessments of ecosystem development: for example, the United States Department of Agriculture–Natural Resources Conservation Service (USDA–NRCS) standard for wetland delineation relies on identifying soil color to determine if soils are capable of supporting wetland ecosystems (Simonson 1989, 1993; Vepraskas et al. 2015).

The Munsell Soil Color Chart (MSCC) has become a key tool in using soil color as an indicator of past and present environmental conditions by providing a means of quantifying a categorically described attribute. While the physical basis of color is derived from quantitative attributes of light, humans struggle to evaluate and communicate perceived differences of multiple colors because its perception is categorical. By providing an ordered and quantitative system to color judgments, the MSCC has thus served an essential purpose in soil science since the 1930s (Kellogg 1987; Al-rasheed 2015). In particular, the chart standardizes color descriptions and allows for color comparisons by noting three qualities of color: hue ($H$), or spectral attribute of color consisting of red, yellow, green, blue, and purple; value ($V$), or color lightness; and chroma ($C_M$), or color purity (Munsell 1905). 440 color chips of discrete hue, value, and chroma combinations, designed to resonate with perceivable color differences, span over 13 hue pages in a common version of the chart (Torrent and Barrón 1993; Munsell Color 2009). The adoption of the MSCC revolutionized the field of soil science by providing a standardized method of color measurement while also opening investigations into soil color relationships with environmental factors (Genthner et al. 1998; Gupta et al. 2008).

Soil color's relationship to hydrology has been thoroughly investigated to the point where a subset of soils, called hydric soils, have been defined based on indicators related to soil morphology, many of which rely on color. Hydric soils are defined by unique colors and patterns related to iron/manganese reduction and oxidation because they have "formed under conditions of saturation, flooding, or ponding long enough during the growing season to develop anaerobic conditions in the upper part" (Federal Register 1994; USDA–NRCS 2018) . Reddish ferric iron ($Fe^{3+}$) oxides typical in terrestrial soils become reduced to $Fe^{2+}$, dissolved, and subsequently translocated within or (with enough time) below the soil profile when anaerobic conditions arise, leaving behind light and gray-colored soil grains (Schwertmann and Lentze 1966; Simonson and Boersma 1972; Richardson and Hole 1979; Schwertmann 1993; Simonson 1993). The USDA's Field Indicators of Hydric Soils in the United States includes 51 indicators that outline specific soil characteristics, primarily color patterns, which indicate historical or recent hydrological conditions that indicate the soil is in fact a hydric soil (USDA–NRCS 2018). While wetland delineation and monitoring incorporate hydrologic, vegetative, and soil aspects, soils are particularly informative: they can respond more swiftly than vegetation to changing hydrology, but also form lasting morphological features that indicate long-term conditions even after saturation, flooding, or ponding conditions disappear (He et al. 2003; Vepraskas et al. 2004; Vepraskas and Lindbo 2012).

Many hydric soil field indicators designate thresholds of $H$, $V$, and $C_M$ to discriminate between hydric and nonhydric soils. For example, over 10 indicators identify a soil as hydric based on the presence of iron and/or manganese depletions, defined as "bodies of low chroma (2 or less) having a value of 4 or more where Fe–Mn oxides have been stripped…"; identifying depletions thus requires both $C_M \leq 2$ and $V \geq 4$. Furthermore, almost all indicators require certain soil layers to "have a dominant chroma of 2 or less" (USDA–NRCS 2018). Field and laboratory studies have corroborated that anaerobic environments capable of supporting wetland ecosystems will produce low-chromas soils ($C_M \leq 2$) when initial iron concentrations are sufficient (Vepraskas 2015). In conjunction with the hydric soil field indicators, the MSCC thus serves as a bridge between human observations of color and the capacity to identify wetland soils.

The MSCC is not without its disadvantages; for decades, one of the foci within soil science has been researching alternative methods of soil color determination that can complement or supersede the MSCC. Color readings using the MSCC are based on human judgment, and the MSCC requires training and practice to increase accuracy and diminish user-based variability in color determinations. Thus, while laypeople unfamiliar with the MSCC may be able to perceive soil colors, they cannot easily utilize the MSCC for accurate rapid soil color determination. Additionally, MSCC color readings are affected by manufacturing variability and aging, lighting conditions affected by time of day and weather, MSCC aging over time, and anatomical and psychological differences between individuals perceiving colors (Brainard et al. 2001; Sánchez-Marañón et al. 2011; Rabenhorst et al. 2015).

Given these shortcomings, a subset of soil studies concerned with soil color have focused on field alternatives to the MSCC, including handheld colorimetry (Shields et al. 1966; Torrent and Barrón 1993; Campos and Demattê 2004; Viscarra Rossel et al. 2009; Summers et al. 2011; Jones and McBratney 2016), and digital photography using medium- to high-end cameras and mobile phone cameras (Viscarra Rossel et al. 2008; O'Donnell et al. 2010; Gómez-Robledo et al. 2013; Moonrungsee et al. 2015; Han et al. 2016; Aitkenhead et al. 2016a; Fan et al. 2017). While most alternatives are not field-based, app-based color measurement instruments like the Nix Color Sensor (Nix) may provide a means of field-based color determination that is resistant to the human judgment and subjective aspects of MSCC readings. The Nix uses a highly consistent pre-calibrated LED light to scan a surface, which is isolated from ambient light by the sensor's diamond shape and 1.5 cm diameter aperture (Schmidt and Ahn 2019). When a surface is scanned, colors are automatically measured, transmitted to a Bluetooth-linked smartphone app, and stored. In contrast to the MSCC, the Nix offer a promising avenue of rapidly identifying soil colors without requiring experience and familiarization or additional data recording. It has been successfully deployed in nonhydric soil color determination and education endeavors; promising findings of its accuracy encourage further investigation into its utility for hydric soil identification (Stiglitz et al. 2016a,b, 2017a,b; Mikhailova et al. 2017).

The goal of this study was to better understand how the Nix can complement and/or act as a substitute for the MSCC in observing soil color. We investigated if the Nix can identify hydric soils, as identified by hydric field indicators reliant on the MSCC, for the purpose of wetland delineation. We observed and analyzed soil colors in forested ecosystems with mapped hydric soils in Northern Virginia using both the MSCC and Nix. The main objectives were: (1) to create a methodology to characterize color variables used by the Nix and compare them with those of the MSCC; (2) to assess correlations between MSCC and Nix variables for soil colors in order to identify the most suitable Nix variable(s) to represent each of the three commonly observed Munsell variables ($H$, $V$, and $C_M$); (3) to investigate the explanatory power of each Nix variable for respective MSCC variables through regression; and (4) to better understand if the Nix can aid in discriminating between hydric and nonhydric soil colors as identified through use of the MSCC.

## Materials and Methods

### Site description

The study was conducted at four wetland sites within Northern Virginia, all located in the Chesapeake Bay Watershed: Mason Neck Wildlife Refuge (MN) in Fairfax County, Julie J. Metz – Neabsco Creek Wetland Bank (JJM) in Prince William County, and Banshee Reeks Nature Preserve (BR) and Algonkian Regional Park (ARP) in Loudoun County (Figure 2).

Both MN and JJM sites fall within the Coastal Plain physiographic province of Northern Virginia. The four study plots at MN (38° 38' 28" N, 77° 9' 54" W) belong to a hardwood forest and palustrine forested wetland with rolling microtopography consisting of high points (hummocks) and low points (hollows) adjacent to a riverine freshwater marsh. Hydrologic inputs originate primarily from precipitation. Hollow locations are composed of the hydric Gunston silt loam and experience occasional to frequent standing or flowing water, depending on seasonal weather patterns (Ahn et al. 2009). Hummock locations, mapped as the nonhydric Matapeake silt loam and Mattapex loam, are conversely rarely to never ponded or flooded (USDA–NRCS Soil Survey Staff 2020). Adjacent to Neabsco Creek near the Potomac River, JJM (38° 36' 25" N, 77° 16' 34" W) is the first created mitigation wetland in the nation and contains both tidal and nontidal sections. Monitoring up to 20 years after its creation in 1994 confirmed the presence of wetland hydrologic conditions per the Army Corps of Engineers wetland delineation manual (Environmental Laboratory 1987; Wetland Studies and Solutions Inc. 2020). Several plots are flooded year-round, whereas others experience frequent to occasional surface saturation. Soils at JJM plots are mapped as hydric and include the very poorly drained Featherstone mucky silty loam and the Hatboro–Codorus complex (USDA–NRCS Soil Survey Staff 2020). Plots receive water inputs from a range of hydrologic sources such as tidal freshwater, groundwater recharge, precipitation, and stream surface flow.

BR (39° 1' 48" N, 77° 35' 46" W) and ARP (39° 3' 25" N, 77° 21' 50" W) fall within the Piedmont physiographic province. BR plots experience occasional to frequent flooding or ponding, and have been mapped to contain both the hydric Albano silt loam as well as the nonhydric Codorus and Manassas silt loams (Fuller 2007; USDA–NRCS Soil Survey Staff 2020). Plots have dynamic hydrologic characteristics: some regions of the preserve are primarily influenced by groundwater connection with subsurface flow from Goose Creek, while others primarily receive inputs from precipitation and surface runoff near small tributaries of Goose Creek (Paul 2017). Finally, ARP plots along the Sanctuary Trail occur within riparian forests, freshwater forested wetlands, and at the fringes of a freshwater emergent wetland. Mapped soil series include the Rowland silt loam on floodplains and Lindside silt loam on terraces; while neither is classified as hydric, vegetative and hydrologic scouting before sampling began indicated a propensity of flooding and/or ponding at plots to support wetland vegetation (USDA–NRCS Soil Survey Staff 2020). Water inputs include overland flow from the Potomac River, overland flow and groundwater connection with nearby emergent wetlands, and precipitation. Water tables range from 0 cm near emergent habitat and reach 60 cm within forested floodplains (U.S. Fish and Wildlife Service 2010).

**Soil collection**

Per site, 4 to 5 randomly selected plots (each 1 m x 1 m) were visited in March-April, June–July, and August–September of 2018 and 2019 for soil sampling. A 10-cm diameter auger (AMS) was used for soil profiling; while augering cannot provide an in-tact and undisturbed core from sampling, it provides an adequate sample size for identifying present redoximorphic features in a relatively short time period without large plot disturbance, allowing it to be scaled to both professional and nonprofessional soil investigations (O'Donnell et al. 2011).

After removing surface debris, soil was collected from each plot. Given variability in plots' soil textures, moisture, and compactness, a variable amount of soil ranging from 10 to 30 cm in depth was removed at a time and laid on a white sheet to reflect in-situ soil horizonation. Concurrent measurement of soil depth was conducted, and every 5 to 10 cm interval was noted to establish depth markers. While peds were naturally separated during transfer from the auger to the sheet, care was taken to maintain in-situ ordering. After all 60 cm of soil had been sampled and transferred, color recordings began.

Only interior colors were examined as to avoid including smudged colors in the readings. Starting at the top of the profile, each ped was broken in half. For each ped, the two halves were inspected for interior colors, and colors were recorded using both the MSCC and the Nix at each site visit. When scanning matrix colors, relatively flat surface areas of the peds were chosen for Nix scanning to reduce sources of error. After colors were recorded, each half was iteratively broken along structural voids to form smaller peds. At each stage of the process, newly exposed interior soils were visually scanned for new colors; when new colors were identified, MSCC and Nix colors were recorded. This process was repeated to a ped diameter of roughly 3–5 cm. Color readings did not go past the 3–5 cm diameter ped size for either the MSCC or Nix because of the size of the aperture of the Nix (~1.5 cm): as the Nix requires a planar surface to ensure the edges surrounding its aperture are tightly touching the surface of color recording, smaller fractions (e.g., diameter <3–5 cm) risk the introduction of uneven interior and edge surfaces which would introduce error into the measurements. Per initial ped, this required about 3 to 5 steps of halving.

This process was repeated for all peds down to 60 cm; however, for peds of the same horizon with visible equivalences in interior matrix and RMF colors, MSCC and Nix color recording were not repeated. When possible, surfaces were smoothed using pressure to create an even surface for measuring color with the Nix; this was not always possible when physical pressure affected the visibility of the color. The identification and recording of each color took one to two minutes for the MSCC, and one minute or less for the Nix.

**Determination of soil colors**

For each identified color, 18 measured (M) variables were collected: 3 from the MSCC ($H$, $V$, and $C_M$), and 15 from the Nix ($L$, $a$, $b$, $C$, $h$, $X$, $Y$, $Z$, $R$, $G$, $B$, $C_K$, $M_K$, $Y_K$, and $K_K$). Per color, the three variables from the Munsell color space ($H$, $V$, and $C_M$) and the 15 variables from the Nix were measured and recorded (Table 8). Procedures for MSCC use were followed, such as reading soil colors from the chart in daylight and with moist soil samples. While specific "gley" or bluish gray or greenish gray colors with low chroma ($C_M \leq 2$) and high value ($V \geq 4$) are common to wetland soils and were observed, they were not included in the analysis given their coincidence with high soil moisture that, in the context of the data set, reduced replicability and reproducibility.

As hue is an alphanumeric variable (e.g., "10YR"; Figure 6) a numeric variable *H#* was recorded as a quasi-equivalent expression to aid in statistical analyses. *H#* was recorded by denoting hues with negative values equal to numerical distances from 10R if redder than 10R (5R and 7.5R), and with positive values equal to numerical distances from 10R if yellower than red (2.5YR to 5Y). Thus, *H#* = -5 for 5R and 15 for 5Y (Kirillova et al. 2015). All further discussion of MSCC variables used in statistical analyses relies on the "measured" (M), or directly measured, variables *H#* (as a proxy for *H*), *V*, and $C_M$.

The Nix was concurrently used to measure all identified colors with exception to those unable to fit within the Nix aperture (e.g., color feature diameters < 1.5 cm). Measurements were made in triplicate by moving the sensor to three areas of a perceptually uniformly colored soil fraction. To record and store colors, the Nix was connected to a smartphone running the Nix Pro Color Sensor app, which automatically recorded and stored scanned colors alongside timestamps and typed descriptors. The use of the Nix and resulting color measurement results on the smartphone app and CSV file (Figure 6). Each color measurement made by the Nix is automatically represented as 15 measured variables from five color spaces: (1) The International Commission on Illumination (CIE) L*a*b*, or CIE–Lab; (2) CIE L*C*h or CIE–LCh, which shares the variable $L^*$ with the CIE–Lab space; (3) CIE–XYZ; (4) the RGB model (including color spaces RGB, sRGB, and Lin.sRGB) commonly used with digital displays; and (5) CMYK (Table 8). Each space is named according to the variables which define colors in said space; for example, a color defined in the LCh space is represented as a three-dimensional vector composed of an $L^*$ dimension, a $C^*$ dimension, and an $h$ dimension, respectively. For the purposes of this study, only the first RGB space data was utilized from the RGB color model; furthermore, asterisks for CIE color spaces L*a*b* and L*C*h are omitted, and variables are referred to as $L$, $a$, $b$, $C$, and $h$. More information on the genesis and applicability of these color spaces is outlined in Viscarra Rossel et al. (2006).

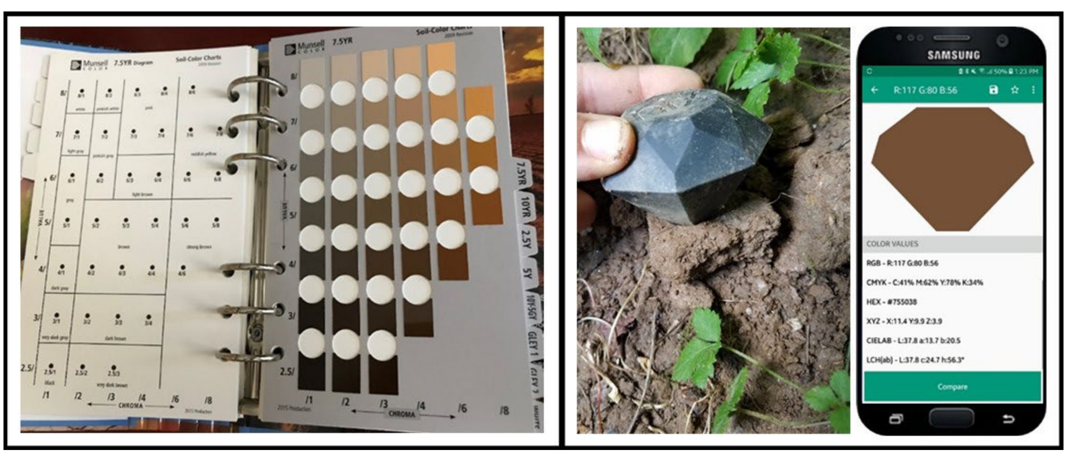


**Figure 6.** Demonstration of color measurements in the field using the Munsell Soil Color Chart (MSCC; left) and the Nix paired with the smartphone app (right)

**Table 8**. Summary of all measured and calculated color (space) variables obtained using the Munsell Soil Color Chart (MSCC) and Nix

| Measured or Calculated [b] | Instrument | Color Space | Description | Variable Name [Study Label] | Variable Description (where applicable) | Range for common soil colors |
|---|---|---|---|---|---|---|
| **Measured** | Munsell Soil Color Chart (MSCC) | Munsell | Perceptually linear color space with 24 hues and discrete, independent luminance / chroma variables | Hue [H] [a] | Spectral attribute of color (e.g., yellow, red); MSCC is composed of 9 hue pages:<br>red: 5R, 7.5R, 10R (most red)<br>yellow-red: 2.5YR, 5YR, 7.5YR, 10YR<br>yellow: 2.5Y, 5Y (most yellow) | 5R – 10Y |
| | | | | (Numeric) Hue [H#] | Linear ranking of MSCC hues, where 10R=0. Each 2.5-unit increase in H equates to a 2.5-step increase (yellower) from 0<br><br>10R = 0; 2.5YR = 2.5; 5YR = 5; 7.5YR =7.5; 10YR = 10; 2.5Y = 12.5; 5Y = 15 | 2.5 – 15 (5Y) |
| | | | | Value [V] | Lightness of color (0=black, 10=white) | 0 – 8 |
| | | | | Chroma [$C_M$] | Intensity or purity of color (0=achromatic) | 0 – 8 |
| | Nix Color Sensor (Nix) | CIE Lab [d] | Device-independent color space with separate luminance/chroma variables | L* [L] | Lightness | 0 – 100 |
| | | | | a* [a] | Chromaticity, where -: green; +: red | Hue dependent |
| | | | | b* [b] | Chromaticity, where - : blue; + : yellow | Hue dependent |
| | | CIE XYZ | Device-independent color space with virtual components X and Z | X | Virtual and nonnegative mix of shorter- and higher- wavelength light; orthogonal to Y | Hue dependent or 0 – 15 |
| | | | | Y | Luminance | Hue dependent |
| | | | | Z | Shorter-wavelength light (corresponds to blue) | Hue dependent |
| | | CIE LCh [c, d] | Device-independent color space which separates luminance / chroma | L* [L] | Lightness | 0 – 100 |
| | | | | C* [C] | Chroma | 0 – 100 |
| | | | | h* [h] | Hue | 0° – 360° |

| Measured or Calculated [b] | Instrument | Color Space | Description | Variable Name | Variable Description (where applicable) | Range for common soil colors |
|---|---|---|---|---|---|---|
| **Measured** | Nix Color Sensor (Nix) | RGB, sRGB, Lin.sRGB | Additive and device-dependent cube-shaped space | R | Red | 0 – 255 |
| | | | | G | Green | 0 – 255 |
| | | | | B | Blue | 0 – 255 |
| | | CMYK | Subtractive space used for printing | C [$C_K$] | Cyan | 0 – 100% |
| | | | | M [$M_K$] | Magenta | 0 – 100% |
| | | | | Y [$Y_K$] | Yellow | 0 – 100% |
| | | | | K [$K_K$] | Black | 0 – 100% |
| **Calculated** | | CIE XYZ | Device-independent color space with virtual components X and Z | X / (X+Y+Z) [$\hat{x}$] | Proportion of X in X+Y+Z | 0 – 1 |
| | | | | Y / (X+Y+Z) [$\hat{y}$] | Proportion of Y in X+Y+Z | 0 – 1 |
| | | | | Z / (X+Y+Z) [$\hat{z}$] | Proportion of Z in X+Y+Z | 0 – 1 |
| | | RGB, sRGB, Lin.sRGB | Additive and device-dependent cube-shaped color space | (2G – R – B)/4 [$H_{RGB}$] | Linearly independent combinations of RGB variables from linearly dependent R, G, and B (Viscarra Rossel et al. 2006) | -25 – 25 |
| | | | | (R + G + B)/3 [$I_{RGB}$] | | 30 – 200 |
| | | | | (R – B)/2 [$S_{RGB}$] | | 0 – 80 |
| | | CMYK | Subtractive space used for printing | $C_K – Y_K$ [Co] | Linearly independent combinations of CMYK variables from linearly dependent $C_K$, $M_K$, $Y_K$ and $K_K$ (Malvar et al. 2008) | -1 – 0 |
| | | | | $Y_K + (C_K - Y_K)/2$ [Cg] | | 0.50 – 0.75 |
| | | | | $1–(2M_K+Y_K+C_K)/4$ [Ym] | | 0.25 – 0.75 |

[a] H is an inherent variable of the MSCC but is not included in statistical analyses or variable counts mentioned in results and discussion

[b] Measured variables were directly measured using the prescribed method (MSCC or Nix); calculated variables required arithmetical operations (addition, subtraction, multiplication, and/or division) to combine multiple variables belonging to a single color space into one variable

[c] While total number of measured variables from the Nix sums to 16 from this table, L is a part of CIE–Lab and CIE–LCh color spaces; thus there are 15 measured Nix variables

[d] The asterisks that follow the alphabetical notations of the CIE variables L*, a*, b*, C*, and h* are inherent aspects of the variable names and are not additions relevant to a footnote

## Formulation of calculated variables

Calculated (C) variables were identified as a relatively rapid and accessible method for arithmetically manipulating measured MSCC and Nix variables to increase the potential likelihood for moderate to strong relationships to surface between the two methods. A list of calculated variables to consider was produced from color science literature indicating the formulation of color-relevant variables from measured color space variables. For Nix color variables, calculations were based in literature recommendations on (1) the de-correlation of linearly dependent color variables and the reduction of color space dimensions; and (2) the basis of absent color spaces non-identical but linked to the color spaces provided by the Nix. In all cases, measured variables from one color space were used as the basis of derivation for each new variable.

## Processing of soil color data

For the set of measured (n = 18) and final calculated variables (n provided in Results), descriptive and normality statistics were conducted on all variables using Microsoft® Excel 2013 to better understand variable distribution. Next, a stepwise investigation of variable relationships was conducted via Spearman correlation analysis to yield a final list of one Nix variable most capable of relating to MSCC variables representative of $H$, $V$, and $C_M$. The analysis contained two key procedures: the identification of strong Spearman correlation coefficients (ρ) for MSCC−Nix variable pairs, and the removal of variables with high intra-method (MSCC−MSCC or Nix−Nix) correlations, i.e., collinearity, from further consideration.

Correlation coefficients were studied between the set of all measured and calculated MSCC variables and (1) all measured Nix variables plus (2) final calculated Nix variables. Generally, 0.70 is accepted as a threshold separating moderately strong from strong relationships (Mukaka 2012; Dancey and Reidy 2017; Akoglu 2018); thus, strong correlations, i.e., those with $|\rho| \geq 0.70$, were flagged for further analysis. If the threshold was not met by at least one Nix variable for either $H$, $V$, or $C_M$ variables, the threshold was lowered in steps of 0.05 until at least one Nix variable met the threshold. Strong ($|\rho| \geq 0.70$) correlations with $V$ and $C_M$ variables, and modest ($|\rho| \geq 0.50$) correlations with $H$ variables, were subsequently flagged. Nix and MSCC variables showing zero strong or modest correlations with variables of the opposing method (i.e., MSCC and Nix, respectively) were removed.

Intra-method variable redundancy was identified by flagging very strong MSCC−MSCC and Nix−Nix correlations ($|\rho| \geq 0.90$), i.e., collinear pairs (Mukaka 2012; Schober et al. 2018). Where one collinear variable was more strongly correlated with variables of the opposing method ($|\Delta\rho| > 0.02$), all other collinear variables were removed. Where collinearity was found between variables that shared similar correlation coefficients with variables of the opposing method ($|\Delta\rho| \leq 0.02$), the following ordered criteria were used to give preference to: (1) measured over calculated variables; (2) variables commonly used in the literature (e.g., $L$ for $V$) (Torrent and Barrón 1993; Yang et al. 2001; Viscarra Rossel et al. 2006; Mahyar et al. 2010; Marqués-Mateu et al. 2015; Moonrungsee et al. 2015); and (3) visual goodness of fit of scatterplots when plotted against the most highly correlated variable of the opposing method. A similar set of criteria were subsequently used to eliminate all but one Nix variable per $H$, $V$, and $C_M$ variables—i.e., yielding three variable pairs. Maximal |ρ| was used as the single criterion to choose between variable pairs for a given MSCC variable when $|\Delta\rho| > 0.02$. Where $|\Delta\rho| \leq 0.02$, one MSCC−Nix variable pair was chosen with preference using the three criteria.

For final MSCC−Nix variable pairs, simple linear regressions were conducted to identify explanatory or predictive power of each Nix variable with respect to its MSCC pair using $R^2$ statistics (at $p < 0.01$). Regression models with $R^2 \geq 0.50$ were assessed to be adequate, as this threshold is common for appropriately identifying predictor variables that outweigh other noncontrolled variables or sources of error (Sanyal et al. 2017). For regression models that were deemed inadequate (i.e., $R^2 < 0.50$), the dataset was split by physiographic province (Coastal Plain [MN, JJM] versus Piedmont [BR, ARP]) to identify if more control over soil physiography—e.g., where Coastal Plain sites are sandier and less iron-rich—would improve predictive power.

Additionally, colors were separated into two sets: one with colors that, after MSCC readings, satisfied a necessary condition of any hydric soil field indicator (e.g., depleted matrix colors; prominent concentration colors; gley colors; n = 162) and those not indicative of hydric soils (e.g., faint concentration colors; non-depleted or reduced matrices; n = 57) (USDA–NRCS 2018). Using these datasets, descriptive statistics and 2-sample t-tests were conducted on $V$ and $C_M$, plus final Nix variables related to $V$ and $C_M$ (total n = 4), to compare colors related to hydric soils ("hydric") versus colors not related to hydric soils ("nonhydric").

## Results

### Describing measured variables for MSCC and Nix

#### *Measured MSCC variables.*

The MSCC contains 9 hue pages most commonly used by MSCC users representing quarter-steps of Munsell hues red (R), yellow–red (YR), and yellow (Y), and are ordered from 5R (most red) to 5Y (most yellow). Each page includes up to 40 color chips with discrete values for $V$ (vertical axis) and $C_M$ (horizontal axis) each ranging from 0 up to 8 depending on hue (Table 8). Higher $V$ corresponds to lighter colors; higher $C_M$ corresponds to purer colors (Figure 4; Figure 6). $C_M$ and $V$ are discrete variables denoted as whole numbers (0, 1, 2, 3, … , 8). Half-step judgments are possible, but not easily judged, between each unit (Table 8).

#### *Measured Nix variables.*

The color spaces included in the Nix app represent common color spaces and variables used across color science and color-related subdisciplines. While some Nix variables are meaningless in terms of perceptual attributes of color such as hue or saturation (e.g., the virtual $X$ from the XYZ color space), most variables are related to properties of hue, value, and/or chroma (Table 8). $L$ (CIE–Lab and CIE–LCh) corresponds to lightness like MSCC $V$, with lower numbers representing darker colors. The Lab variables $a$ and $b$ provide spectrums of green ($-a$) to red ($+a$) and yellow ($-b$) to blue ($+b$), respectively. The LCh space is similar to the Munsell space, with variable meanings for $L$, $C$, and $h$ directly linking to those of their MSCC counterparts $V$, $C_M$, and $H$, respectively. CMYK and RGB color spaces have variables related to specific hues—cyan, magenta, yellow, and black for CMYK, and red, green, and blue for RGB. For each of these color spaces, all variables encompass a quality of lightness and are not linearly independent. For example, in the RGB (red, green, and blue) color space, a unit-increase for each variable relates to an overall lightening of color, as the red, green, and blue components "add" to increase lightness. The opposite is true of the subtractive CMYK (cyan, magenta, yellow, and black) color space.

**Calculation of variables to increase MSCC–Nix variable pairs**

The method of identifying calculated variables relevant for relating Nix and MSCC measurements led to an expansion of measured (M) variables (MSCC: n = 3; Nix: n = 15) to include an additional 9 calculated (C) variables (MSCC: n = 0; Nix: n = 9), yielding 27 total variables (Table 8).

For the MSCC, three calculated variables were considered for analysis—(1) angular hue, or $H°$, which represents hues as angles on a circular color wheel; (2) $sinH°$; and (3) $cosH°$. However, zero were deemed useful for this study's application. Because angular hue ($H°$) was defined with 5R set equal to 0° (Sánchez-Marañón et al. 2011; Ruck and Brown 2015), it shared a direct linear relationship with $H\#$ and added no value to the study. Additionally, while $sinH°$ and $cosH°$ could have benefited our research aims, they were redundant: the dataset only included hue calculations for $H\#$ that, when transformed to $H°$, fell within quadrant one (i.e., yielding monotonic changes to both *cosH°* and *sinH°*, respectively). Indexing *H#* and *H°* differently and independently (e.g., 5R = 0 for *H#* but 10R = 0° for *H°*) was deemed unnecessary and nonproductive due to the absence of colors with hues redder than 2.5YR (e.g., 10R, 7.5R, …; n = 0). For soils of Northern Virginia which are not often redder than 5YR, it was determined that derivations of MSCC variables are simply not necessary to augment the color information provided by MSCC.

With respect to $V$ and $C_M$, zero calculated variables were deemed suitable for relating Nix-measured colors to MSCC-measured colors. While other calculations exist in the literature, transformations that characterize soil color patterns instead of color (e.g., redoximorphic features) or combine variables into multivariable expressions do not serve the need of linking Nix color variables to the MSCC color aspects hue, value, and chroma. Thus, arithmetic operations including more than one of $H$, $V$ and $C_M$ or relating to color patterns instead of colors were deemed unsuitable (Evans and Franzmeier 1988; Thompson and Bell 1996; Jien et al. 2004).

In contrast to the MSCC, calculated variables (C) derived from the Nix measured variables were deemed useful to color relationship studies between the Nix and the MSCC. RGB and CMYK include dependent variables; thus, linearly independent variables from the RGB and CMYK color space were calculated from transformations delineated by Malvar et al. (2008). The derived variables provide a simple algebraic transformation of $R$, $G$, and $B$ and $C_K$, $M_K$, $Y_K$, and $K_K$, respectively, and have been shown to be useful in color science (Viscarra Rossel et al. 2006; Malvar et al. 2008). Calculations to normalize the XYZ color space and create variables used in the CIE–xyY color space, not included in Nix measurements, were also made (Viscarra Rossel et al. 2006).

This approach led to the inclusion of 9 calculated variables for the Nix: (1–3) $\hat{x}$, or $X/(X+Y+Z)$; $\hat{y}$, or $Y/(X+Y+Z)$; and $\hat{z}$, or $Z/(X+Y+Z)$ from the XYZ color space; (4–6) $H_{RGB}$, or $[(2G) - R - B)] \cdot 4^{-1}$ ; $I_{RGB}$, or $(R+G+B) \cdot 3^{-1}$; and $S_{RGB}$, or $(R - B) \cdot 2^{-1}$ from the RGB color space; and (7– 9) $Co$, or $C_K - Y_K$; $Cg$, or $Y_K + [(C_K - Y_K) \cdot 2^{-1}]$ ; and $Ym$, or $1 - [(2M_K + Y_K + C_K) \cdot 4^{-1}]$ from the CMYK color space. The XYZ color space variables provide chromaticity coordinates between 0 and 1 and provide a means of including the CIE Yxy color space in the analysis. While $Z/(X+Y+Z)$ is usually ignored in color sciences due to its linear dependence with $X/(X+Y+Z)$ and $Y/(X+Y+Z)$, it is included here as not all normalized variables were to be used in concert.

**Describing observed colors through MSCC and Nix variables**

Descriptive statistics for all measured (n = 3) MSCC variables indicate *H#* ranged from 2.5 (= 2.5R) to 15 (= 5Y) with a mean of 8.4, or 8.4YR; this most closely mirrors the MSCC hue page 7.5YR, with *H#* = 7.5 (Table 9). *V* ranged from 2 to 7 with a mean of 4.3 ± 0.1, and $C_M$ ranged from 1 to 6 with a mean of 3.1 ± 0.1. Measured variables *V* and $C_M$ were nonnormal per the Shapiro test for normality ($p < 0.001$).

Descriptive and normality statistics for all measured (n = 15) and calculated (n = 9) Nix variables indicate that *L* and *R* were the only measured variables to display normal distributions per the Shapiro test ($p > 0.05$; Table 9). Additionally, *X* and *Y* from the XYZ color space were almost identically distributed with similar means, medians, ranges, and skewness and kurtosis. From $R$, $G$, and $B$, $B$ displayed the lowest range and did not surpass 99 out of a possible 355. At the $\alpha = 0.10$ level, all calculated variables were significantly nonnormal. $H_{RGB}$ and $Co$ were primarily negative whereas $I_{RGB}$, $S_{RGB}$, $Cg$, and $Ym$ consisted exclusively of positive values.

**Table 9.** Descriptive statistics for all measured and calculated variables from the MSCC and Nix for soil colors among the study's four sites

| Variable Type | Color Space | Variable | Shapiro Normality [a] | Median | Mean ± SE | Kurtosis | Skewness | Range | (Min, Max) |
|---|---|---|---|---|---|---|---|---|---|
| **Measured** | MSCC | H# | <0.001 | 7.5 | 8.4 ± 0.2 | -0.328 | -0.083 | 12.5 | (2.5, 15) |
| | | V | <0.001 | 4 | 4.3 ± 0.1 | -0.363 | -0.074 | 5.0 | (2, 7) |
| | | $C_M$ | <0.001 | 3 | 3.1 ± 0.1 | -0.327 | 0.154 | 5.0 | (1, 6) |
| | Nix – Lab | L | **0.113** † | 36.7 | 37.6 ± 0.7 | -0.271 | -0.016 | 47.4 | (13.2, 60.5) |
| | | a | 0.010 * | 7.9 | 7.9 ± 0.2 | -0.787 | 0.205 | 12.7 | (1.9, 14.6) |
| | | b | 0.006 | 16.0 | 16.8 ± 0.4 | -0.830 | 0.223 | 22.4 | (5.4, 27.8) |
| | Nix – LCh | C | *0.002* | 18.4 | 18.7 ± 0.4 | -1.062 | 0.022 | 23.5 | (6.2, 29.7) |
| | | h | <0.001 | 65.3 | 64.9 ± 0.5 | -1.206 | 0.202 | 24.3 | (54.6, 78.9) |
| | Nix – XYZ | X | <0.001 | 10.3 | 11.5 ± 0.4 | 0.335 | 0.782 | 28.0 | (1.7, 29.6) |
| | | Y | <0.001 | 9.4 | 10.8 ± 0.4 | 0.469 | 0.875 | 27.1 | (1.6, 28.7) |
| | | Z | <0.001 | 4.2 | 4.9 ± 0.2 | 0.029 | 0.787 | 11.0 | (0.9, 12.0) |
| | Nix – RGB | R | **0.629** † | 108 | 107.8 ± 1.9 | -0.330 | -0.039 | 131 | (40, 171) |
| | | G | 0.006 | 81 | 83.9 ± 1.6 | -0.296 | 0.243 | 108 | (32, 140) |
| | | B | 0.009 | 60 | 61.9 ± 1.2 | -0.431 | 0.168 | 73 | (26, 99) |
| | Nix – CMYK | $C_K$ | <0.001 | 0.47 | 0.47 ± 0.06 | -0.552 | 0.132 | 0.32 | (0.32, 0.64) |
| | | $M_K$ | <0.001 | 0.60 | 0.58 ± 0.06 | -0.170 | -0.829 | 0.27 | (0.41, 0.67) |
| | | $Y_K$ | 0.002 | 0.74 | 0.73 ± 0.04 | 0.724 | -0.536 | 0.23 | (0.60, 0.83) |
| | | $K_K$ | 0.005 | 0.36 | 0.35 ± 0.14 | -0.280 | 0.339 | 0.70 | (0.06, 0.76) |
| **Calculated** | Nix – XYZ | $\hat{x}$ | 0.045 * | 0.405 | 0.423 ± 0.001 | -0.075 | -0.229 | 0.086 | (0.377, 0.462) |
| | | $\hat{y}$ | 0.008 | 0.467 | 0.396 ± 0.001 | -0.449 | 0.320 | 0.036 | (0.381, 0.416) |
| | | $\hat{z}$ | 0.001 | 0.178 | 0.181 ± 0.002 | -0.217 | 0.465 | 0.105 | (0.135, 0.240) |
| | Nix – RGB | $H_{RGB}$ | <0.001 | -0.25 | -0.50 ± 0.12 | -0.798 | 0.154 | 6.75 | (-3.50, 3.25) |
| | | $I_{RGB}$ | **0.082** + | 82.7 | 84.5 ± 1.45 | -0.322 | 0.064 | 103 | (32.7, 136.0) |
| | | $S_{RGB}$ | <0.001 | 22.5 | 22.9 ± 0.5 | -1.034 | 0.062 | 31.5 | (7.0, 38.5) |
| | Nix – CMYK | Co | 0.003 | -0.266 | -0.267 ± 0.006 | -0.777 | 0.234 | 0.340 | (-0.410, -0.070) |
| | | Cg | <0.001 | 0.599 | 0.599 ± 0.003 | 0.268 | -0.124 | 0.170 | (0.505, 0.675) |
| | | Ym | <0.001 | 0.403 | 0.413 ± 0.003 | 0.035 | -0.697 | 0.210 | (0.333, 0.543) |

[a] Shapiro normality refers to the p-value obtained from the Shapiro test for normality. A statistically significant p value ($p < 0.01$) indicates a non-normal distribution
† Not significant ($p > 0.10$)
+ Significant at $0.05 < p < 0.10$
* Significant at $0.01 < p < 0.05$

## Correlation

***Pre-screening results: MSCC–Nix variable correlations.***

An assessment of Spearman correlations between MSCC variables (n = 3) and measured Nix variables (n = 15) highlighted that Nix variables $a$, $Z$, $B$, $C_K$, $M_K$, and $Y_K$ failed to hold strong ($V$, $C_M$) or modest ($H$) correlations with MSCC variables (Table 10). These variables were thus removed from further analysis. *H#* was modestly correlated with $h$ only ($|\rho| = 0.53$; $p < 0.001$). $V$ was strongly positively correlated with $L$, $X$, $Y$, and $G$ ($\rho = 0.73$) and strongly negatively correlated with $K_K$ ($\rho = -0.73$); $V$ also showed strong correlation with $R$ ($\rho = 0.72$) ($p < 0.001$). $C_M$ was strongly correlated with $b$ ($\rho = 0.76$) and $C$ ($\rho = 0.77$) ($p < 0.001$).

**Table 10.** Spearman correlation matrix for all measured color variables from the MSCC and Nix

| Nix Color Sensor – Measured (n = 15) | Munsell Soil Color Chart – Measured (n = 3) | | |
|---|---|---|---|
| | ***H#*** | ***V*** | ***$C_M$*** |
| ***L*** | 0.31 | **0.73** [a] | 0.39 |
| ***a*** | -0.24 | 0.15 | 0.60 |
| ***b*** | 0.20 | 0.61 | **0.76** [a] |
| ***C*** | 0.12 | 0.56 | **0.77** [a] |
| ***h*** | *0.54* [b] | 0.44 | -0.08 |
| ***X*** | 0.29 | **0.73** [a] | 0.43 |
| ***Y*** | 0.31 | **0.73** [a] | 0.39 |
| ***Z*** | 0.32 | 0.66 | 0.18 |
| ***R*** | 0.25 | **0.72** [a] | 0.49 |
| ***G*** | 0.33 | **0.73** [a] | 0.34 |
| ***B*** | 0.32 | 0.63 | 0.12 |
| ***$C_K$*** | -0.13 | -0.62 | -0.67 |
| ***$M_K$*** | -0.47 | -0.63 | -0.13 |
| ***$Y_K$*** | -0.11 | -0.06 | 0.53 |
| ***$K_K$*** | -0.31 | **-0.73** [a] | -0.37 |

*Note.* All correlations with $|\rho| \geq 0.21$ are significant at $p < 0.001$
[a] $|\rho| \geq 0.70$
[b] $|\rho| \geq 0.50$ (only highlighted for MSCC H#)

Several variable sets displayed high intra-method (MSCC–MSCC or Nix–Nix) correlations: (1) *L*, *X*, *Y*, *Z*, *R*, *G*, *B*, and $K_K$ and (2) *C* and *b*. The collinearity criteria outlined in the methods were used to remove Nix variables *X*, *Y*, *R*, *G*, $K_K$ from further analysis. In conjunction with Nix variables removed for failing to hold strong (*V*, $C_M$) or modest ($H$) correlations with Nix variables, Nix variables $L$, $C$, and $h$ remained for further analysis, and remaining correlation pairs were $V$ and $L$; $C_M$ and $C$; and $H\#$ and $h$.

Between all MSCC variables (n = 3) and calculated Nix variables (n = 9), $\hat{z}$, $H_{RGB}$, $I_{RGB}$, and $Co$ displayed strong ($V$, $C_M$) or modest ($H$) correlations with MSCC variables; $\hat{x}$, $\hat{y}$, $S_{RGB}$, $Cg$, and $Ym$ were only weakly ($H$) or moderately ($V$, $C_M$) correlated with MSCC variables and were thus removed from further analysis (Table 11). $H_{RGB}$ was modestly correlated with $H\#$ ($\rho = 0.56$). V was not more strongly correlated with calculated Nix variables than measured Nix variables; the maximum coefficient was $\rho = 0.72$ between $V$ and $I_{RGB}$ ($p < 0.001$). $C_M$ showed strong correlations with $\hat{z}$ ($\rho = -0.80$), $Co$ ($\rho = -0.80$) and $S_{RGB}$ ($\rho = 0.74$) ($p < 0.001$). No pairs of Nix calculated variables were highly collinear ($|\rho| < 0.90$). Given the remaining four calculated Nix variables, strong ($V$, $C_M$) and modest ($H$) correlation pairs were $V$ and $I_{RGB}$; $C_M$ and $\hat{z}$; $C_M$ and $S_{RGB}$; $C_M$ and $Co$; and $H\#$ paired with $H_{RGB}$.

**Table 11.** Spearman correlation matrix between measured MSCC variables and calculated variables from the Nix

| Nix Color Sensor – Calculated (n = 9) | Munsell Soil Color Chart – Measured (n = 3) | | |
|---|---|---|---|
| | ***H#*** | ***V*** | ***$C_M$*** |
| ***$\hat{x}$*** | -0.18 | 0.14 | 0.69 |
| ***$\hat{y}$*** | 0.42 | 0.53 | 0.69 |
| ***$\hat{z}$*** | -0.01 | -0.35 | **-0.80** [a] |
| ***$H_{RGB}$*** | *0.56* [b] | 0.41 | -0.05 |
| ***$I_{RGB}$*** | 0.30 | **0.72** [a] | 0.36 |
| ***$S_{RGB}$*** | 0.12 | 0.57 | **0.74** [a] |
| ***Co*** | -0.06 | -0.47 | **-0.80** [a] |
| ***Cg*** | -0.20 | -0.62 | -0.30 |
| ***Ym*** | 0.36 | 0.68 | 0.21 |

*Note.* All correlations with $|\rho| \geq 0.21$ are significant at $p < 0.001$
[a] $|\rho| \geq 0.70$
[b] $|\rho| \geq 0.50$ (only highlighted for MSCC H#)

### *Choosing final variables.*

From the remaining MSCC–Nix variable pairs for *H*, selection criteria were employed to choose between *H#–h* and *H#–$H_{RGB}$*. After comparing the scatterplots of similarly correlated pairs *H#–$H_{RGB}$* and *H#–h* ($|\Delta\rho| \leq 0.02$; Tables 10 and 11), $H_{RGB}$ was chosen as the most suitable variable for relating to MSCC *H*. Next, to choose between *V–L* and *V–$I_{RGB}$* ($|\Delta\rho| \leq 0.02$; Tables 10 and 11), *L* was chosen over $I_{RGB}$ due to being a measured versus calculated variable as well as its prevalence in soil and color science literature. Finally, for $C_M$ correlations with *b*, *C*, $\hat{z}$, *Cg*, and *Co*, $C_M$–$\hat{z}$ and $C_M$–*Co* were most strongly correlated than the other pairs ($|\Delta\rho| > 0.02$). Scatter was similar between $C_M$ vs. $\hat{z}$ and $C_M$ vs. *Co* plots. Ultimately, $\hat{z}$ was selected due to the relationship between $\hat{z}$

and the pre-established CIE–xyY (or $\hat{x}\hat{y}$Y using our notation), a color space discussed in color science literature where $\hat{z} = 1 - (\hat{x} + \hat{y})$ (Viscarra Rossel et al. 2006).

In summary, three MSCC–Nix variable pairs were ultimately chosen to allow MSCC measurements to be complemented with the Nix: *H#* and $H_{RGB}$ ($\rho = 0.56$); *V* and *L* ($\rho = 0.73$); and $C_M$ and $\hat{z}$ ($\rho = -0.80$) ($p < 0.001$).

**Quantification of relationships between MSCC and Nix**

Regression analysis indicated that variable pairs *H#* and $H_{RGB}$, *V* and *L*, and $C_M$ and $\hat{z}$ can be defined through linear relationships in which 26% of variation in *H#* can be explained by $H_{RGB}$ calculations; 54% of variation in *V* can be explained by *L* measurements; and 62% of variation in $C_M$ can be explained by $\hat{z}$ calculations (Figure 7; $p < 0.01$ for all).

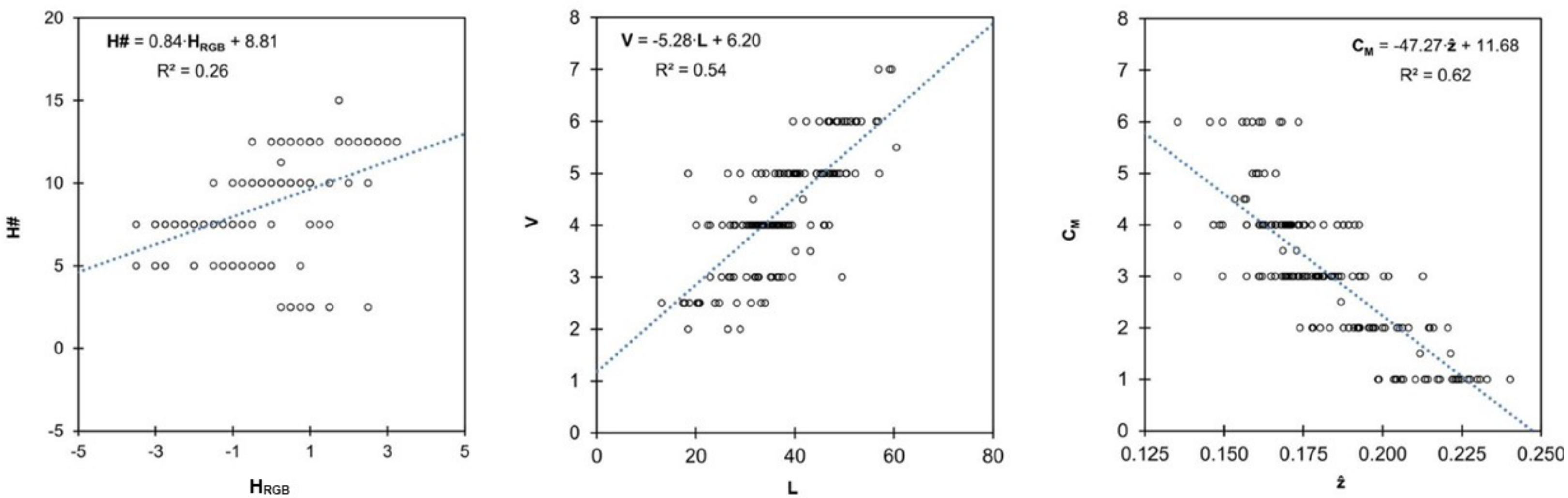


**Figure 7.** Scatterplots including regression model trendlines and $R^2$ coefficients for final Nix–MSCC variable pairs

The regression between $H\#$ and $H_{RGB}$ is weak; residuals are not randomly distributed, and a pattern is evident where low $H\#$ values (H# $\leq 5$) have the largest residuals and tend to share a distinct relationship with $H_{RGB}$ when compared to the pattern for $H\# \geq 5$ (Figure 7). When separated by physiographic province, regression results between $H_{RGB}$ and $H\#$ did not improve ($R^2 = 0.07$ for Coastal Plain sites, $p > 0.01$; $R^2 = 0.33$ for Piedmont sites, $p < 0.01$). The regression between $V$ and $L$ indicates a moderately strong linear relationship with more pronounced scatter for more frequently observed values like 3 through 5, but the model tended to overestimate $V$ for low (< 3) values, and underestimate $V$ for high (> 6) values. Finally, the regression model for $C_M$ versus $\hat{z}$ highlights a moderately strong negative linear relationship. Residuals are generally negative for $C_M < 3$ and positive for $C_M \geq 4$; in particular, the model underestimates observed $C_M$ for all observations above $C_M = 4$.

In summary, $H\#$ and $H_{RGB}$ ranged from 2.5 to 15 and -3.5 to 3.25, respectively, with medians of 7.5 (7.5YR) for $H\#$ and -0.25 for $H_{RGB}$. Mean $H\#$ (8.4YR) falls between 7.5YR and 10YR but is best approximated by the hue page 7.5YR. $V$ and $L$ ranged from 2 to 7 ($V$) and 13.2 to 60.5 ($L$), with medians of 4 and 36.7, respectively. Finally, $C_M$ and $\hat{z}$ ranged from 0 to 6 and 0.172 to 0.240 with medians of 4 ($C_M$) and 0.179 ($\hat{z}$) (Table 12).

**Table 12.** Summary statistics for final variables of the Munsell Soil Color Chart (MSCC) and Nix for wetland soil color reading

| Soil Color Attribute | Munsell Variable | (Min., Max.) | Median | Mean ± SE | 95% Confidence Interval | **ρ / $R^2$** | Nix variable | (Min., Max.) | Median | Mean ± SE | 95% Confidence Interval |
|---|---|---|---|---|---|---|---|---|---|---|---|
| **Hue** [a] | *H#* | (2.5, 15) | 7.5 | 8.4 ± 0.2 | (7.8, 8.8), | 0.56<br>0.26 | $H_{RGB}$ | (-3.5, 3.25) | -0.25 | -0.50 ± 0.12 | (-0.73, -0.27) |
| | *H* | (2.5YR, 5Y) | 7.5YR | ~7.5YR [b] | (7.8YR, 8.8YR) | | | | | | |
| **Value** | *V* | (2, 7) | 4 | 4.3 ± 0.1 | (4.2, 4.5) | 0.73<br>0.54 | *L* | (13.2, 60.5) | 36.7 | 37.6 ± 9.5 | (36.1, 38.9) |
| **Chroma** | $C_M$ | (1, 6) | 3 | 3.1 ± 0.1 | (2.8, 3.4) | -0.80<br>0.62 | $\hat{z}$ | (0.135, 0.240) | 0.178 | 0.181 ± 0.001 | (0.177, 0.185) |
| **Set of colors used to identify hydric soils** | Nonhydric *V* | (2, 7) | 4 | 4.1 ± 1.1 | (4.0, 4.3) | | *L* | (13.2, 60.5) | 36.7 | 37.6 ± 0.8 | (36.1, 39.1) |
| | Hydric | (4, 6) | 5 | 4.6 ± 0.9 | (4.4, 4.8) | | | (27.5, 52.8) | 36.7 | 39.4 ± 1.0 | (37.4, 41.4) |
| | Nonhydric $C_M$ * | (1, 6) | 4 | 3.3 ± 1.2 | (3.1, 3.5) | | $\hat{z}$ * | (0.135, 0.231) | 0.171 | 0.174 ± 0.001 | (0.171, 0.176) |
| | Hydric | (1, 2) | 1 | 1.3 ± 0.5 | (1.1, 1.4) | | | (0.172, 0.240) | 0.202 | 0.204 ± 0.002 | (0.200, 0.209) |

[a] Represented as both *H#* and Munsell *H*

[b] Mean *H#* of 8.4 is the most comparable to the MSCC hue page 7.5YR

[*] $p < 0.05$ for the 2-sample t-test

Table 12 also indicates statistics for colors that aided in identifying hydric soils and those that did not; t-distribution confidence intervals highlight that statistically significant differences in $C_M$ and $\hat{z}$ occurred between colors involved in hydric soil identification and all other colors ($p < 0.05$). However, $L$ did not differ between hydric versus nonhydric groups ($p > 0.05$).

## Discussion

### MSCC and Nix variables

The 15 variables recorded by the Nix provide a broader set of variables and meanings to describe soil color beyond the MSCC. The color spaces supplied through the Nix are not relatable to MSCC variables through well-defined mathematical equations, but certain color spaces have been constructed in such a way—and thoroughly researched with respect to the MSCC—to render them relevant to our study's objective. For example, Lab and LCh were specifically created to relate to human perception of color (e.g., hue, lightness or tone, and chroma or saturation) similar to the MSCC; additionally, the transformation from MSCC to CIE–XYZ, followed by a transformation to CIE–Lab or CIE–LCh, has been studied extensively, making CIE variables attractive for MSCC color space conversions (Torrent and Barrón 1993; Viscarra Rossel et al. 2006, 2008; Mahyar et al. 2010; Moonrungsee et al. 2015; Fan et al. 2017; Kirillova et al. 2018). While RGB and CMYK variables are device-dependent and not directly related to human perception of color qualities like the MSCC, they have been the focus of previous soils research

(Gómez-Robledo et al. 2013; Moonrungsee et al. 2015; Stiglitz et al. 2016a), and their inclusion in our statistical analysis improved chances of identifying strong inter-space correlations. Because each Nix instrument is calibrated before consumer use with guaranteed high inter-instrument agreement, the device dependence of $H_{RGB}$, selected as the variable most representative of hue, was not deemed an issue for this study. Furthermore, CMYK was chosen as the color space for analysis in a previous study relating the Nix to MSCC soil color measurements, giving precedence to the suitability of such spaces in soil science (Stiglitz et al. 2016a).

**Correlation between soil color variables**

The correlation analysis produced promising albeit not affirmative correlations between the Nix and MSCC methods of soil color determination. Intuitively understood Nix variables—for example, $L$, $C$, and $h$—proved most useful for relating Nix colors to MSCC value, but not chroma or hue (Table 10). While $V$ was best correlated with $L$, $C_M$ was more strongly correlated with calculated variables like $\hat{z}$ than with measured chroma-related variables like $C$.

The correlation results were not optimal for several reasons. First, the relatively weak correlation coefficients between all Nix variables and MSCC variables—in particular, $H\#$—was unexpected. Research has identified that the mathematical relationship between $H$ and $h$ is more complex than would be expected from their shared meaning (Simon and Frost 1987). Beyond differences associated with complex color theory, this relatively weak result may be attributable to the relatively low number of MSCC hue pages (and thus values for *H#*). The introduction of multiple subdivisions between hue pages within the MSCC could provide a higher correlation between MSCC and Nix hue determinations, but would not aid in allowing the Nix to complement conventional color descriptions. Incorporating more complicated calculations such as a redness index, which includes a quotient with cubed variables, may have allowed nonredundant relationships to surface and subsequently may have augmented correlation strengths with h, but would also hinder the goal of this study to find accessible and relatively simple Nix variables to use as proxies for MSCC variables (Viscarra Rossel et al. 2006; Sánchez-Marañón et al. 2011; Kirillova et al. 2015).

A one-to-one transformation between Nix and MSCC color measurements was not achievable from this sample data, but the strong correlation between $C_M$ and $\hat{z}$ highlights a utility of the XYZ color space for relating Nix measurements to the MSCC. It was expected that $L$ and $V$ would have a strong correlation closer to 0.90, demonstrated in past laboratory studies ($r > 0.90$) (Viscarra Rossel et al. 2006); however, the field focus in this study greatly affected the potential to obtain such high correlations. In relating observed MSCC colors to recorded Nix colors, Stiglitz et al. (2016a) found "moderately strong" correlations between MSCC and $M_K$, $Y_K$, and $K_K$ of the CMYK color space, where correlation coefficients were 0.51, 0.59, and 0.58 in moist soils, respectively. Our study thus contributes to the literature the finding that, while MSCC and Nix colors may be moderately strongly correlated, there exists a high degree of variation among MSCC observations in the field that cannot be explained by Nix measurements. Stiglitz et al. (2016a) converted Munsell readings to CMYK; therefore, it is not possible to tell if the variance for each MSCC reading for $V$ and $C_M$ mirrored that found in this study. Another study used a model to predict MSCC observations from Nix measurements and found that predictions differed by 0.5 to 3 units in $V$ and 0 to 3 units in $C_M$ (Mancini et al. 2020). Most relevant to using the Nix for hydric soil identification, Mancini et al. (2020) observed that low-chroma colors identified using the MSCC were correctly estimated by the Nix. Their results generally show potential for using the Nix for color measurements when a model has first been calibrated and validated in relating Nix to MSCC. Thus, simple measurements of soil color using both the Nix and MSCC would benefit from models that are calibrated using Nix measurements of MSCC chips.

Within our study, deviations from strong correlations ($|\rho| \geq 0.80$) may be explained by an inability to control for surface texture and soil moisture in the field. These are variables that are always controlled under laboratory settings when high correlations have been determined between MSCC readings and other device readings, and a history of strong evidence exists that indicates they influence both perceived and objective soil color determinations (Torrent and Barrón 1993; Moonrungsee et al. 2015; Fan et al. 2017; Malone et al. 2018). Nonetheless, these are properties of soil that cannot always be controlled in the field; one recommendation for future studies using the Nix in the field would be to moisten soils enough to be able to form a flat smooth surface upon which the Nix can be placed when doing color measurements and avoiding soil saturated beyond a certain extent. However, as soil colors can become homogenized when rubbed, such a protocol may risk a loss of in-situ soil colors. Because high soil moisture is likely to be encountered when investigating wetland soil colors, further study is necessary to quantify the relationship between the hydrologic conditions of sites and their soil colors to build a much stronger and universal relationship for many different types of soils over a large geographic extent.

**Relationships between Nix and MSCC variables**

Overall, the high collinearity identified within each method makes a strong case for relying on univariate regression instead of using a multi-dimensional approach that requires multiple Nix variables to explain each MSCC variable. Nonetheless, while the regression analysis highlights that $V$ and $C_M$ can be explained by Nix variables to a modest degree identified as adequate by this study's standards ($R^2 \geq 0.50$), large spread and nonrandom residuals indicate that MSCC readings may not be dependably estimated from Nix variables using our regression models (Figure 7).

Particularly for the weak $H\#-H_{RGB}$ regression model ($R^2 = 0.26$), large ranges in Nix measurements for a given discrete MSCC measurement (e.g., $H_{RGB} = 0.5$) suggest inadequate control over sources of error using the Nix. Controlling for physiographic province reduced predictive power of the regression models, with high standard errors in Nix measurements for each discrete $H\#$ despite similar ranges; this indicates that measuring soils with similar texture characteristics may not be sufficient to reduce error.

Instead, increasing the predictive power of MSCC−Nix regression models should focus on the standardization of methods after sampling soils and before measuring color—e.g., controlling for soil moisture, surface roughness, lighting conditions when using the MSCC.

Stiglitz et al. (2016a) highlighted the strong capacity for the Nix to detect color changes due to moisture, which suggests that the Nix measurements may be more sensitive than human-dependent MSCC judgments concerning color changes due to moisture. Furthermore, light scattering is known to depend on surface roughness or evenness, and this relationship can extend to micro-scale roughness within the Nix aperture that affects color determinations (Wu et al. 2009). Finally, while standard operating procedures for MSCC use advise users to take measures to limit misinterpretations due to lighting conditions, field operations—particularly in forested wetlands—are not necessarily able to work around time of day or micro-habitat lighting conditions that are affected by canopy cover and may affect MSCC judgments (Turk and Young 2020). While lab-based studies can better control moisture content, surface evenness, and lighting-dependent judgments of soil color, steps can nonetheless be taken in the field to minimize the error due to these issues. For example, higher priority should be placed on creating a smooth surface for each soil ped using a knife while minimizing the mixing of colors present on the soil surface. Additionally, when using both methods of color determination, taking Nix measurements before MSCC measurements, or ensuring that each soil ped is re-wetted before utilizing the opposing method, may reduce changes in soil moisture that affect objective and perceived soil color. Further study should focus specifically focus on how to control these issues without manipulating in-situ soil colors through reducing roughness and without overcomplicating the efficiency that the Nix can offer to the process.

Regression models between MSCC variables and $H_{RGB}$, $L$, and $\hat{z}$ may also improve through increasing the sample size and diversity of measured colors, as the observations of this study were comprised of only 53 unique combinations of ($H$, $V$, $C_M$) common to the Virginia Piedmont and Coastal Plain. For example, very few soils with colors redder than 5YR were identified at our field sites. If the medians of $H_{RGB}$ are examined for each discrete $H\#$ in Figure 7, it appears that the more commonly observed colors—i.e., $H\# = 5$ (5YR), 7.5 (7.5YR), 10 (10YR), and 12.5 (2.5Y) – follow a slightly different trend with a steeper slope than identified using the regression equation; this is the result of $H_{RGB}$ values for $H\# = 2.5$ ($H$ = 2.5YR) plotting considerably higher than would be expected from the perceivable $H\#$–$H_{RGB}$ relationship for yellower hues (higher $H\#$). More measurements for soils with hues of 2.5YR and redder may be necessary to determine if our data accurately depict an inability for the Nix to follow a predictable trend in soil redness past a certain threshold.

The scatterplots of Figure 7 also indicate large spread and nonrandom residuals for the $C_M$–$\hat{z}$ model despite the pair's high correlation coefficient. For $C_M = 1$, outliers appear to be decreasing the explanatory power of the line of best fit; for $C_M > 5$, the onset of a nonlinear trend produces systematically positive residuals (Figure 7). The results of the regression may be improved by creating a regression modeled from the median and interquartile range associated with each discrete chroma rather than using the entire dataset; for example, obtaining $\hat{z} < 0.175$ would be indicative of $C_M > 2$ with a higher degree of certainty. The nonlinear relationship for $C_M > 5$ may suggest a nonlinear relationship even with improved quality control and method standardization, warranting further study.

Overall, the discrete nature of *H#*, *V*, and $C_M$ complicate regression interpretation even with normal residuals: MSCC versus Nix scatterplots are unlikely to be either onto or one-to-one, with a spectrum of Nix variable measurements mapped to a single MSCC variable measurement, and multiple MSCC measurements mapped to a single Nix variable measurement. Therefore, using the Nix as a color determination tool is more likely to provide range estimates of MSCC variables instead of point estimates. However, point estimates can still be useful and can be improved through regression analyses with reduced variances and randomly distributed residuals.

**Utility of methodology for soil science and education**

Our analysis does not support the notion that the Nix can be depended upon by professionals to identify soil colors, including wetland soil colors, without greater method standardization and quality control. An important aspect of color determination in assisting hydric field indicators is the capacity to discriminate between chromas of 2 or less and chromas greater than 2, but large overlap occurred for $\hat{z}$ between these two sets such that professionals characterizing soil color would not be able to discern the hydric nature of a soil if $\hat{z}$ fell within this range of overlap (e.g., 0.175 to 0.225).

Nonetheless, the methodology of identifying relationships between Nix and MSCC variables was able to identify moderately strong to strong correlations that suggest a focus on characterizing Nix variables is relevant to its application to soil science and education. Certain Nix measured and calculated variables can be linked to the aspects of color from the MSCC—hue, value, and chroma—in a generalized way through identifying trends in increasing/decreasing Nix variables as a signal of higher or lower numbers for MSCC variables, or extrema in Nix variable ranges highlighting extrema in MSCC variable ranges. For example, citizen science education endeavors using the Nix in Northern Virginia could identify light (high value) and dull (low chroma) colors indicative of redox depletions by finding Nix $L$ to be greater than ~50 and $\hat{z}$ to be greater than ~0.22 (Table 12), and highlight the high probability that colors do not meet the hydric soil thresholds for depletions if $L$ and $\hat{z}$ do not fall in these ranges. Such an approach would augment the shortcomings of using the MSCC—requiring familiarity for proper judgment, influenced by sunlight and moisture, and requiring sometimes time-consuming judgments—and provide an accessible, relatively fast method of exploring soil colors.

Furthermore, the Nix has the capacity to be used cautiously in assisting MSCC measurements and identifying hydric soils in less technical and more education-focused endeavors when users are more familiar with alternative color spaces like CIE–Lab, RGB, or CMYK. While variables like $H_{RGB}$ and $\hat{z}$ may be unfamiliar to users, their introduction into soil science and education could yield a new pathway of characterizing and parametrizing soil colors that ultimately appear less like algebraic calculations and more like intuitive indicators of color. With future efforts focused on improving the breadth of colors measured using both measurement devices and removing sources of error by working to standardize surface texture, moisture, and other confounding variables met during field work, the shortcomings highlighted in this study can be addressed with promising applications.

## Conclusions

This study shows that Nix variables can be characterized and quantitatively related to MSCC variables to a modest or strong degree. The correlation and regression analyses of the two field methods for soil color measurement indicate that MSCC $H$, $V$, and $C_M$ variables of soil colors, commonly observed and reported for wetland delineation, can be represented from modest ($H$), moderately strong ($V$), and strong ($C_M$) relationships with Nix variables $H_{RGB}$, $L$, and $\hat{z}$, respectively. With over 35% of variation in each MSCC variable left unexplained by matching Nix variables, field use of the Nix by professionals cannot yet be supported using the methods of this study; nonetheless, correlations between MSCC $V$ and $C_M$ and Nix variables indicate a promising role of the Nix in characterizing soil colors with further refinement following similar calculations and statistical analyses presented herein. More fine-tuning is necessary to properly harness what the Nix can offer, and future endeavors should determine if a standardization of field methods can render the Nix able to measure color accurately and reliably as related to MSCC measurements.

# CHAPTER FIVE:
# PREDICTING FOREST WETLAND SOIL CARBON USING QUANTITATIVE COLOR SENSOR MEASUREMENTS IN THE REGION OF NORTHERN VIRGINIA, USA

## Introduction

Estimated to hold over 2300 Gt C in its top 3 meters, soil is one of the largest carbon reservoirs on Earth (Schlesinger 1990; Jobbágy and Jackson 2000; Köchy et al. 2015). Efforts to minimize soil carbon losses and augment soil carbon sequestration have assumed a prominent role in natural climate solutions, given the key role that soil organic carbon (SOC) dynamics play in regulating atmospheric greenhouse gases (Guo and Gifford 2002; Sahoo et al. 2019; Bossio et al. 2020). Wetlands have received particular attention for their carbon storage potential due to high rates primary productivity paired with anaerobic biogeochemical settings that slow decomposition of organic matter (Mitsch and Gosselink 2015; Villa and Mitsch 2015). Some wetland types, such as subarctic peatlands with thawing permafrost, tend to act as carbon sources rather than sinks (Johansson et al. 2006); conversely, wetlands with mineral soils, including forested palustrine wetlands, can serve as promising carbon sinks due to a seasonal or intermittent reduction of the soil environment that slows decomposition of recalcitrant soil organic matter (SOM), encourages high productivity, and minimizes methane emission potential (Whiting and Chanton 2001; Chimner and Ewel 2005; Bridgham et al. 2006; Bernal and

Mitsch 2013; Villa and Mitsch 2015; Villa and Bernal 2018). In areas with natural forested wetland cover, their conservation and restoration have thus become attractive strategies to counter greenhouse gases emissions through augmented soil carbon sequestration (Bae and Ryu 2015; Pulighe et al. 2016; Säynäjoki et al. 2018; Xue et al. 2019; Virginia Department of Environmental Quality 2019).

Measuring SOC within the top 30 cm of forested wetland soils where carbon concentrations and fluxes are highest can be useful for drafting climate adaptation strategies, for which preliminary assessments and sustained monitoring of carbon storage potentials and fluxes are essential (Yu et al. 2012; Nahlik and Fennessy 2016; Lees et al. 2018). Furthermore, estimates of SOC can aid wetland ecosystem health and development assessments through the connection between SOC and root development, water retention and infiltration rates, cation exchange and buffering capacity, and reduction–oxidation reactions with nitrate-nitrite and iron/manganese (Bishel-Machung et al. 1996; Ahn and Jones 2013). Therefore, measuring SOC over time can provide critical information to watershed planners, managers, and scientists. Because current estimates of SOC commonly rely on laboratory analyses that are unavailable at the time of field observations and require great expense, labor, and time (Post et al. 2001; Rawlins et al. 2008; Meersmans et al. 2009; Roper et al. 2019), various methodology-focused studies have sought to link SOC to more rapid and/or accessible field- or laboratory-based measurements.

Soil color has emerged as a strong predictor of SOC and soil total carbon (TC) contents (Wills et al. 2007; Pretorius et al. 2017; Stiglitz et al. 2017a), with researchers first linking soil darkness to SOM as early as the 1920s (Brown and O'Neal 1923). Using A.H. Munsell's Munsell Soil Color Chart (MSCC) that standardizes perceived colors via observations of *hue*, *value*, and *chroma* (Munsell 1905), color variables—most notably value and chroma—have been shown to be strong predictors of SOC (Konen et al. 2003; Wills et al. 2007; Pretorius et al. 2017). The MSCC is nonetheless imperfect for rapid field-based determinations and SOC predictions, as it is dependent on factors that introduce error into measured colors: aging of the MSCC color chips, soil texture and moisture, lighting conditions, subjective color judgments, and training that is required to increase user familiarity (Torrent and Barrón 1993; Neitz et al. 2002; Sánchez-Marañón et al. 2011; Elliot 2015; Schmidt and Ahn 2019). Additionally, the MSCC relies on semiquantitative data and requires transformations for statistical analysis (Viscarra Rossel et al. 2009; Kirillova et al. 2015). Other soil color methodologies have been utilized to identify and quantify soil colors, with various devices like mobile phone cameras, handheld spectrophotometers, and handheld colorimeters investigated as rapid field-based methods to complement and/or substitute for the MSCC in field monitoring. Cameras can capture an entire soil profile for color determination but require color correction cards, standardized photography conditions, and specific processing algorithms to accurately and reproducibly determine color (Aitkenhead et al. 2015; Han et al. 2016). Handheld spectrophotometers and colorimeters can greatly aid in rapidly and objectively identifying soil colors but can cost over $1,000 compared to the more accessible $250 of the MSCC; furthermore, both suffer from error introduced from light scattering through heterogeneity in soil texture and surface evenness that renders them more suitable for laboratory-based methodologies (Gómez-Robledo et al. 2013; Moritsuka et al. 2014; Stiglitz et al. 2016a; Fan et al. 2017; Schmidt and Ahn 2019).

The Nix Pro Color Sensor (*"Nix"*; www.nixsensor.com/nix-pro/) is an app-based color measurement device that has been shown to be complementary to the MSCC with a similar price ($349) (Schmidt and Ahn 2021b). Through its continuous numerical and objective measurements of soil color using 15 variables from 5 color spaces including the Commission on Illumination (CIE) L*a*b* (CIE–Lab), it represents an opportunity to predict SOC from field-based soil color measurements (see Schmidt and Ahn [2021a] for further information about color spaces and color variables). While strong relationships between the Nix and SOC have been established—with coefficient of determination ($R^2$) strengths up to 0.98 (Mikhailova et al. 2017; Stiglitz et al. 2018; Mukhopadhyay et al. 2020)—all investigations have focused on upland soils in specific geographic settings, and have relied on lab-based methods using dried and homogenized soils for color determinations. Field assessments that target different physiographic, hydrologic, and ecological settings are necessary to more fully assess the Nix's capability to assess soil carbon from on-site color determinations.

The goal of this study was thus to explore the potential use of a quantitative color sensor, the Nix, to predict carbon contents and stocks in the top layer of forested wetland soils. By using total carbon (TC) as a proxy for SOC in a non-calcareous soilscape, research objectives were to (1) collect, assess, and compare (a) field-based soil color data using the Nix color sensor and (b) soil carbon contents and stocks across different sites and physiographic provinces in NOVA; (2) assess relationships between all color variables collected by the Nix and soil carbon contents and stocks via correlation analysis; and (3) identify predictive power of single and multiple linear regression models relying on Nix color variables to predict soil carbon..

## Material and Methods

### Site description

Field research was carried out in 2020 at four forested wetlands in Northern Virginia: Algonkian Regional Park (ARP), Banshee Reeks Nature Preserve (BR), Julie J. Metz Wetlands Bank (JJM), and Elizabeth Hartwell–Mason Neck National Wildlife Refuge (MN) (Figure 2). Sites were selected to be balanced across the Piedmont (ARP, BR) and Coastal Plain (JJM, MN) physiographic provinces; additionally, their local watersheds include impervious surface percentages (% ISC) ranging from non-urbanized (% ISC < 5%; BR and MN) to urbanized (% ISC > 20%; ARP and JJM), representative of regional variation in landcover. Each site was sampled at 5 randomly selected plots spaced roughly > 200 m apart (Chi et al. 2018). Table 1 describes the characteristics of the four sites, including geomorphology, dominant soils, and vegetation communities.

In the Piedmont, ARP (39°3'28" N, 77°21'51" W) includes riparian forests and freshwater forested and emergent wetlands influenced by overland flow from the Potomac River, a groundwater connection with nearby emergent wetlands, and precipitation. Mapped soil series include Rowland silt loams and Lindside silt loams; while neither is hydric, ARP was observed to be capable of supporting wetland vegetation before sampling began (USDA–NRCS Soil Survey Staff 2020). BR (39°1'31" N, 77°35'30" W) includes occasionally to frequently saturated forested areas mapped as the hydric Albano silt loam plus the nonhydric Codorus and Manassas silt loams (USDA–NRCS Soil Survey Staff 2020). Floodplains and riparian zones are influenced by subsurface flow from Goose Creek, precipitation, and surface runoff from tributaries.

In the Coastal Plain, JJM (38°36'23" N, 77°16'38" W) lies adjacent to Neabsco Creek, a tributary of the Potomac River, and has sustained wetland hydrology since its construction as a mitigation wetland in 1994 (Environmental Laboratory 1987). The wetland contains occasionally, frequently, and permanently flooded soils mapped as the hydric Featherstone mucky silty loam and Hatboro–Codorus Complex, which are influenced by groundwater recharge, precipitation, and stream surface flow (USDA–NRCS Soil Survey Staff 2020) (USDA–NRCS Soil Survey Staff, 2020). MN (38°38'38" N, 77°09'57" W) includes a hardwood forest and forested wetland with rolling microtopography consisting of high points (hummocks) and low points (hollows). The occasionally to frequently saturated hollows are mainly influenced by precipitation and are mapped as the hydric Gunston silt loams; the rarely saturated hummocks are mapped as the nonhydric Matapeake silt loams and Mattapex loams (Ahn et al. 2009; USDA–NRCS Soil Survey Staff 2020).

**Field methods**

Soils were sampled in spring (March–April), summer (June–July), and fall (August–September) of 2018 and 2019 to capture seasonal fluctuations in color over two growing seasons. Average temperatures were 13.5˚C (-13.9˚C to 35.0˚C) in 2018 and 14.0˚C (-18.9˚C to 37.8˚C) in 2019; total precipitation was 169.5 cm in 2018 and 103.7 cm in 2019, with 2018 being the wettest year of the decade by 50-plus cm (Menne et al. 2012). At each plot (n = 16), a 10-cm (4") diameter auger (AMS) was used for soil profiling; while augering cannot provide an in-tact and undisturbed core from sampling, it provides an adequate sample size for identifying present soil colors in a relatively short time period without large plot disturbance, allowing it to be scaled to both professional and nonprofessional soil investigations (O'Donnell et al. 2011).

After removing surface debris, soil was augered down to 60 cm and laid on a white sheet to reflect in-situ soil horizonation. For each 10-cm depth interval (0–10 cm, 10–20 cm, and 20–30 cm), peds were split and identified interior colors were scanned with the Nix after it was connected to an Android smartphone running the Nix Pro Color Sensor app, which automatically recorded and stored scanned colors alongside timestamps and typed descriptors. Each scan is composed of 15 *Nix color variables* (grouped by color spaces, with names related to their respective variables): *L*, *a*, *b* (CIE–

Lab), $C$, $h$ (CIE–LCh), $X$, $Y$, $Z$ (CIE–XYZ), $R$, $G$, $B$ (RGB), and $C_K$, $M_K$, $Y_K$, and $K_K$ (CMYK) (Schmidt and Ahn, 2021). After initial scans, peds were iteratively halved along structural voids to form smaller peds; for each 10-cm depth interval, newly identified interior colors were also scanned using the Nix. This process was repeated until a ped diameter of 3–5 cm was reached or until peds were unable to maintain an even intact surface for Nix color recording. Before using the Nix, soils were wetted if dry, and surfaces were smoothed without mixing colors to create an even surface. Independent of ped boundaries, perceptibly identical colors within a given soil horizon were not repeatedly scanned. Colors were not measured when they could not fit within the Nix aperture (i.e., features less than 1 cm in diameter).

At three subplots per plot, soil samples were obtained for bulk density ($D_b$) and carbon analyses using a probe handcrafted from a PVC pipe with saw-tooth edges and notches at 10, 20, and 30 cm (modified from (Caldwell et al. 2005; Giannopoulos et al. 2019)) Caldwell et al. [2005] and Giannopoulos et al. [2019]). Undisturbed 30-cm cores were sampled and separated into three equally sized 10-cm depth intervals (0–10 cm, 10–20 cm, and 20–30 cm). Because one plot at both JJM and BR included large rocks below 20 cm (diameters > 5–10 cm), 20 to 30 cm samples were not collected at 6 subplots, totaling 138 soil samples collected for both $D_b$ and carbon analysis (i.e., 4 sites · 4 plots · 3 subplots · 3 depth intervals =144 minus 6).

**Lab analysis**

Wet masses were obtained for 10-cm-length soil core samples within 4 hours of collection using a Sartoruis Miras 2 scale with 5 g readability. Samples were placed into a drying oven between 85°C and 105°C for at least 72 hours until a constant dry mass was achieved; $D_b$ ($g{\cdot}cm^{-3}$) was subsequently calculated as the ratio between soil dry mass and the soil probe core volume.

Dried soil cores were crushed using a mortar and pestle then passed through a 2-mm sieve three times. Dry-weight percentages of total carbon (*TC*) were obtained from 5–10 mg samples using a Perkin–Elmer 2400 Series II CHNS/O Analyzer (Perkin–Elmer Corporation, Norwalk, CT, USA). Total carbon stocks (*TC stocks*, $kgC{\cdot}m^{-2}$) were calculated at each depth interval by multiplying TC, $D_b$, and interval length (10 cm) and converting to proper units: $TC\ stocks = D_b\ [g{\cdot}cm^{-3}] \cdot 10\ cm \cdot 10^4\ cm^2/m^2 \cdot (TC\ [\%] / 100)\ [g\ C / 100\ g] \cdot 1/10^3\ kg/g\ C$; i.e., *TC stocks* ($kgC{\cdot}m^{-2}$) = $D_b \cdot TC$. TC and TC stocks are herein referred to as *carbon variables*. TC (stocks) for the region's Piedmont and Coastal Plain are virtually equivalent to SOC (stocks) given the non-calcareous nature of the studied soilscape (Konen et al. 2003).

**Data analysis**

Using Microsoft (MS) Excel (Version 2012, 2021), carbon contents and bulk densities were averaged across subplots to yield plot-specific TC (%) and TC stock calculations for 0–10 cm, 10–20 cm, and 20–30 cm depth intervals. Soil color measurements were subsequently matched with plot averages for carbon contents and stocks. Data were scanned and screened to remove (1) outliers, defined as colors that fell outside 2 standard deviations of the mean for a given TC percentage, or coordinate pairs with simple linear regression residuals exceeding 3% in TC for Nix color variable *L*; (2) non-matrix redoximorphic features (gley colors, depletions, and concentrations); and (3) duplicates (e.g., identical color scans taken from same color at a specific plot and depth interval), leaving a sample size of 134. These samples are referred to as the *aggregate dataset* (n = 134), comprised of all recorded colors and respective soil carbon contents and stocks for all study plots and depth intervals (e.g., one sample would include a color observed at JJM plot 2 from 10–20 cm with its respective carbon contents and stocks).

After verifying assumptions of normality and homogeneity of variances on color and carbon variables, ANOVA, correlation, and regression analyses were conducted. Correlation analysis was conducted between Nix color variables and carbon contents and stocks plus three transformations of carbon contents and stocks (natural log [Ln(x)], square root [$\sqrt{x}$], and inverse [$x^{-1}$]), which were included to potentially strengthen correlations and regressions (Becker et al. 2019; Pek et al. 2019). Pearson correlations between measured Nix color variables and measured and transformed carbon variables were evaluated to yield finally-chosen (*final*) Nix color variables and one finally-chosen (final) carbon variable with priority placed on measured variables, but ultimately based on strength of correlations; $|r| \geq 0.70$ was used to indicate strong correlations (Mukaka 2012; Dancey and Reidy 2017; Akoglu 2018). For Nix color variables of the same color space with similar correlation coefficients ($|\Delta r| \leq 0.02$), a maximum of one variable was selected on the basis of user familiarity and innate relation to colors common in soil (e.g., from RGB, *R* [red] is more relevant for describing soil color than *G* [green]).

Final Nix color variables were used in four subsequent regression analyses. First, using the aggregate dataset, linear regression models were conducted on soil carbon and each final Nix color variable; scatterplots were also visually assessed to identify nonrandom patterns in residuals. To identify if relationships depended on physiographic province, regressions were also conducted using data separated by levels of each factor (i.e., physiographic province [factor] separated by Piedmont and Coastal Plain [factor levels]). Third, to remove noise in the regression models conducted on the aggregate dataset—in which each plot and depth interval had more than one corresponding color observed— linear regression models were conducted on soil carbon using Nix color variables that were averaged at each carbon percentage level (i.e., averaged by each plot and depth interval). Finally, using IBM SPSS software (Version 26, 2019), a backward stepwise multiple linear regression (MLR) model was also conducted with all Nix color variables as inputs to assess the added value of employing multiple Nix color variables in soil carbon predictions.

## Results

### Soil color and carbon by site

Table 13 displays all quantitative Nix color variables as well as TC and TC stocks for study sites. Colors showed high variability for several Nix color variables, specifically Lab *L*, or lightness (13.2 to 60.5) and CMYK $K_K$, or black (0.06 to 0.76). Variability depended on site for certain variables, where LCh *C* (i.e., chroma) was the only variable that did not significantly differ between sites (Table 13; $p > 0.10$). Piedmont soils (ARP, BR) showed higher values of Lab *a* and lower values of LCh *h*—both indicative of redder hues—than Coastal Plain soils (JJM, MN; $p < 0.05$). In contrast, CMYK $M_K$, magenta, and RGB *R*, red, did not significantly differ due to the combination of lightness and hue in these subtractive (CMYK) and additive (RGB) color spaces. With respect to soil lightness (corresponding to MSCC value), BR and JJM soils were significantly darker than MN soils, with lower Lab *L* (lightness) and higher CMYK $K_K$ (black) ($p < 0.01$); coinciding with these differences, JJM soils had lower values of RGB *R* (additive red) and *B* (additive blue) compared to ARP and MN ($p < 0.05$), where lower values of RGB *R*, *G*, and *B* in tandem relate to darker soils. While MN contained lighter soils than JJM and BR as seen through differences in *L, R*, *G*, and *B* ($p < 0.05$), MN also included the largest range for almost all Nix color variables—specifically Lab *L* (lightness)*,* LCh *C* (chroma) and *h* (hue), RGB *R* (additive red)*, G* (additive green), and *B* (additive blue)*,* and CMYK $C_K$ (cyan) and $K_K$ (black) (Table 13).

Table 13 also displays carbon characteristics at each site, represented as TC (%) and TC stocks (kg·m$^{-2}$) where the latter is reported only for the top 10 cm that was responsible for the majority (>50%) of soil carbon from 0 to 30 cm. Average TC and TC stocks ranged from 0.34% to 4.11% and from 0.40 kg·m$^{-2}$ to 5.7 kg·m$^{-2}$, respectively, with values that were comparable to other studies on Mid-Atlantic Piedmont and Coastal Plain forested wetlands in or near NOVA. However, several plots included TC and TC stocks not indicative of wetland development, e.g., TC < 2–3% (Giese et al. 2000; Giese and Flannagan 2006); in particular, ARP plots were consistently low in TC (0.9% to 2.0%; $p > 0.05$) and significantly lower in TC stocks (1.2 to 2.0 kg·m$^{-2}$; $p < 0.05$) compared to other sites. Conversely, JJM plots were consistently high in TC (2.6% to 3.3%; $p > 0.05$) with higher TC stocks than other sites (3.6 to 5.7 kg·m$^{-2}$; $p < 0.05$). While BR and MN had higher variability in TC (1.3% to 4.1% and 0.3% to 4.1%, respectively), both included the study's highest reported carbon contents ( >4.0%), where MN's carbon content variability matches its high variability in Nix color variables (Table 13).

**Table 13.** Nix color variables (n = 15) from five color spaces and carbon contents and stocks measured at each forested wetland site (mean ± standard error)

| | Algonkian Regional Park (ARP) | Banshee Reeks (BR) | Julie J. Metz Neabsco Creek (JJM) | Mason Neck (MN) |
|---|---|---|---|---|
| **Nix Color Variables** | | | | |
| Lab | | | | |
| *L* ** | 37.9 ± 3.0 [ab] | 34.4 ± 5.1 [b] | 27.3 ± 4.0 [b] | 42.2 ± 11.3 [a] |
| *a* ** | 9.9 ± 1.0 [a] | 8.4 ± 3.1 [a] | 5.6 ± 0.6 [b] | 6.6 ± 2.3 [b] |
| *b* * | 15.7 ± 1.2 [a] | 16.4 ± 3.4 [a] | 13.9 ± 1.5 [a] | 18.1 ± 6.7 [a] |
| LCh | | | | |
| *C* | 18.6 ± 1.5 [c] | 18.5 ± 4.3 [c] | 14.9 ± 1.6 [c] | 19.3 ± 7.0 [c] |
| *h* ** | 57.6 ± 1.3 [c] | 63.6 ± 5.3 [b] | 68 ± 1.1 [a] | 69.3 ± 4.9 [a] |
| XYZ | | | | |
| *X* ** | 10.4 ± 1.8 [b] | 9.2 ± 2.9 [b] | 5.6 ± 1.4 [b] | 14.8 ± 7.4 [a] |
| *Y* ** | 9.5 ± 1.6 [b] | 8.5 ± 2.5 [b] | 5.3 ± 1.4 [b] | 14.3 ± 7.2 [a] |
| *Z* ** | 4.5 ± 0.9 [b] | 3.7 ± 1.0 [b] | 2.4 ± 0.7 [b] | 6.4 ± 3.0 [a] |
| RGB | | | | |
| *R* ** | 108.0 ± 8.3 [ab] | 100.1 ± 16.1 [bc] | 78.3 ± 10.3 [c] | 118.6 ± 34.8 [a] |
| *G* ** | 80.3 ± 7.1 [b] | 75.8 ± 11.0 [b] | 61.2 ± 8.7 [b] | 96.2 ± 28.6 [a] |
| *B* ** | 61.7 ± 6.8 [ab] | 55.4 ± 7.8 [bc] | 43.7 ± 7.3 [c] | 70.4 ± 19.9 [a] |
| CMYK | | | | |
| $C_K$ ** | 0.46 ± 0.02 [b] | 0.48 ± 0.05 [ab] | 0.53 ± 0.02 [a] | 0.45 ± 0.08 [b] |
| $M_K$ ** | 0.60 ± 0.02 [a] | 0.60 ± 0.03 [a] | 0.61 ± 0.02 [a] | 0.53 ± 0.07 [b] |
| $Y_K$ ** | 0.72 ± 0.02 [b] | 0.75 ± 0.02 [a] | 0.77 ± 0.02 [a] | 0.71 ± 0.04 [b] |
| $K_K$ ** | 0.36 ± 0.05 [bc] | 0.40 ± 0.09 [ab] | 0.52 ± 0.07 [a] | 0.29 ± 0.19 [c] |
| **Soil Carbon** | | | | |
| TC (%) ** | 1.19 ± 0.35 [b] | 2.31 ± 1.01 [a] | 2.87 ± 0.35 [a] | 1.24 ± 1.14 [b] |
| TC Stocks (kg·m$^{-2}$) ** | 1.5 ± 0.3 [c] | 3.1 ± 1.1 [b] | 4.3 ± 1.0 [a] | 1.5 ± 1.1 [c] |

*significant at $p < 0.05$
** significant at $p < 0.01$

Significant differences in TC between sites, with higher TC at BR and JJM than ARP and MN ($p < 0.01$), mirrored several trends in soil color variable differences between sites—for example, BR and JJM soils had lower values of Lab $L$ (34.4 ± 5.1; 27.3 ± 4.0) than MN (42.2 ± 11.3; $p < 0.05$) and ARP (37.9 ± 3.0; $p < 0.10$); and higher values of CMYK $K_K$ (0.40 ± 0.09; 0.52 ± 0.07) than MN (0.29 ± 0.19; $p < 0.05$) and ARP (0.36 ± 0.05; $p < 0.10$), respectively, indicating a link between soil carbon and color lightness ($L$) or darkness ($K_K$).

**Correlations**

Table 14 shows the correlation results between Nix color variables and carbon contents and stocks; in addition to TC and TC stocks, natural log transformations (but neither square root nor inverse transformations) are included in further analyses due to augmented correlation coefficients ($\Delta r > 0.02$) with Nix color variables when compared to Nix correlations with untransformed TC and TC stock variables. In general, Lab $a$, LCh $h$, and CMYK $Y_K$ displayed the lowest correlations with soil carbon. Conversely, correlation coefficients with Ln(TC) exceeded 0.70 ± 0.02 in magnitude for six Nix color variables: Lab (1) $L$, XYZ (2) $X$ and (3) $Y$, RGB (4) $R$ and (5) $G$, and CMYK (6) $K_K$ ($|r| > 0.68$; $p < 0.01$; Table 14).

**Table 14.** Pearson correlation coefficients between Nix color variables (n = 15) and soil carbon variables (TC [%], TC stocks [$kg \cdot m^{-2}$], Ln[TC], and Ln([TC stocks])

| Nix Color Variables | TC (%) | TC Stocks ($kg \cdot m^{-2}$) | Ln(TC) | Ln(TC Stocks) |
|---|---|---|---|---|
| Lab | | | | |
| *L* [1] | -0.64 | -0.58 | -0.70 | *-0.65* |
| *a* | -0.24 | -0.11 | -0.21 | -0.13 |
| *b* | -0.52 | -0.42 | -0.61 | -0.53 |
| LCh | | | | |
| *C* | -0.50 | -0.39 | -0.58 | -0.49 |
| *h* | -0.19 | -0.21 | -0.29 | -0.29 |
| XYZ | | | | |
| *X* [1] | -0.61 | -0.56 | -0.70 | *-0.65* |
| *Y* | -0.61 | -0.57 | *-0.69* | *-0.65* |
| *Z* | -0.59 | -0.57 | *-0.65* | -0.62 |
| RGB | | | | |
| *R* [1] | -0.64 | -0.57 | -0.70 | -0.64 |
| *G* | -0.63 | -0.58 | -0.70 | *-0.65* |
| *B* | -0.61 | -0.58 | *-0.66* | -0.62 |
| CMYK | | | | |
| $C_K$ | 0.58 | 0.48 | 0.64 | 0.56 |
| $M_K$ | 0.55 | 0.54 | 0.64 | 0.61 |
| $Y_K$ | 0.28 | 0.37 | 0.26 | 0.31 |
| $K_K$ [1] | *0.65* | 0.59 | 0.70 | *0.65* |

[1] Denotes Nix variables with $|r| \geq 0.70$ for at least one carbon variable (excluding G, as explained in the methods and results).
* Note: all correlations where $|r| > 0.30$ are statistically significant ($p < 0.01$).
*Italics* : $0.70 > |r| \geq 0.65$
Underline: $|r| \geq 0.70$

$X$ and $Y$ from the XYZ color space, as well as $R$ and $G$ from the RGB color space, showed high collinearity, respectively ($|r| \geq 0.90$; see Schmidt and Ahn 2021). From the XYZ space, $X$ was selected over $Y$ as a final Nix color variable to avoid confusion between $Y$ and $Y_K$ (yellow) from the CMYK color space. Despite the lack of one-to-one relationship between RGB $R$ and the hue red, $R$ (red) was selected over $G$ (green) as the best estimate of Ln(TC) from the RGB color space because of the perceptible relationship between soil redness and oxidized irons as well as hydrology (Schwertmann and Taylor 1989; Schwertmann 1993; Viscarra Rossel et al. 2006). Since Ln(TC) has been used in previous research using the Nix (Stiglitz et al. 2017a; Mikhailova et al. 2017; Mukhopadhyay et al. 2020; Mukhopadhyay and Chakraborty 2020) and zero Nix–TC (%) correlations exceeded 0.70 in magnitude (Table 14), Ln(TC) was selected as the final carbon variable for regression analyses. The final four Nix color variables were thus $L$ (CIE–Lab), $X$ (XYZ), $R$ (RGB), and $K_K$ (CMYK).

**Linear regressions models**

Regression models conducted using the aggregate dataset for Ln(TC) versus final Nix color variables ($L$, $X$, $R$, and $K_K$) are displayed in Figure 8. Simple linear regressions between final Nix color variables and Ln(TC) produced adequate models, where $R^2$ = 0.50 for Ln(TC) versus Lab $L$ and RGB $R$, and $R^2$ = 0.49 for Ln(TC) versus XYZ $X$ and CMYK $K_K$, respectively ($p < 0.01$ for all). Residual analyses indicated that models tended to overestimate soil carbon for lower values of Ln(TC) (e.g., Ln[TC] < −5) and underestimate soil carbon for higher values of Ln(TC) (e.g., Ln[TC] > −3.5), with nonnormal residuals (Figure 8). High spread in Nix color measurements for individual carbon contents (i.e., at a given plot and depth interval)—visualized as horizontal spread in Figure 8—decreased each model's explanatory power. Nonetheless, residuals tended to show homoscedasticity, and $R^2$ values that approximate 0.50 highlight the capacity for simple linear regressions to explain a significant portion of Ln(TC) variability.

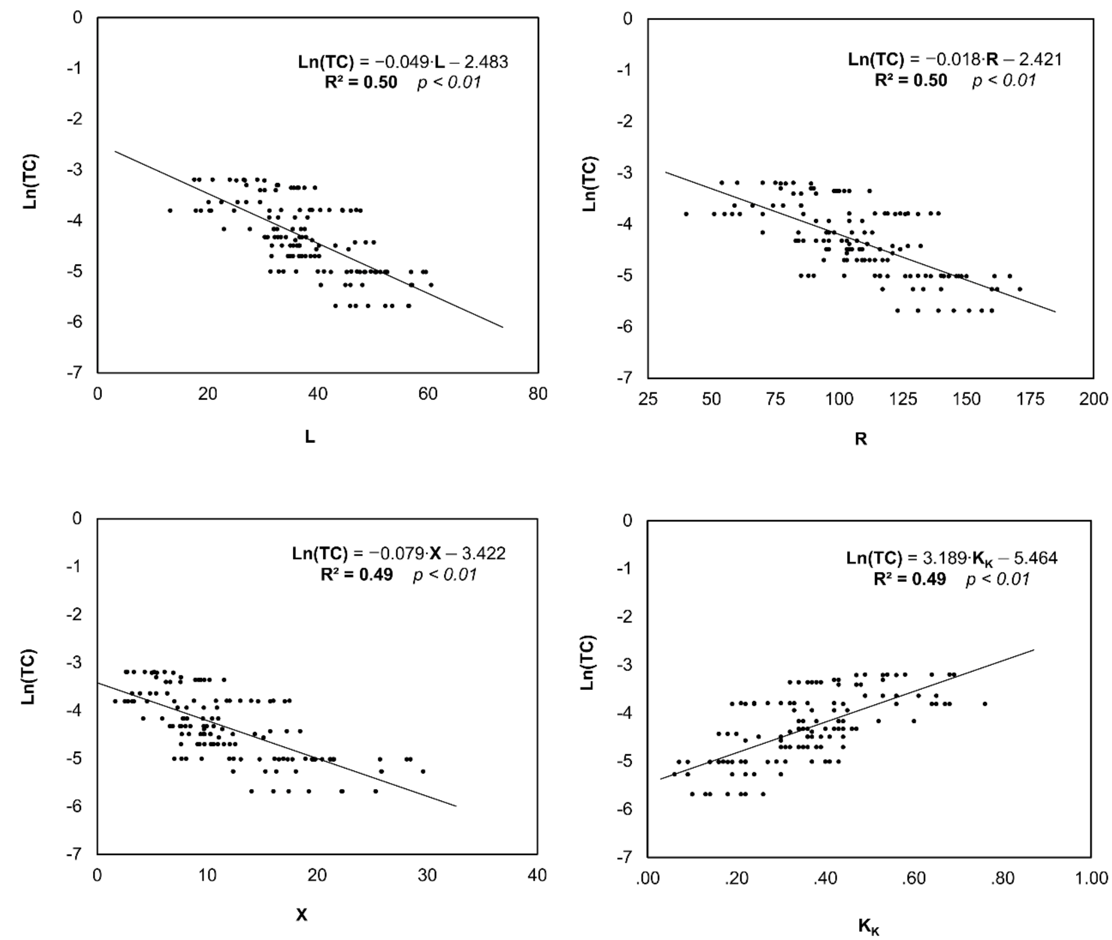


**Figure 8.** Regressions for Ln(TC) versus final Nix color variables (*L*, *X*, *R*, and $K_K$), using coordinate pairs from the aggregate dataset (n = 134) that includes all measured colors and carbon contents / stocks

When Nix–Ln(TC) coordinate pairs were separated by factor levels of physiography (Piedmont, Coastal Plain), regression model slopes and strengths were affected. Coastal Plain, but not Piedmont, regressions were significant; $R^2$ values surpassed those achieved using from the aggregate dataset and ranged from 0.55 ($K_K$) to 0.65 ($R$) ($p < 0.05$; Figure 8; Table 15). In contrast, Piedmont regressions were weak and insignificant ($p > 0.25$).

**Table 15.** Regression model equations and $R^2$ values for Ln(TC) versus final Nix color variables ($L$, $X$, $R$, and $K_K$), by physiographic province (Piedmont vs. Coastal Plain)

| Nix Color Variable | *Physiographic Province* | |
|---|---|---|
| | Piedmont | Coastal Plain |
| **L** | | |
| $R^2$ | 0.05 | **0.62** |
| p-value | > 0.25 | **0.00**** |
| β (slope) | -0.219 | -0.05 |
| Intercept | 1.273 | 2.061 |
| **X** | | |
| $R^2$ | 0.04 | **0.60** |
| p-value | > 0.25 | **0.00**** |
| β (slope) | -0.036 | -0.082 |
| Intercept | 0.844 | 1.159 |
| **R** | | |
| $R^2$ | 0.05 | **0.65** |
| p-value | > 0.25 | **0.00** ** |
| β (slope) | -0.008 | -0.018 |
| Intercept | 1.315 | 2.127 |
| **$K_K$** | | |
| $R^2$ | 0.05 | **0.55** |
| p-value | > 0.25 | **0.00 **** |
| β (slope) | 1.457 | 2.909 |
| Intercept | 0.056 | 0.939 |

*, *italics:* $p < 0.05$
**, **bold:** $p < 0.01$

When color measurements for final Nix variables were first averaged by plot and depth interval (i.e., all colors measured for a given carbon content), averaged colors could explain roughly 70% of the variability in Ln(TC), with $R^2$ ranging from 0.66 ($K_K$) to 0.70 ($R$) (Figure 9; $p < 0.01$ for all). Comparisons between these regression strengths (Figure 9) and those obtained from each individual color scan (Figure 8) suggest that obtaining average color data for all sizeable colors observed at a given depth can provide more reliable estimates of TC than individual color measurements. Furthermore, regression slopes—a sign of model sensitivity—were 40 to 55% higher for averaged data (Figure 9) than aggregate data (Figure 8) ($L$: −0.07 vs. −0.049; $X$: −0.12 vs. −0.08; $R$: −0.03 vs. −0.02; $K_K$: 4.50 vs. 3.19, respectively), suggesting averaged data models are both more robust sensitive to changes in soil carbon.

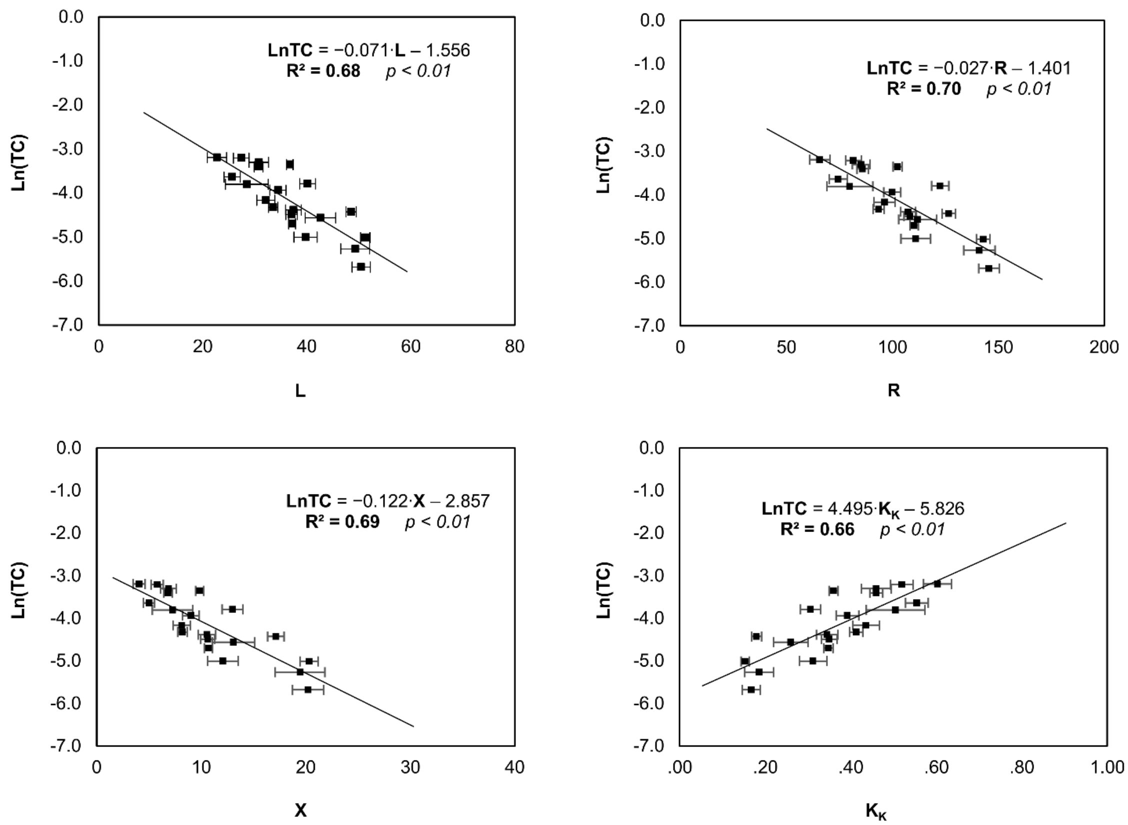


**Figure 9.** Regressions for Ln[TC]) versus final Nix color variables ($L$, $X$, $R$, and $K_K$), using coordinate pairs from averaged data that includes one averaged color measurement and soil carbon content per plot and depth interval ($p < 0.01$ for all)

Finally, the multiple linear regression model revealed that the use of multiple variables recorded by the Nix—*a* (Lab), *Y* (XYZ), *B* (RGB), and all variables of the CMYK color space ($C_K$, $M_K$, $Y_K$, and $K_K$)—can be used to estimate Ln[TC] with an adjusted $R^2$ of 0.60, per the following equation ($p < 0.01$):

**Equation 1.** Multiple linear regression (MLR) equation for the natural log of total carbon, Ln(TC), from Nix color variables

$$\mathrm{Ln(TC)} = 0.431 \cdot a - 0.172 \cdot Y + 0.326 \cdot B + 14.314 \cdot C_K - 20.274 \cdot M_K + 37.070 \cdot Y_K + 31.055 \cdot K_K - 54.525$$

Statistical analysis indicated that Lab *a*, RGB *B*, and CMYK $Y_K$ and $K_K$ were most significant ($p < 0.01$); furthermore, standardized beta coefficients were highest in magnitude for Lab *B* (7.654) and CMYK $K_K$ (6.804). Figure 10 displays predicted versus observed TC (%) derived from Equation 1. Residuals were not independently distributed, and the model tended to underestimate TC for low-carbon soils (observed TC < 1.5%) and overestimate TC where observed TC exceeded 3%.

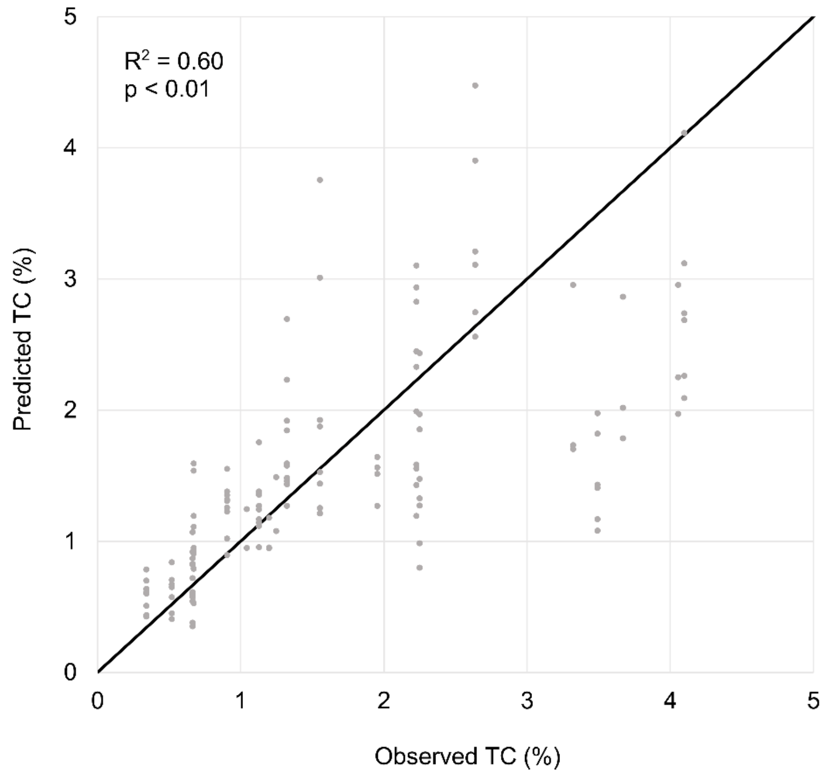


**Figure 10.** Predicted versus observed TC (n = 134) obtained from a multiple linear regression (MLR) model using Nix variables *a*, *Y*, *B*, $C_K$, $M_K$, $Y_K$, and $K_K$ (Equation 1)

## Discussion

### Nix colors and soil carbon

Nix measurements can highlight sitewide differences in colors that may reflect their differences in soil carbon contents and stocks. Variables like Lab *L* and CMYK $K_K$ indicated color differences between (1) BR and JJM and (2) ARP and MN that mirrored differences in carbon contents and stocks (Table 13). When soil carbon comparison rather than prediction is a management or outreach goal, simple comparisons between these Nix color variables may be suitable. Including more sites with varied soil colors and carbon contents would improve the understanding of how the Nix may be used as a carbon comparison tool. Furthermore, certain Nix color variables can be useful for identifying signatures of soil settings that are inexorably linked to soil carbon content—e.g., parent material, physiography, hydrology, and soil biogeochemistry. While the number of study sites was limited in this investigation, differences between Coastal Plain and Piedmont soil colors highlighted through the hue-related variables Lab *a* and LCh *h* likely relate to iron oxide contents that are known to differ between the physiographic provinces (Rossi and Rabenhorst 2016). Furthermore, the large spread, high values for XYZ *X* and RGB *R,* and low values for CMYK $K_K$ at MN might signal the prevalence of depleted (light, low-chroma) soil matrices as well as redox concentrations that were most abundant at MN (Ahn et al. 2009). As soil color determinations are a primary to indicate hydrologic and soil biogeochemical settings, significant differences in variables like CMYK $K_K$—related to both soil moisture and organic matter content—between sites highlight the potential for the Nix to be further investigated for the purpose of hydric soil delineation (USDA—NRCS 2018).

The distributions of Nix soil color variables presented herein add to the potential ranges for Nix color variables successfully used to discern color relationships with soil carbon. Compared to Stiglitz et al. (2016b), the 134 data color measurements of this study included higher ranges for $M_K$ (0.41–0.67 versus 0.31–0.41) and $Y_K$ (0.63–0.83 versus 0.55–0.66), and a wider range for $K_K$ (0.06–0.76 versus 0.55–0.66); these discrepancies may stem from differences in climate, geography, presence/absence of hydric soils, or differences in methodology (i.e., on-site color determinations versus sample processing before color determinations). Color variable ranges for these Piedmont and Coastal Plain soils were comparable to colors that can be observed on the global scale, but ranges for variables like Lab *a* and *b,* LCh *C* and *h,* and RGB *B* were relatively small (Viscarra Rossel et al. 2006).

With respect to soil carbon, forested wetlands in areas with similar landcover patterns have been documented to host carbon stocks of 10 to 14 $kg \cdot m^{-2}$ (Bae and Ryu 2015; Nave et al. 2019). While this research identified carbon stocks that were at most 5.7 $kg \cdot m^{-2}$, ranges reported herein for soil carbon (Table 13) are similar to those reported for forested wetlands within the Mid-Atlantic Piedmont and Coastal Plain physiographic provinces, with common reports of carbon contents ranging from 0.7% to 4.1% up to a depth of 15 cm (Stolt et al. 2000; D'Angelo 2005; Noe 2011; Dee and Ahn 2012; Ahn and Peralta 2012; Ledford et al. 2022); thus, this study provides sufficient variability in soil carbon for assessing sitewide differences between, and relationships with, Nix color variables.

**Relationships between color and carbon in forested wetland soils**

Previous research has unearthed strong relationships between soil color and both carbon contents (Schulze et al. 1993; Wills et al. 2007; Liles et al. 2013; Ibáñez-Asensio et al. 2013; Aitkenhead et al. 2015; Pretorius et al. 2017; Mikhailova et al. 2017; Chen et al. 2018) and carbon stocks (Chaplot et al. 2001; Konen et al. 2003; Viscarra Rossel et al. 2006; Wills et al. 2007; Moritsuka et al. 2014), where many studies based the choice of TC versus TC stocks on application and/or audience rather than regression strengths. The finding herein that Nix color variables are more highly correlated with TC than TC stocks may be inherent to color–carbon relationships, indicating that predictions of soil carbon from Nix color variables may not require further soil physicochemical analyses—e.g., measurement of $D_b$ (Wills et al. 2007). Furthermore, the choice to transform TC using a natural logarithm is both present (Mikhailova et al. 2017; Stiglitz et al. 2018) and absent (Mukhopadhyay et al. 2020) in literature using the Nix. Mukhopadhyay et al. (2020) found a relatively high correlation between Nix variables and SOC (%) as opposed to Ln(SOC); however, an apparent nonrandom residual pattern in their scatterplot gives credence to the conclusion that soil carbon is linearly correlated with variables of soil color only after undergoing a log transformation, and our results extend that conclusion to soil color as measured in the field. Despite Figure 8 revealing nonrandom residual patterns for all four scatterplots—particularly for Ln(TC) vs. $L$—the Ln(TC) function provided the best residual pattern out of TC and the common transformations explored in this study (square root [$\sqrt{x}$] and inverse [$x^{-1}$]). It is recommended that the Nix be used to assess color—carbon relationships with soils that provide a higher range of carbon contents to more thoroughly assess the linearity of Ln(TC) vs. Nix color variable models.

Using Ln(TC) as a proxy for soil carbon, soil carbon can be best predicted using Nix color variables $L$, $X$, $R$, and $K_K$ with moderately strong coefficients of determination ($R^2 \approx 0.50$), deemed to be acceptable by this study's standards ($|r| \geq 0.70$ and $R^2 \geq 0.49$; Table 14; Figure 8). In contrast to a single variable solution, these four variables are offered to allow flexibility in color space choice (CIE–Lab, XYZ, RGB, and/or CMYK). However, compared to XYZ $X$ and CMYK $K_K$, variables $L$ (Lab) and $R$ (RGB) have slightly higher $R^2$ values (0.50 versus 0.49; $p < 0.01$), more randomness in residual patterns, and larger y-intercepts (-2.483 [$L$] and -2.421 [$R$] versus -3.422 [$X$] and -5.464 [$Y$]) that more adequately estimate soil carbon contents when soil color approaches black (Figure 8). Similar results were observed in previous studies, as soil lightness—i.e., Lab $L$—and SOC have been prominently linked (e.g., $r = -0.74$ in Viscarra Rossel et al. 2006) with a linear or curvilinear relationship (Brown and O'Neal 1923; Schulze et al. 1993; Yang et al. 2001; Konen et al. 2003; Wills et al. 2007; Yonekura et al. 2010; Liles et al. 2013; Moritsuka et al. 2014; Pretorius et al. 2017; Mikhailova et al. 2017; Stiglitz et al. 2018). Furthermore, strong correlations between soil carbon and RGB $R$ ($r = -0.79$) have also been identified (Viscarra Rossel et al. 2006; Ibáñez-Asensio et al. 2013).

This study's results corroborated the finding that distinct soil taxonomic and/or landscape settings can produce distinct regression models and strengths (e.g., for *L*: $R^2 = 0.62$ for Coastal Plain soils [Table 15] vs. $R^2 = 0.50$ for all soils from both Coastal Plain and Piedmont [Figure 8]; $p < 0.01$ for both). Nix color measurements may thus be more useful if models are confined to a limited soilscape (Viscarra Rossel et al. 2006; Wills et al. 2007; Ibáñez-Asensio et al. 2013; Moritsuka et al. 2014; Valeeva et al. 2016; Mikhailova et al. 2017; Stiglitz et al. 2018). Unlike Coastal Plain soils, Piedmont soils fall within the Culpeper Triassic Basin and have higher clay and iron oxide contents, which provide abundant binding sites for soil organic carbon. Carbon physicochemistry and resulting color patterns are thus inherently different in the Piedmont than in the Coastal Plain (Elless et al. 1996; Adhikari and Yang 2015). Furthermore, soil carbon has a stronger monotonic (curvi-)linear relationship with sand content than clay content (Breemen and Feijtel 1990; Torn et al. 1997; Baldock and Skjemstad 2000; Six et al. 2002; Wills et al. 2007), and Coastal Plain soils are generally sandier (Markewich et al. 1990). In accordance with previous studies, this research highlights that accurate models for soil carbon estimation from soil color measurements should be constrained to specific mineralogical and physiographic settings with less obfuscation from high clay contents.

Stronger $R^2$ values for Nix−carbon regression models reliant on averaged rather than aggregate data suggests that multiple color measurements for the same soil depth should be averaged when creating carbon regression models. While such averaging requires more sampling and temporal engagement, it bolsters the applications of using color over time to track carbon changes and provide management opportunities to improve wetland carbon storage. Finally, in contrast to previous studies obtaining high (>0.90) $R^2$ values when models were based on Lab *L*, *a*, and/or *b*, this study's MLR analysis rendered a model able to explain 60% of the variation in Ln(TC) in which *L* was excluded ($p \approx 0.25$) and RGB *B* and CMYK $K_K$ were the strongest predictors (Equation 1). The influence of RGB *B*—which had a Pearson correlation coefficient of −0.66 with Ln(TC) (Table 14)—signals that, despite the link between soil color and additive blue, RGB *B* offers additional information than offered through soil lightness (L, $K_K$) alone. The MLR (Figure 10) nonetheless could not predict Ln(TC) to the extent of average color measurements of *L*, *X*, *R*, or $K_K$ alone (Figure 9); in particular, the model tended to under-estimate TC for soils with high TC (>2.5%), bolstering the recommendation that multiple color measurements be taken and averaged when creating and relying on linear regression models.

**Implications and limitations of the study**

The applications of these findings rest upon the on-site nature of color measurements and the accuracy of model predictions. This study is one of the first linking quantitative soil color variables and carbon contents to occur on-site using non-processed samples (see Wills et al. 2007 for others), but the confirmation of relationships between Nix color variables and soil carbon were met with relatively large deviations in regression models (>1 difference in Ln[TC]) with a substantial variance in Ln(TC) left unexplained. Simple linear regressions of Ln(TC) versus Nix variables like *L* may improve with procedural improvements that control for confounding variables like soil moisture, texture, and surface evenness (Stiglitz et al., 2016; Wu et al., 2009). Nonetheless, complete control cannot be attained in a field setting, and it remains to be seen if regression strengths observed in lab studies like Chen et al. (2018; $R^2$ = 0.71), Viscarra Rossel et al. (2006; $R^2$ = 0.76), and Mikhailova et al. (2017; $R^2$ = 0.96) can be achieved in on-site color determinations and carbon estimations. Particularly when using the Nix to forested wetland areas known to contain iron and/or manganese redoximorphic features, heterogeneous color patterns in the soil matrix can complicate the applicability of such regression models by obfuscating the relationship between soil color and carbon contents. Demonstrated through a comparison of $R^2$ and overall scatter between regression models based on aggregate versus averaged datasets (Figure 8; Figure 9), it is recommended that users average Nix color variable values at a certain depth (e.g., $[K_{K(1)} + K_{K(2)}]/2$) when more than one significant color is identified in a soil horizon, and to ignore insubstantial features like concentrations comprising less than 25% of the soil matrix.

Beyond quality control concerns, studies have identified additional variables affecting regression models that may warrant further study for field-based investigations. For example, depth is known to affect the relationship between soil color and soil carbon; while soil colors were matched to each respective depth interval's carbon contents in this study, previous investigations have gone one step further to incorporate depth into their models as an auxiliary variable (Wills et al. 2007; Mikhailova et al. 2017; Stiglitz et al. 2018). This is a promising approach if studies incorporate sufficient sampling points into their analysis, but also complicates model accessibility. Similar to the suggestions of Mukhopadhyay et al. (2020), it is recommended that quality control efforts focus on controlling other variables to augment correlation and regression strengths rather than relying on an additional input for regression models.

## **Conclusions**

The outcome of the study demonstrates that field deployment of the Nix Color Sensor and accompanying app has the potential to not only differentiate soils of contrasting colors and carbon contents, but also predict soil carbon contents through a simple linear regression equation providing an estimate of Ln(TC). Nix color variables—notably $L$ (Lab), $X$ (XYZ), $R$ (RGB), and $K_K$ (CMYK)—were more capable of predicting Ln(TC) in certain physiographic settings, specifically the Coastal Plain, highlighting that refinement of Nix methodologies may be required on a regionally-specific scale. Independent of physicochemical properties, however, it is suggested that investigations into, and/or application of, the Nix as a tool for soil carbon prediction focus on soils within a uniform landscape and with reliance on averaged matrix color measurements.

Unlike the MSCC or more expensive methods, the Nix has the potential to be accessibly integrated into carbon storage and sequestration strategies that would benefit from accurate, relatively inexpensive, and sustained efforts, along with simple statistical models, to predict soil carbon at promising carbon sinks like forested wetlands. While further research is warranted to better understand color–carbon relationships in soils within different physiographic provinces as well as ecosystem types, these findings offer an optimistic basis for potentially incorporating the Nix and its soil color measurements into environmental monitoring and assessments, carbon-focused watershed management, and/or soil science education and training.

# CHAPTER SIX:
# AIDING ENVIRONMENTAL MONITORING AND/OR ASSESSMENT BY IMPLEMENTING A SYSTEMATIC PROCEDURE TO MEASURE SOIL COLORS USING THE NIX COLOR SENSOR

## Introduction

In the era of global change, many ecological challenges researched and addressed by scientists and resource managers benefit from community engagement: monitoring costs can be lowered, monitoring can cover greater physical and/or temporal scopes, and participants can expand their environmental literacy (Conrad and Hilchey 2011). Various Bluetooth-linked sensors exist to support ecological monitoring and environmental literacy, including handheld particular matter sensors like the AirBeam (habitatmap.org/airbeam/) and handheld Light Detection and Ranging (LIDAR) sensors like Spike® by IkeGPS (https://shop.ikegps.com/products/spike) (Stitt et al. 2019). Even more endeavors rely solely on the chief tool for engaging people in ecological inquiry: the smartphone. Apps like iNaturalist serve to not only collect and crowdsource monitoring data, but also teach and engage users through interactions with their smartphones and surroundings.

While many ecological monitoring apps and/or projects serve to bridge gaps in monitoring needs and the layperson's environmental literacy, a 2017 study identifying 509 ecologically- and environmentally- themed citizen science and/or engagement projects across the globe included zero mention of soil as a theme (Pocock et al. 2017); similarly, a 2018 study cited various projects whose main foci included species and/or biodiversity monitoring, air monitoring, and water/stream monitoring, but no foci related to soils or sediments (Palacin-Silva and Porras 2018). While a lack of initiatives related to soil science may stem from a lack of public, government, and nongovernmental organization (NGO) NGO interest, two key aspects of ecological monitoring are missing in soil science compared to other fields of study: simple, scientifically reliable, and cost-effective (1) indicators of soil ecology to be measured, and (2) methods of measuring said indicators. Many soil physicochemical properties like soil moisture require sample processing, and many soil assessments require large disturbances such as soil pits or wide auger holes.

Recently, however, soil color has risen to the forefront of soil indicators due to its link to the dark-colored soil organic carbon (SOC) and organic matter (SOM), hot topics in the realms of soil ecology and climate change (Schmidt and Ahn 2021a). Furthermore, soil color can assess and/or track wetland soil development, linked to wetland ecosystem service development like slowed organic matter decomposition and carbon storage potential. Soil color thus serves as a perceptive measure capable of use in status assessments, while also serving as an indicator for wetland monitoring that can aid in adaptive management of land areas (Conrad and Hilchey 2011). Multiple methods of measuring soil color have been studied (Schmidt and Ahn 2019), yet the conventional method—using a ~$200 chart called Munsell Soil Color Chart (MSCC) to identify

Munsell hue (H), value (V), and chroma ($C_M$) of soil colors—has yet to be replaced given its field applicability and relative ease of use. Nonetheless, the MSCC requires training to overcome perceptual biases, takes time for correct color identification, and is affected by weather conditions. Furthermore, it cannot be used by the colorblind, making up ~10% of the male population.

A Bluetooth-linked device called the Nix Color Sensor (Nix), used in several soil endeavors beginning in 2016 (Stiglitz et al. 2016b, a, 2017b; Schmidt and Ahn 2021b), has the potential to open up soil color and carbon inquiries to the untrained eye. Relatively inexpensive in comparison to other field-applicable colorimeters ($350), the diamond-shaped Nix, roughly the size of a tennis ball, rapidly measures the color of the surface its ~ 2 $cm^2$ aperture lies upon; colors are measured objectively and numerically via 15 color variables from 5 color spaces including the Commission on Illumination (CIE) L*a*b*. Scanned data is sent to a Bluetooth-linked Android or Apple device for easy export. Given its portability and ease of use, the Nix sensor has the potential to be deployed in school and/or community investigations of soil color to allow for a convergence of soil color literacy and ecosystem service literacy in participatory and local place-based learning and data collection (Wals et al. 2014). Furthermore, in urban areas where flooding and stormwater management produce novel wetlands and/or new development of wetland-like ecosystems (Palta et al. 2017), the Nix serves as a tool to connect individuals to their changing environment, allowing them to be better stewards of their urban ecosystems as soil color changes over time signal hydrologic and ecosystem service changes.

Herein presented is a case study outlining the methodology used in the deployment of the Nix color sensor in a university field and lab class taught by Dr. Changwoo Ahn, Ecological Sustainability, designed as an undergraduate research and scholarship intensive course. Under the purview of Dr. Ahn and teaching assistant Stephanie Schmidt, the goal of the class project was to study soil colors in campus green spaces using the Nix color sensor to give students a better understanding of soil ecology. Through the class project, we have identified strengths and/or weaknesses of deploying the Nix in future citizen-based endeavors to monitor and/or assess ecosystems through soil color determination.

## Class project design and implementation

The case study took place on the campus of George Mason University in Fairfax, Virginia, USA. The campus is 677 acres large and contains various green spaces across campus like undisturbed forested areas, rain gardens installed as stormwater controls, a mulched *food forest*, floodplains underneath boardwalks, and the Ahn Wetland Mesocosm Compound and its adjacent ephemeral stream and wetland area. All sampled locations were either upland or showed minor signs of mottling from fluctuating water tables (e.g., a floodplain site).

Our goals were achieved through use of a Standard Operating Procedure (SOP) with required materials including soil probes, trowels, butter knives, the Nix Pro color sensor, and self-provided smartphones. The 2-page SOP was developed to guide ~10 students placed into 3 different groups through (1) Nix best practices, (2) navigating and using the Nix app on their smartphones, (3) soil collection, (4) measuring soil colors at each plot using the Nix, (5) storing samples for processing, and (6) exporting, downloading, and sharing data. The SOP was created with the intent for students to collect soil colors at 3 depths—soil surface, topsoil (0–15 cm), and A horizon (15–30 cm)—at several green spaces across campus, measure and export soil colors, and analyze colors to provide insight for a final report.

**Soil color measurement using the Nix**

All sampling and measurement steps were demonstrated to students before giving them a chance to practice in Dr. Changwoo Ahn's outdoor field space, the Wetland Mesocosm Compound. Students were shown how to remove surface debris before measuring colors of the soil surface colors (i.e., ground color) and how to use a ~ 30 cm soil probe to obtain a core to be used for 0–15 cm and 15–30 cm measurements and soil samples. A summary of the procedure is outlined in Table 16.

**Table 16.** General procedure from the Standard Operating Procedure (SOP) that students were to follow to measure soil colors using the Nix

| | |
|---|---|
| **Before Sampling** | |
| | Download Nix Pro Color Sensor App |
| | Turn on picture geotagging |
| | Make sure Nix is charged and paired to phone/tablet |
| **At Sampling Plot** | |
| | Have trowel, soil probe, water (spray bottle), Nix, and Bluetooth-linked phone/tablet on hand |
| | Clear litter from soil surface at desired location |
| | Take geotagged pictures of plot and surrounding area |
| **Soil surface color** | |
| | Use trowel to clear soil surface of any woody debris / leaves and ensure a smooth soil surface |
| | Place the Nix on top of cleared soil surface with subtle pressure on top to ensure aperture edges are in contact with soil |
| | In Nix app, press "Scan"; save color scan in desired folder named to a standard convention "SitePlot_0cm" |
| **0-15 cm and 15-30 cm color preparation** | |
| | Using a ~30 cm soil probe, push the probe into the soil; once it is all the way inserted, pull the probe out |
| | Create a longitudinal "cross section" by cutting down the length of the core using a knife held parallel to the probe |
| **0-15 cm colors** | |
| | Within the top half of the probe, find a uniformly colored area under the very dark upper layer for the 1st scan location |
| | At the selected location, smooth/flatten the cross-section surface by gently pressing down without blending colors |
| | Place the Nix on the chosen location with subtle pressure on top to ensure aperture edges are in contact with soil/probe |
| | In Nix app, press "Scan"; save color scan in desired folder named to a standard convention "SitePlot_0to15cm" |
| **15-30 cm colors** | |
| | In the bottom half of the probe, find a uniformly colored area, under the very dark upper layer, for the second scan |
| | At the selected location, smooth/flatten the cross-section surface by gently pressing down without blending colors |
| | Place the Nix on the chosen location with subtle pressure on top to ensure aperture edges are in contact with soil/probe |
| | In Nix app, press "Scan"; save color scan in desired folder named to a standard convention "SitePlot_15to30cm" |
| **Tips for all measurements** | |
| | Make sure to moisten site of measurement with spray bottle until soil is moist enough that it does not change color |
| | Place the Nix on the soil surface with subtle pressure on top to ensure aperture edges are in contact with soil |
| | Do your best to avoid very mottled areas; if color uniformity cannot be guaranteed, simply find a representative area |
| **After Sampling** | |
| | From each site, all scans will be saved in the Nix app within the folder ("swatch") name given to them |
| | Export them in the app by navigating to Menu → Settings → Export Scanned Colors, and find the folder you created with your saved scans |
| | The resulting .csv file will have the color name in column A, time stamp in column C, and color variables in columns D through AB. Geotagged information (latitude, longitude) can be matched to color names manually |

Techniques demonstrated and encouraged with each scan to obtain accurate color measurements included moistening the soil if needed, a standard when determining color via the MSCC, and ensuring the Nix aperture edges were firmly in contact with the soil surface in question (i.e., not allowing the aperture to shine light onto anything but the sample area). For measurements conducted from soils collected using the soil probe, students were taught how to use a knife to slide along the soil probe and longitudinally cut the core, providing a cross-section "surface" for measurement. Furthermore, they were to procure a smooth and flat topographic profile of the core cross-section by delicately pressing into its surface (to the effect of removing cracks, bumps, protruding roots, etc.); and ensure that the area of soil chosen for measurement—i.e., on which the Nix aperture would be placed—displayed uniform coloring. This final technique emphasized flexibility over rigidity in measurement depth/location along the core due to the inaccuracy of Nix color measurements that ensues when the surface it is observing displays heterogeneous color patterns. Nonetheless, if soils with patterns of concentrations and depletions amidst matrix colors were observed, students were told to preserve in-situ colors rather than smudging them when flattening the surface of the cross section.

Groups were allowed to choose 3 to 5 plots per site, several of which were chosen based on contrasting environmental conditions (e.g., upland vs. lowland; high versus low canopy coverage). Once sampling began, students were directed to measure colors (n = 3: surface, 0–15 cm, 15–30 cm) at each plot.

While the Nix links to phones via Bluetooth technology, only one device can be connected at a time; thus, each group had one student “in charge” of using the Nix app, which was comprised of (1) scanning colors; (2) creating color folders, or “swatches”, for each site; (3) naming colors with an ID which were to follow the convention “Site(acronym)_Plot#_Depth" (e.g., “AFC1_0to15” for the first plot at the Aquatic Fitness Center and for the color between 0 and 15 cm); and, finally, (4) saving and exporting the color measurements, from which .csv files would be obtained for each swatch of saved color scans. As the Nix app does not save GPS data per scan, a secondary student was directed to record GPS data through geotagged pictures at each plot.

**Comprehensive understanding through a final report**

Using their Nix .csv files and GPS data, students were tasked with writing a final report that connected their field methods to data analysis (Figure 11).

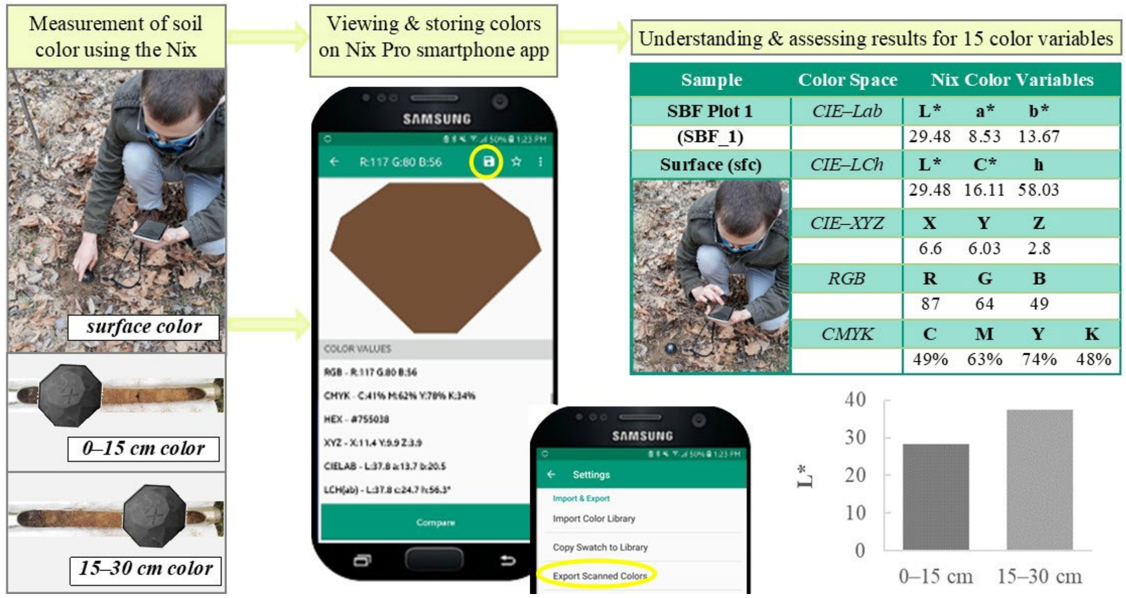


**Figure 11.** Summary of the process students participated in for the Ecological Sustainability class, starting with field measurements of soil color using the Nix, and culminating in an assessment of colors they scanned across campus

Several students focused on color differences across depth intervals, using Nix variables like $L^*$ (lightness) and $C^*$ (chroma) from the Commission on International Illumination (CIE) Lab and LCH color spaces, as $L^*$ and $C^*$ mirror the Munsell space variables $V$ (value) and $C_M$ (chroma) respectively. The 15 color space variables overwhelmed some students, but our previous research linking Nix color variables to the MSCC variables gave them several variables to focus on, such as $L^*$ and the easily-calculated $X/(X+Y+Z)$ from the CIE–XYZ color space (Schmidt and Ahn 2021b).

## Learning outcomes: Improved environmental literacy

While data organization and analysis were key aspects of students' reports, the success of the project was more measured qualitatively by students' gauged engagement and learning during and after the project. During a time when most classes were virtual, students reported a connection to their environment missing from the online lectures and Zoom sessions of other classes. Moreover, many students reported a better understanding of the role of soil and urban hydrology in sustainable land management—for example, more highly flooded areas near the wetland mesocosm compounded tended to show "gley" colors than did the sandy, dark orange colors in the upland forest. While the Nix automates the color determination in comparison to the MSCC and thus may remove some tangibility gained through the subjective judgment-based MSCC method, students nonetheless expressed a similar sense of interaction and connection to the soils underneath their feet using the Nix. This was enhanced by one key capability of the Nix: side-by-side comparison of two colors to one another, both numerically (e.g., $RGB_{1st\ plot}$ versus $RGB_{2nd\ plot}$) and perceptually via the side-by-side half-diamond display in the app. Through the comparison feature, students could take a 15–30 cm color measurement at the wetland area (gleyed) and visually compare its color to that of the upland forest while also seeing differences in variables like CIE–Lab $L^*$ and CMYK $M_K$ (magenta).

Ecological literacy goes beyond gained interaction and requires the use of ecological understanding in "living in, enjoying, and/or studying the environment" (Berkowitz et al. 2005). Although birdwatching and plant/wildlife photography may have no direct analogy within the pedosphere, many students gained curiosity into the mysteries of the soils underneath their feet, viewing soil as another medium worthy of monitoring and appreciating (indicated through personal communication). While such appreciation can be gained using a Munsell chart without a gadget like the Nix, the latter's app component provides a way to transform color measurements into digital content, rendering a sense of digital achievement and desire to study and "achieve" more. Furthermore, several students were excited to spread community awareness of soil monitoring opportunities by showing what they found with the Nix, culminating in an undergraduate student presentation that analyzed soil color measurements across campus broadcast to all conference attendees.

## Development and refinement of the procedure

In applications of using color as an indicator of ecosystem function such as SOM or SOC contents, color alone often still needs to be supplemented with further soil analysis due to the modest rather than >90% regressions between field-based soil color measurements and SOM and/or soil carbon (Schmidt and Ahn 2021a); however, proper and standardized techniques using the Nix modified from those presented here can transform objective measurements of soil colors into informative ecosystem and/or land characterizations.

A key challenge to standardizing the act of soil color measurements at a specific location—be it with the MSCC or Nix—is the added variable of depth often not present in other environmental monitoring endeavors. Birdwatching is arguably a 3-dimensional activity, but the meaning of a bird siting 20 feet aboveground versus 30 feet aboveground is not key to successful citizen science. In contrast, depth and thickness of observed colors are significant variables in the monitoring of soil colors, and, ideally, both must be standardized, controlled, and/or noted in monitoring data. A key application of such monitoring is wetland soil, or *hydric soil*, identification, in which the presence of a depleted soil matrix at 15 cm provides a different implication from its presence at 35 cm, and a depleted soil matrix at 15 cm with a 1-cm thickness means something different than a depleted soil matrix at 15 cm with a 15-cm thickness (USDA–NRCS 2018). An amendment to the procedure would better control for thicknesses and starting depths by requiring students to also record starting depth and thickness when making their soil probe color measurements, requiring only the addition of a ruler.

Furthermore, soils across the world exhibit different patterns of horizonation, with various arrangements and thicknesses of soil horizons such as the organic (O) surface horizon that may or may not be present, the A horizon, and the B horizon (subsoil). The purpose of our procedure calling for 3 colors was to capture the O horizon (undisturbed surface measurement), A horizon (0–15 cm), and B horizon (15–30 cm), given both A and B horizons were present above 30 cm. Flexibility in measuring depth allowed students to use their discretion to find an area of homogenous color for each scan that did not rely on an understanding of soil horizonation, but was implicit in their decision-making. However, future amendments to the procedure could allow for more universal comparison of scans by more explicitly introducing the idea of horizonation into monitoring endeavors. This would first require a determination of a threshold value for ΔE—the color difference between two scans that is calculated by the Nix in its comparison feature—below which 0–15 cm and 15–30 cm samples would be deemed identical, and above which samples would be determined distinct and thus from two separate horizons. While such determinations could be made in post-processing, in order to account for soils with very thick O horizons, the procedure should require students to note if either their 0–15 cm or 15–30 cm sample came from the topmost organic layer of the soil when sampling. The inclusion of a surface color measurement provided a useful *reference* depth independent of soil horizonation, and future research could focus on the relationship between surface colors and functional attributes of soil ecology to provide a very universally applicable and easy-to-monitor feature of soils beneath our feet.

With exception to the wetland site near the Ahn Mesocosm Compound, this case study did not have students focusing on wetland areas, which tend to have redoximorphic features with highly mottled color patterns. Given color heterogeneity in soils without a soil matrix color comprising ≥60–70% of the matrix, the Nix poorly approximates soil color. Nonetheless, as seen with the highly gleyed soils at the lowest elevation within the wetland site, the Nix can still accurately assess surface colors, topsoil colors, and matrix colors of layers with low frequencies of redoximorphic features, rendering it most appropriate for seasonally to permanently flooded wetland soils that display gley or depleted horizons above 30 cm.

Overall, the procedure allowed students to (1) collect and monitor soils in less time than required using the MSCC, (2) produce numerical and digital data prime for crowdsourcing, and (3) compare colors across campus and between depth intervals. Because the Nix is not set up for crowdsourced and geotagged data, students were responsible for separately noting locations and descriptions, adding these notes into their spreadsheet of Nix-provided color data, and using GIS software if they were interested in graphically displaying their color results. To properly advocate for the use of the Nix in a greater community and/or global setting, the transfer of color measurements to a crowdsourced medium would require minor additional software development to append Nix measurement data. Such development could allow for a map of all colors across an area with a filter on depth (e.g., *surface*) showing which areas require greater investment and which areas may exhibit signs of wetland development (e.g., gleyed colors above 30 cm). Students were excited to brainstorm such ideas that were not yet fully developed during the execution of this class project, but are well within reach for the future of Nix-based color monitoring.

## **Applications for land and watershed management**

Even without a crowdsourced component to the Nix color sensor and app, the Nix provides ample opportunity for establishing citizen science and/or management-based monitoring programs for local, regional, and/or global soil colors that can dually enhance community environmental literacy. More relevant to wetland ecology is the monitoring and/or tracking of colors that may indicate the presence or development of a wetland ecosystem. Recently, "accidental," or unplanned, wetlands have been documented in areas that become flood-prone after altered weather patterns, landcover, and/or stormwater management lead to increased urban flood frequencies and intensities (Palta et al. 2017). As soil biogeochemical processes can lead to the gray/gley colors common of hydric soils in as little as 21 days (He et al. 2003), color measurements from the Nix can act as indicators of either well established or novel hydrologic regimes. Nix variable ranges can be linked to indicators of hydric soils—e.g., relationships to Munsell chroma $C_M \leq 2$ [hydric] and $C_M > 2$ [nonhydric] (Schmidt and Ahn 2021b)—thus transforming Nix measurements into an ecological radar that can act significantly faster than that of the MSCC, quickly connecting users to the unseen footprints of climate change and development.

Deliberate advancement of both monitoring scope and environmental literacy can be gained by the development of a citizen science and/or outreach program with local Soil and Water Conservation Districts, Master Naturalists, or other ecological education and advocacy focused groups. For individual monitoring events, it is not practical to expect interested parties to individually own Nix sensors, but community centers such as local libraries are prime candidates for hubs that can rent out Nix sensors to community members and/or groups. In tandem with scientist-led trainings and/or monitoring events, citizen monitoring can be guided by our Ecological Sustainability SOP with minor modification, allowing users to measure soil colors in the field, identify wetland or wetland-like areas, and/or augment their connection and understanding to soil ecology. With or without crowdsourced data, citizens would be faced with an opportunity to become better environmental stewards by documenting, explaining, and appreciating soil colors in their communities.

## Conclusions

Enhancing the capacity for soil color to be measured and assessed is a key aspect of making knowledge of soil functions more accessible and cost-effective. As we successfully deployed the Nix Color Sensor in a small-scale student setting, we are optimistic that larger-scale citizen science programs can similarly connect citizens to their pedosphere while expanding the scope of soil monitoring activities. Some modifications including software development may allow the Nix to be used in a crowdsourced setting, and we encourage interested researchers to connect with us for future methodological refinement and collaboration.

# CHAPTER SEVEN:
# CONCLUDING REMARKS—CONTRIBUTIONS TO SOIL SCIENCE, WETLAND ECOLOGY AND MANAGEMENT, AND SOCIETY

Even in the face of national agendas and policies that may alone fail the successful conservation and protection wetlands in urbanizing regions of the US, increased efficiency, accessibility, and both spatial and temporal extents of monitoring soil colors—key indicators of wetland ecosystem functions—is paramount to improving the sustainability of land management practices that ultimately govern ecological sustainability in a region (Xie et al. 2020). Using a tool like the Nix to complement the MSCC in both professional and lay citizen projects can enhance the process of delineating wetlands, identifying spaces that show promising signs of hydric soil development, mapping soil carbon storage and identifying key areas to conserve, and teaching stakeholders and students about soil colors in their own yards and green spaces.

In accordance with the urban ecology framework that investigates systems as mosaics of both the biological/physical and the social, development of appropriate land management practices to conserve/restore desired wetland services requires new perspectives not only related to soil management, but also the encouragement of positive interactions between humans and their soilscapes that can render such management practical and culturally valuable. Independent of the technical aspects of this dissertation that may require further study and refinement before a translation into to wetland science and management practices, the proposed methodologies and applications of measuring and monitoring soil colors provides a much-needed instigation of cultural appreciation for soils within the traditionally flora- and macrofauna-focused interpretations of wetlands. In promoting a more intuitive connection between ecosystem functions and observable and/or easily measurable ecosystem properties like soil color, I am optimistic that my research will benefit both wetland conservation and various stakeholders by fostering stronger connections to, and understanding of, an otherwise unseen soilscape.

## REFERENCES


Adams WA (1973) The effect of organic matter on the bulk and true densities of some uncultivated Podzolic soils. Journal of Soil Science 24:10–17. https://doi.org/10.1111/j.1365-2389.1973.tb00737.x

Adhikari D, Yang Y (2015) Selective stabilization of aliphatic organic carbon by iron oxide. Scientific Reports 5:11214. https://doi.org/10.1038/srep11214

Adhikari K, Hartemink AE (2016) Linking soils to ecosystem services — A global review. Geoderma 262:101–111. https://doi.org/10.1016/j.geoderma.2015.08.009

Ahn C, Gillevet PM, Sikaroodi M, Wolf KL (2009) An assessment of soil bacterial community structure and physicochemistry in two microtopographic locations of a palustrine forested wetland. Wetlands Ecology and Management 17:397–407. https://doi.org/10.1007/s11273-008-9116-4

Ahn C, Jones S (2013) Assessing organic matter and organic carbon contents in soils of created mitigation wetlands in Virginia. Environmental Engineering Research 18:151–156. https://doi.org/10.4491/eer.2013.18.3.151

Ahn C, Peralta RM (2012) Soil properties are useful to examine denitrification function development in created mitigation wetlands. Ecological Engineering 49:130–136. https://doi.org/10.1016/j.ecoleng.2012.08.039

Aitkenhead M, Coull M, Gwatkin R, Donnelly D (2016a) Automated soil physical parameter assessment using smartphone and digital camera imagery. Journal of Imaging 2:35. https://doi.org/10.3390/jimaging2040035

Aitkenhead M, Donnelly D, Coull M, Gwatkin R (2016b) Estimating soil properties with a mobile phone. In: Hartemink AE, Minasny B (eds) Digital Soil Morphometrics. Springer International Publishing, Cham, pp 89–110

Aitkenhead M, Donnelly D, Coull M, Hastings E (2014) Innovations in environmental monitoring using mobile phone technology – a review. International Journal of Interactive Mobile Technologies (iJIM) 8:42–50. https://doi.org/10.3991/ijim.v8i2.3645

Aitkenhead MJ, Donnelly D, Sutherland L, et al (2015) Predicting Scottish topsoil organic matter content from colour and environmental factors. European Journal of Soil Science 66:112–120. https://doi.org/10.1111/ejss.12199

Akoglu H (2018) User's guide to correlation coefficients. Turkish Journal of Emergency Medicine 18:91–93. https://doi.org/10.1016/j.tjem.2018.08.001

Al-rasheed AS (2015) Categorical perception of color: Evidence from secondary category boundary. Psychology Research and Behavior Management 8:273–285. https://doi.org/10.2147/PRBM.S78348

de Aquino RE, Marques J, Campos MCC, et al (2016) Characteristics of color and iron oxides of clay fraction in Archeological Dark Earth in Apuí region, southern Amazonas. Geoderma 262:35–44. https://doi.org/10.1016/j.geoderma.2015.07.010

Axt JR, Walbridge MR (1999) Phosphate removal capacity of palustrine forested wetlands and adjacent uplands in Virginia. Soil Science Society of America Journal 63:1019–1031. https://doi.org/10.2136/sssaj1999.6341019x

Bae J, Ryu Y (2015) Land use and land cover changes explain spatial and temporal variations of the soil organic carbon stocks in a constructed urban park. Landscape and Urban Planning 136:57–67. https://doi.org/10.1016/j.landurbplan.2014.11.015

Baldock JA, Skjemstad JO (2000) Role of the soil matrix and minerals in protecting natural organic materials against biological attack. Organic Geochemistry 31:697–710. https://doi.org/10.1016/S0146-6380(00)00049-8

Ballantine K, Schneider R (2009) Fifty-five years of soil development in restored freshwater depressional wetlands. Ecological Applications 19:1467–1480. https://doi.org/10.1890/07-0588.1

Barrett LR (2002) Spectrophotometric color measurement in situ in well drained sandy soils. Geoderma 108:49–77. https://doi.org/10.1016/S0016-7061(02)00121-0

Barron V, Torrent J (1986) Use of the Kubelka—Munk theory to study the influence of iron oxides on soil colour. Journal of Soil Science 37:499–510. https://doi.org/10.1111/j.1365-2389.1986.tb00382.x

Becker TE, Robertson MM, Vandenberg RJ (2019) Nonlinear transformations in organizational research: Possible problems and potential solutions. Organizational Research Methods 22:831–866. https://doi.org/10.1177/1094428118775205

Berkowitz AR, Ford ME, Brewer CA (2005) A framework for integrating ecological literacy, civics literacy, and environmental citizenship. In: Johnson EA, Mappin MJ (eds) Environmental Education and Advocacy: Changing Perspectives of Ecology and Education. Cambridge University Press, Cambridge, pp 227–266. http://www.bioed.org/pubs/EE_chapter_berkowitz_et_al.pdf. Accessed 28 May 2020

Berkowitz JF (2012) Updating Regional Supplements to the Corps of Engineers Wetland Delineation Manual. USACE Engineer Research and Development Center, Vicksburg, MS. https://apps.dtic.mil/sti/pdfs/ADA571250.pdf. Accessed 5 Apr 2022

Berkowitz JF, Page S, Noble CV (2014) Potential disconnect between observations of hydrophytic vegetation, wetland hydrology indicators, and hydric soils in unique pitcher plant bog habitats of the southern Gulf Coast. Southeastern Naturalist 13:721–734. https://doi.org/10.1656/058.013.0410

Berkowitz JF, VanZomeren CM, Currie SJ, Vasilas L (2017) Application of α,α’-dipyridyl dye for hydric soil identification. Soil Science Society of America Journal 81:654–658. https://doi.org/10.2136/sssaj2016.12.0431

Bernal B, Mitsch WJ (2013) Carbon sequestration in two created riverine wetlands in the midwestern United States. Journal of Environmental Quality 42:1236–1244. https://doi.org/10.2134/jeq2012.0229

Bestelmeyer BT, Tugel AJ, Peacock GL, et al (2009) State-and-transition models for heterogeneous landscapes: a strategy for development and application. Rangeland Ecology and Management 62:1–15. https://doi.org/10.2111/08-146

Bishel-Machung L, Brooks RP, Yates SS, Hoover KL (1996) Soil properties of reference wetlands and wetland creation projects in Pennsylvania. Wetlands 16:532–541. https://doi.org/10.1007/BF03161343

Blavet D, Mathe E, Leprun JC (2000) Relations between soil colour and waterlogging duration in a representative hillside of the West African granito-gneissic bedrock. CATENA 39:187–210. https://doi.org/10.1016/S0341-8162(99)00087-9

Blumm MC (2018) The Clinton Wetlands Plan: No net gain in wetlands protection. Florida State University Journal of Land Use and Environmental Law 9:1. https://ir.law.fsu.edu/jluel/vol9/iss2/1. Accessed 8 Jan 2019

Bollman MA, Storm MJ, King GA, Watrud LS (2012) Wetland and riparian plant communities at risk of invasion by transgenic herbicide-resistant Agrostis spp. in central Oregon. Plant Ecology 213:355–370. https://doi.org/10.1007/s11258-011-0015-z

Bossio DA, Cook-Patton SC, Ellis PW, et al (2020) The role of soil carbon in natural climate solutions. Nature Sustainability 3:391–398. https://doi.org/10.1038/s41893-020-0491-z

Bouma J, Fox C, Miedema R (1990) Micromorphology of hydromorphic soils: Applications for soil genesis and land evaluation. Developments in Soil Science 19:257–278. https://doi.org/10.1016/S0166-2481(08)70338-6

Brady NC, Weil RR (2008) The nature and properties of soils, Rev. 14. ed., Pearson Education International, Upper Saddle River, NJ

Brainard D, Smelser NJ, Baltes PB (2001) Color vision theory. In: International Encyclopedia of the Social and Behavioral Sciences. Elsevier, Oxford, pp 2256–2263. https://color2.psych.upenn.edu/brainard/papers/ColorTheory1.pdf. Accessed 5 Apr 2022

van Breemen N, Feijtel T (1990) Soil processes and properties involved in the production of greenhouse gases, with special relevance to soil taxonomic systems. In: Bouwman AF (eds) Soils and the greenhouse effect. International Soil Reference and Information Centre, Wageningen, Netherlands, pp 195–223

Bridgham SD, Megonigal JP, Keller JK, et al (2006) The carbon balance of North American wetlands. Wetlands 26:889–916. https://doi.org/10.1672/0277-5212(2006)26[889:TCBONA]2.0.CO;2

Brown P, O'Neal A (1923) The color of soils in relation to organic matter content. Iowa Agriculture and Home Economics Experiment Station Research Bulletin 75.

Caldwell PV, Adams AA, Niewoehner CP, et al (2005) Sampling device to extract intact cores in saturated organic soils. Soil Science Society of America Journal 69:2071–2075. https://doi.org/10.2136/sssaj2005.0150

Campbell DA, Cole CA, Brooks RP (2002) A comparison of created and natural wetlands in Pennsylvania, USA. Wetlands Ecology and Management 10:41–49. https://doi.org/10.1023/A:1014335618914

Campos RC, Demattê JAM (2004) Cor do solo: uma abordagem da forma convencional de obtenção em oposição à automatização do método para fins de classificação de solos. Revista Brasileira de Ciência do Solo 28:853–863. https://doi.org/10.1590/S0100-06832004000500008

Chaplot V, Bernoux M, Walter C, et al (2001) Soil carbon storage prediction in temperate hydromorphic soils using a morphologic index and digital elevation model. Soil Science 166:48–60. https://doi.org/10.1097/00010694-200101000-00008

Chaplot V, Walter C, Curmi P (2000) Improving soil hydromorphy prediction according to DEM resolution and available pedological data. Geoderma 97:405–422. https://doi.org/10.1016/S0016-7061(00)00048-3

Chen Y, Zhang M, Fan D, et al (2018) Linear regression between CIE-Lab color parameters and organic matter in soils of tea plantations. Eurasian Soil Science 51:199–203. https://doi.org/10.1134/S1064229318020011

Chi Y, Zheng W, Shi H, et al (2018) Spatial heterogeneity of estuarine wetland ecosystem health influenced by complex natural and anthropogenic factors. Science of The Total Environment 634:1445–1462. https://doi.org/10.1016/j.scitotenv.2018.04.085

Chimner RA, Ewel KC (2005) A tropical freshwater wetland: II. Production, decomposition, and peat formation. Wetlands Ecology and Management 13:671–684. https://doi.org/10.1007/s11273-005-0965-9

Cole CA, Brooks RP, Wardrop DH (2001) Assessing the relationship between biomass and soil organic matter in created wetlands of central Pennsylvania, USA. Ecological Engineering 17:423–428. https://doi.org/10.1016/S0925-8574(00)00171-3

Conrad CC, Hilchey KG (2011) A review of citizen science and community-based environmental monitoring: Issues and opportunities. Environmental Monitoring and Assessment 176:273–291. https://doi.org/10.1007/s10661-010-1582-5

Craft C, Broome S, Campbell C (2002) Fifteen years of vegetation and soil development after brackish-water marsh creation. Restoration Ecology 10:248–258. https://doi.org/10.1046/j.1526-100X.2002.01020.x

Dahl TE (1990) Wetland losses in the United States 1780s to 1980s. US Department of the Interior, Fish and Wildlife Service, Washington, D.C. https://www.fws.gov/wetlands/documents/Wetlands-Losses-in-the-United-States-1780s-to-1980s.pdf. Accessed 17 Dec 2018

Dahl TE (2000) Status and trends of wetlands in the conterminous United States 1986 to 1997. US Department of the Interior, Fish and Wildlife Service, Washington, D.C. https://www.fws.gov/wetlands/documents/Status-and-Trends-of-Wetlands-in-the-Conterminous-United-States-1986-to-1997.pdf. Accessed 17 Dec 2018

Dahl TE (2006) Status and trends of wetlands in the conterminous United States 1998 to 2004. US Department of the Interior, Fish and Wildlife Service, Washington, D.C. https://www.fws.gov/wetlands/documents/Status-and-Trends-of-Wetlands-in-the-Conterminous-United-States-1998-to-2004.pdf. Accessed 17 Dec 2018

Dahl TE (2011) Status and trends of wetlands in the conterminous United States 2004 to 2009. US Department of the Interior, Fish and Wildlife Service, Washington, D.C. https://www.fws.gov/wetlands/documents/status-and-trends-of-wetlands-in-the-conterminous-united-states-2004-to-2009.pdf. Accessed 17 Dec 2018

Dancey CP, Reidy J (2017) Statistics without maths for psychology, Seventh Edition. Pearson, New York

D'Angelo EM (2005) Phosphorus sorption capacity and exchange by soils from mitigated and late successional bottomland forest wetlands. Wetlands 25:297–305. https://doi.org/10.1672/6

Daniels RB, Gamble EE (1967) The edge effect in some ultisols in the North Carolina Coastal Plain. Geoderma 1:117–124. https://doi.org/10.1016/0016-7061(67)90003-1

Daniels RB, Gamble EE, Nelson LA (1971) Relations between soil morphology and water-table Levels on a dissected North Carolina Coastal Plain surface 1. Soil Science Society of America Journal 35:781–784. https://doi.org/10.2136/sssaj1971.03615995003500050041x

Daniels RB, Simonson GH, Handy RL (1961) Ferrous iron content and color of sediments. Soil Science 91:378–382

Davis L (1995) A handbook of constructed wetlands: A guide to creating wetlands for agricultural wastewater, domestic wastewater, coal mine drainage, and stormwater in the Mid-Atlantic region. Volume 1: General considerations. USDA–NRCS and the US Protection Agency, Washington, D.C. http://biblioteca.cehum.org/bitstream/CEHUM2018/1287/1/Davis.%20A%20Handbook%20of%20Constructed%20Wetlands%2C%20Volume%201%2C%20General%20Considerations.pdf. Accessed 5 Dec 2021

Dee SM, Ahn C (2012) Soil properties predict plant community development of mitigation wetlands created in the Virginia Piedmont, USA. Environmental Management 49:1022–1036. https://doi.org/10.1007/s00267-012-9838-1

Dewey JC, Schoenholtz SH, Shepard JP, Messina MG (2006) Issues related to wetland delineation of a Texas, USA bottomland hardwood forest. Wetlands 26:410–429. https://doi.org/10.1672/0277-5212(2006)26[410:IRTWDO]2.0.CO;2

Dorau K, Wessel-Bothe S, Milbert G, et al (2020) Climate change and redoximorphosis in a soil with stagnic properties. CATENA 190:104528. https://doi.org/10.1016/j.catena.2020.104528

Ehrenfeld JG (2005) Vegetation of forested wetlands in urban and suburban landscapes in New Jersey. The Journal of the Torrey Botanical Society 132:262–279. https://doi.org/10.3159/1095-5674(2005)132[262:VOFWIU]2.0.CO;2

Ehrich EL (2010) Pedogenic fate and transport of total mercury across subaerial and subaqueous soils in an Appalachian plateau impoundment. Master Thesis, Pennsylvania State University. https://etda.libraries.psu.edu/files/final_submissions/1783. Accessed 5 Dec 2021

Elless MP, Rabenhorst MC, James BR (1996) Redoximorphic features in soils of the Triassic Culpeper Basin. Soil Science 161:58–69. https://doi.org/10.1097/00010694-199601000-00008

Elliot AJ (2015) Color and psychological functioning: a review of theoretical and empirical work. Frontiers in Psychology 6:368. https://doi.org/10.3389/fpsyg.2015.00368

Environmental Laboratory (1987) Corps of Engineers Wetland Delineation Manual. USACE Environmental Laboratory, Vicksburg, MS. https://www.lrh.usace.army.mil/Portals/38/docs/USACE%2087%20Wetland%20Delineation%20Manual.pdf. Accessed 5 Jan 2021

Evans CV, Franzmeier D (1986) Saturation, aeration, and color patterns in a toposequence of soils in North-central Indiana 1. Soil Science Society of America Journal 50:975–980

Evans CV, Franzmeier DP (1988) Color index values to represent wetness and aeration in some Indiana soils. Geoderma 41:353–368. https://doi.org/10.1016/0016-7061(88)90070-5

Fan Z, Herrick JE, Saltzman R, et al (2017) Measurement of soil color: A comparison between smartphone camera and the Munsell Color Charts. Soil Science Society of America Journal 81:1139–1146. https://doi.org/10.2136/sssaj2017.01.0009

Federal Register (1994) Changes in hydric soils of the United States. https://www.loc.gov/item/fr027074/. Accessed 17 Sept 2018

Fiedler S, Sommer M (2004) Water and redox conditions in wetland soils—their influence on pedogenic oxides and morphology. Soil Science Society of America Journal 68:326–335. http://dx.doi.org/10.2136/sssaj2004.0326

Franzmeier DP, Yahner JE, Steinhardt GC, Sinclair HR (1983) Color patterns and water table levels in some Indiana soils. Soil Science Society of America Journal 47:1196–1202. https://doi.org/10.2136/sssaj1983.03615995004700060027x

Fretwell JD, Williams JS, Redman PJ (1996) National Water Summary on Wetland Resources. United States Geological Survey. https://doi.org/10.3133/wsp2425

Fuller BG (2007) Banshee Reeks Nature Preserve General Management Plan. Loudoun County Department of Parks, Recreation, and Community Services – Division of Facilities Planning and Development

Genthner MH, Daniels W, Hodges RL, Thomas P (1998) Redoximorphic features and seasonal water table relations, upper Coastal Plain, Virginia. In: Rabenhorst MC, Bell JC, McDaniel PA (eds) Quantifying Soil Hydromorphology, pp 43–60. https://doi.org/10.2136/sssaspecpub54.c3

Giannopoulos G, Lee DY, Neubauer SC, et al (2019) A simple and effective sampler to collect undisturbed cores from tidal marshes. bioRxiv 515825. https://doi.org/10.1101/515825

Giese L, Flannagan C (2006) Soil properties in Northern Virginia created forested wetlands. In: Hydrology and Management of Forested Wetlands, Proceedings of the International Conference, April 8-12, 2006, New Bern, North Carolina. American Society of Agricultural and Biological Engineers

Giese LA, Aust WM, Trettin CC, Kolka RK (2000) Spatial and temporal patterns of carbon storage and species richness in three South Carolina coastal plain riparian forests. Ecological Engineering 15: S157-S170. http://dx.doi.org/10.1016/S0925-8574(99)00081-6

Gómez-Robledo L, López-Ruiz N, Melgosa M, et al (2013) Using the mobile phone as Munsell soil-colour sensor: An experiment under controlled illumination conditions. Computers and Electronics in Agriculture 99:200–208. https://doi.org/10.1016/j.compag.2013.10.002

Guertal WR, Hall GF (1990) Relating soil color to water table levels. The Ohio Journal of Science 90:118–124

Guo LB, Gifford RM (2002) Soil carbon stocks and land use change: a meta-analysis. Global Change Biology 8:345–360. https://doi.org/10.1046/j.1354-1013.2002.00486.x

Gupta RK, Abrol IP, Finkl CW, et al (2008) Soil color. In: Chesworth W (ed) Encyclopedia of Soil Science. Springer Netherlands, Dordrecht, pp 641–643. https://doi.org/10.1007/978-1-4020-3995-9_534

Guthrie RL, Hajek BF (1979) Morphology and water regime of a Dothan soil 1. Soil Science Society of America Journal 43:142–144. https://doi.org/10.2136/sssaj1979.03615995004300010027x

Han P, Dong D, Zhao X, et al (2016) A smartphone-based soil color sensor: For soil type classification. Computers and Electronics in Agriculture 123:232–241. https://doi.org/10.1016/j.compag.2016.02.024

He X, Vepraskas MJ, Lindbo D, Skaggs R (2003) A method to predict soil saturation frequency and duration from soil color. Soil Science Society of America Journal 67:961–969

Heath RC (1984) Ground-water regions of the United States. U.S. Department of the Interior, Geological Survey, Washington, D.C. https://doi.org/10.3133/wsp2242

Heller DL (2019) Research Guides: Clean Water Act Legal Research: Overview. In: Pace Law School Library Research Guides. https://libraryguides.law.pace.edu/c.php?g=319426&p=2133615. Accessed 8 Jan 2019

Hodgen J (2016) Comparison of Nix Color Sensor and Nix Color Sensor Pro to standard meat science research colorimeters. Meat Science 112:159. https://doi.org/10.1016/j.meatsci.2015.08.129

Holman BW, Kerr MJ, Morris S, Hopkins DL (2019) The identification of dark cutting beef carcasses in Australia, using Nix Pro Color Sensor™ colour measures, and their relationship to bolar blade, striploin and topside quality traits. Meat Science 148:50–54. https://doi.org/10.1016/j.meatsci.2018.10.002

Holman BWB, Collins D, Kilgannon AK, Hopkins DL (2018) The effect of technical replicate (repeats) on Nix Pro Color Sensor™ measurement precision for meat: A case-study on aged beef colour stability. Meat Science 135:42–45. https://doi.org/10.1016/j.meatsci.2017.09.001

Holman BWB, Hopkins DL (2019) A comparison of the Nix Colour Sensor Pro™ and HunterLab MiniScan™ colorimetric instruments when assessing aged beef colour stability over 72 h display. Meat Science 147:162–165. https://doi.org/10.1016/j.meatsci.2018.09.009

Hossler K, Bouchard V (2010) Soil development and establishment of carbon-based properties in created freshwater marshes. Ecological Applications 20:539–553. https://doi.org/10.1890/08-1330.1

Hunt RWG, Pointer MR (2011) Measuring Colour. John Wiley & Sons, Chichester, West Sussex, United Kingdom

Ibáñez-Asensio S, Marqués-Mateu A, Moreno-Ramón H, Balasch S (2013) Statistical relationships between soil colour and soil attributes in semiarid areas. Biosystems Engineering 116:120–129. https://doi.org/10.1016/j.biosystemseng.2013.07.013

Ibraheem NA, Hasan MM, Khan RZ, Mishra PK (2012) Understanding color models: a review. ARPN Journal of Science and Technology 2:265–275

Jackson CR, Thompson JA, Kolka RK (2014) Wetland soils, hydrology and geomorphology. In: Batzer D, Sharitz R (eds) Ecology of Freshwater and Estuarine Wetlands. Berkeley, CA, University of California Press, pp 23-60. https://doi.org/10.1525/9780520959118-004

Jacobs PM, West LT, Shaw JN (2002) Redoximorphic features as indicators of seasonal saturation, Lowndes County, Georgia. Soil Science Society of America Journal 66:315–323. https://doi.org/10.2136/sssaj2002.3150

Jien S-H, Hseu Z, Chen Z (2004) Relations between morphological color index and soil wetness condition of anthraquic soils in Taiwan. Soil Science 169:871–882. https://doi.org/10.1097/01.ss.0000149364.73688.68

Jien S-H, Hseu Z-Y, Tsai C-C, Chen Z-S (2016) Soil profile imaging for estimating the depth distributions of clay, iron, and hydrological conditions of soils under rice in Northern Taiwan. In: Hartemink AE, Minasny B (eds) Digital Soil Morphometrics. Springer International Publishing, Cham, pp 145–163. http://dx.doi.org/10.1007/978-3-319-28295-4_10

Jobbágy EG, Jackson RB (2000) The vertical distribution of soil organic carbon and its relation to climate and vegetation. Ecological Applications 10:423–436. https://doi.org/10.1890/1051-0761(2000)010[0423:TVDOSO]2.0.CO;2

Johansson T, Malmer N, Crill PM, et al (2006) Decadal vegetation changes in a northern peatland, greenhouse gas fluxes and net radiative forcing. Global Change Biology 12:2352–2369. https://doi.org/10.1111/j.1365-2486.2006.01267.x

Johnston C, Pinay G, Arens C, Naiman R (1995) Influence of soil properties on the biogeochemistry of a beaver meadow hydrosequence. Soil Science Society of America Journal 59:1789–1799. https://doi.org/10.2136/sssaj1995.03615995005900060041x

Jolliffe IT, Cadima J (2016) Principal component analysis: a review and recent developments. Philosophical Transactions of the Royal Society A: Mathematical, Physical and Engineering Sciences 374:20150202. https://doi.org/10.1098/rsta.2015.0202

Jones EJ, McBratney AB (2016) In situ analysis of soil mineral composition through conjoint use of visible, near-infrared and X-ray fluorescence spectroscopy. In: Hartemink AE, Minasny B (eds) Digital Soil Morphometrics. Springer International Publishing, Cham, pp 51–62. https://doi.org/10.1007/978-3-319-28295-4_4

Kachergis E, Rocca ME, Fernandez-Gimenez ME (2011) Indicators of ecosystem function identify alternate states in the sagebrush steppe. Ecological Applications 21:2781–2792. https://doi.org/10.1890/10-2182.1

Kellogg CE (1987) Soil Survey Manual (1938). US Department of Agriculture, Washington, D.C. https://www.nrcs.usda.gov/Internet/FSE_DOCUMENTS/nrcseprd1335010.pdf. Accessed 4 Apr 2022

Ketterings QM, Bigham JM (2000) Soil color as an indicator of slash-and-burn fire severity and soil fertility in Sumatra, Indonesia. Soil Science Society of America Journal 64:1826–1833. https://doi.org/10.2136/sssaj2000.6451826x

Kirillova N, Vodyanitskii YN, Sileva T (2015) Conversion of soil color parameters from the Munsell system to the CIE-L* a* b* system. Eurasian Soil Science 48:468–475. https://doi.org/10.1134/S1064229315050026

Kirillova NP, Grauer-Gray J, Hartemink AE, et al (2018) New perspectives to use Munsell Color Charts with electronic devices. Computers and Electronics in Agriculture 155:378–385. https://doi.org/10.1016/j.compag.2018.10.028

Köchy M, Hiederer R, Freibauer A (2015) Global distribution of soil organic carbon – Part 1: Masses and frequency distributions of SOC stocks for the tropics, permafrost regions, wetlands, and the world. SOIL 1:351–365. https://doi.org/10.5194/soil-1-351-2015

Konen ME, Burras CL, Sandor JA (2003) Organic carbon, texture, and quantitative color measurement relationships for cultivated soils in north central Iowa. Soil Science Society of America Journal 67:1823–1830. https://doi.org/10.2136/sssaj2003.1823

Lal R (2004) Soil carbon sequestration impacts on global climate change and food Security. Science 304:1623–1627. https://doi.org/10.1126/science.1097396

Ledford K, Schmidt SA, Ahn C (2022) Assessing carbon storage potential of forested wetland soils in two physiographic provinces of Northern Virginia, USA. Sustainability 14:2048. https://doi.org/10.3390/su14042048

Lees KJ, Quaife T, Artz RRE, et al (2018) Potential for using remote sensing to estimate carbon fluxes across northern peatlands – a review. Science of The Total Environment 615:857–874. https://doi.org/10.1016/j.scitotenv.2017.09.103

Li X, McCarty GW, Lang M, et al (2018) Topographic and physicochemical controls on soil denitrification in prior converted croplands located on the Delmarva Peninsula, USA. Geoderma 309:41–49. https://doi.org/10.1016/j.geoderma.2017.09.003

Liles GC, Beaudette DE, O'Geen AT, Horwath WR (2013) Developing predictive soil C models for soils using quantitative color measurements. Soil Science Society of America Journal 77:2173–2181. https://doi.org/10.2136/sssaj2013.02.0057

Lima O (2014) Interactive Munsell Color Space Simulator. https://munsell.com/color-blog/interactive-color-space-simulator/. Accessed 5 Jan 2019

Lindig-Cisneros R, Desmond J, Boyer KE, Zedler JB (2003) Wetland restoration thresholds: Can a degradation transition be reversed with increased effort? Ecological Applications 13:193–205. https://www.jstor.org/stable/3099959

Loudoun County Office of Mapping and Geographic Information (2021) Aerial Archive, 1957 Imagery. https://logis.loudoun.gov/archive/ Accessed 5 Dec 2021

Mahyar F, Cheung V, Westland S (2010) Different transformation methods between CIELAB coordinates and Munsell hue. Coloration Technology 126:31–36. https://doi.org/10.1111/j.1478-4408.2010.00224.x

Malone BP, McBratney AB, Budiman Minasny (2018) Description and spatial inference of soil drainage using matrix soil colours in the Lower Hunter Valley, New South Wales, Australia. PeerJ. https://doi.org/10.7717/peerj.4659

Malvar HS, Sullivan GJ, Srinivasan S (2008) Lifting-based reversible color transformations for image compression. In: Applications of Digital Image Processing XXXI 7073:707307. http://dx.doi.org/10.1117/12.797091

Mancini M, Weindorf DC, Monteiro MEC, et al (2020) From sensor data to Munsell color system: Machine learning algorithm applied to tropical soil color classification via Nix$^{TM}$ Pro sensor. Geoderma 375:114471. https://doi.org/10.1016/j.geoderma.2020.114471

Markewich HW, Pavich MJ, Buell GR (1990) Contrasting soils and landscapes of the Piedmont and Coastal Plain, eastern United States. Geomorphology 3:417–447. https://doi.org/10.1016/0169-555X(90)90015-I

Marqués-Mateu Á, Balaguer-Puig M, Moreno-Ramón H, Ibáñez-Asensio S (2015) A laboratory procedure for measuring and georeferencing soil colour. In: The International Archives of Photogrammetry, Remote Sensing and Spatial Information Sciences; Gottingen. Copernicus Gesellschaft mbH, Gottingen, Germany, pp 57–64

Martens DA, Frankenberger Jr. WT (1992) Modification of infiltration rates in an organic-amended irrigated soil. Agronomy Journal 84:707–717. https://doi.org/10.2134/agronj1992.00021962008400040032x

Marutho D, Handaka SH, Wijaya E, Muljono (2018) The determination of cluster number at k-mean using elbow method and purity evaluation on Headline News. In: 2018 International Seminar on Application for Technology of Information and Communication, pp 533–538. https://doi.org/10.1109/ISEMANTIC.2018.8549751

Meersmans J, Wesemael BV, Molle MV (2009) Determining soil organic carbon for agricultural soils: a comparison between the Walkley & Black and the dry combustion methods (north Belgium). Soil Use and Management 25:346–353. https://doi.org/10.1111/j.1475-2743.2009.00242.x

Megonigal JP, Patrick WH, Faulkner SP (1993) Wetland identification in seasonally flooded forest soils: Soil morphology and redox dynamics. Soil Science Society of America Journal 57:140–149. https://doi.org/10.2136/sssaj1993.03615995005700010027x

Menne MJ, Durre I, Korzeniewski B, et al (2012) Global Historical Climatology Network - Daily (GHCN-Daily), Version 3 [Daily Summaries]. NOAA National Climatic Data Center. https://doi.org/10.7289/V5D21VHZ

Mikhailova EA, Stiglitz RY, Post CJ, et al (2017) Predicting soil organic carbon and total nitrogen in the Russian Chernozem from depth and wireless color sensor measurements. Eurasian Soil Science 50:1414–1419. https://doi.org/10.1134/S106422931713004X

Mitsch WJ, Gosselink JG (2015) Wetlands, 5th edn. John Wiley & Sons Inc, Somerset, NJ

Mokma D, Cremeens D (1991) Relationships of saturation and B horizon colour patterns in soils of three hydrosequences in south-central Michigan, USA. Soil Use and Management 7:56–60. https://doi.org/10.1111/j.1475-2743.1991.tb00848.x

Mokma D, Sprecher S (1994) Water table depths and color patterns in soils developed from red parent materials in Michigan, USA. CATENA 22:287–298. https://doi.org/10.1016/0341-8162(94)90039-6

Moonrungsee N, Pencharee S, Jakmunee J (2015) Colorimetric analyzer based on mobile phone camera for determination of available phosphorus in soil. Talanta 136:204–209. https://doi.org/10.1016/j.talanta.2015.01.024

Moore T (1974) Gley morphology and soil water regimes in some soils in south-central England. Geoderma 11:297–304. https://doi.org/10.1016/0016-7061(74)90056-1

Morgan CP, Stolt MH (2004) A comparison of several approaches to monitor water-table fluctuations. Soil Science Society of America Journal 68:562–566. https://doi.org/10.2136/sssaj2004.5620

Moritsuka N, Matsuoka K, Katsura K, et al (2014) Soil color analysis for statistically estimating total carbon, total nitrogen and active iron contents in Japanese agricultural soils. Soil Science and Plant Nutrition 60:475–485. https://doi.org/10.1080/00380768.2014.906295

Mukaka MM (2012) Statistics corner: A guide to appropriate use of correlation coefficient in medical research. Malawi Medical Journal 24:69–71

Mukhopadhyay S, Chakraborty S (2020) Use of diffuse reflectance spectroscopy and Nix pro color sensor in combination for rapid prediction of soil organic carbon. Computers and Electronics in Agriculture 176:105630. https://doi.org/10.1016/j.compag.2020.105630

Mukhopadhyay S, Chakraborty S, Bhadoria PBS, et al (2020) Assessment of heavy metal and soil organic carbon by portable X-ray fluorescence spectrometry and NixPro$^{TM}$ sensor in landfill soils of India. Geoderma Regional 20:e00249. https://doi.org/10.1016/j.geodrs.2019.e00249

Munsell AH (1905) A Color Notation. G. H. Ellis Company, Boston, MA

Munsell Color (2010). Munsell soil-color charts: With genuine Munsell color chips. Munsell Color, Grand Rapids, MI

Nahlik AM, Fennessy MS (2016) Carbon storage in US wetlands. Nature Communications 7:13835. https://doi.org/10.1038/ncomms13835

National Research Council (1995) Wetlands: Characteristics and Boundaries. The National Academies Press, Washington, D.C. https://doi.org/10.17226/4766

National Research Council (2001) Compensating for wetland losses under the Clean Water Act. The National Academies Press, Washington, D.C. https://doi.org/10.17226/10134

Nave LE, DeLyser K, Butler-Leopold PR, et al (2019) Effects of land use and forest management on soil carbon in the ecoregions of Maryland and adjacent eastern United States. Forest Ecology and Management 448:34–47. https://doi.org/10.1016/j.foreco.2019.05.072

Neitz J, Carroll J, Yamauchi Y, et al (2002) Color perception is mediated by a plastic neural mechanism that is adjustable in adults. Neuron 35:783–792. https://doi.org/10.1016/s0896-6273(02)00818-8

Nix Sensor Ltd. (2022) Nix Device Comparison. https://www.nixsensor.com/compare-nix/ Accessed 2 Mar 2022

Noe GB (2011) Measurement of net nitrogen and phosphorus mineralization in wetland soils using a modification of the resin-core technique. Soil Science Society of America Journal 75:760–770. https://doi.org/10.2136/sssaj2010.0289

Odeh IOA, McBratney AB (2005) Pedometrics. In: Hillel D (ed) Encyclopedia of Soils in the Environment. Elsevier, Oxford, pp 166–175. https://doi.org/10.1016/B0-12-348530-4/00020-5

O'Donnell TK, Goyne KW, Miles RJ, et al (2010) Identification and quantification of soil redoximorphic features by digital image processing. Geoderma 157:86–96. https://doi.org/10.1016/j.geoderma.2010.03.019

O'Donnell TK, Goyne KW, Miles RJ, et al (2011) Determination of representative elementary areas for soil redoximorphic features identified by digital image processing. Geoderma 161:138–146. https://doi.org/10.1016/j.geoderma.2010.12.011

O'Driscoll M, Clinton S, Jefferson A, et al (2010) Urbanization effects on watershed hydrology and in-stream processes in the southern United States. Water 2:605–648. https://doi.org/10.3390/w2030605

Page RW, Wilcher LS (1990) Memorandum of agreement between the Department of the Army and the EPA concerning the determination of mitigation under the Clean Water Act Section 404(b)(1) Guidelines. US Army/EPA, Washington, D.C. https://www.epa.gov/sites/default/files/2019-05/documents/1990_army-epa_mitigation_moa.pdf. Accessed 17 Dec 2018

Palacin-Silva M, Porras J (2018) Shut up and take my environmental data! A study on ICT enabled citizen science practices, participation approaches and challenges. EPiC Series in Computing 52:270–288. https://doi.org/10.29007/mk4k

Palta MM, Ehrenfeld JG, Giménez D, et al (2016) Soil texture and water retention as spatial predictors of denitrification in urban wetlands. Soil Biology and Biochemistry 101:237–250. https://doi.org/10.1016/j.soilbio.2016.06.011

Palta MM, Grimm NB, Groffman PM (2017) "Accidental" urban wetlands: Ecosystem functions in unexpected places. Frontiers in Ecology and the Environment 15:248–256. https://doi.org/10.1002/fee.1494

Paul J (2017) In our backyard: Banshee Reeks, a Virginia treasure. In: Loudoun Now. http://loudounnow.com/2017/03/24/in-our-backyard-banshee-reeks-a-virginia-treasure/. Accessed 18 Dec 2018

Pek J, Wong O, Wong A (2019) Data transformations for inference with linear regression: Clarifications and recommendations. Practical Assessment, Research, and Evaluation 22, Article 9. https://doi.org/10.7275/2w3n-0f07

Pendleton RL, Nickerson D (1951) Soil colors and special Munsell Soil Color Charts. Soil Science 71:35–44. http://doi.org/10.1097/00010694-195101000-00004

Peralta RM, Ahn C, Gillevet PM (2013) Characterization of soil bacterial community structure and physicochemical properties in created and natural wetlands. Science of the Total Environment 443:725–732. https://doi.org/10.1016/j.scitotenv.2012.11.052

Pocock MJO, Tweddle JC, Savage J, et al (2017) The diversity and evolution of ecological and environmental citizen science. PLoS One 12:e0172579. https://doi.org/10.1371/journal.pone.0172579

Post WM, Izaurralde RC, Mann LK, Bliss N (2001) Monitoring and verifying changes of organic carbon in soil. In: Rosenberg NJ, Izaurralde RC (eds) Storing Carbon in Agricultural Soils: A Multi-Purpose Environmental Strategy. Springer Netherlands, Dordrecht, pp 73–99. https://doi.org/10.1007/978-94-017-3089-1_4

Pretorius M, Huyssteen C, Brown L (2017) Soil color indicates carbon and wetlands: Developing a color-proxy for soil organic carbon and wetland boundaries on sandy coastal plains in South Africa. Environmental Monitoring and Assessment 189:1–18. https://doi.org/10.1007/s10661-017-6249-z

Pruitt BA (2001) Hydrologic and soil conditions across hydrogeomorphic settings. Dissertation, University of Georgia. https://getd.libs.uga.edu/pdfs/pruitt_bruce_a_200108_phd.pdf. Accessed 26 March 2021

Pulighe G, Fava F, Lupia F (2016) Insights and opportunities from mapping ecosystem services of urban green spaces and potentials in planning. Ecosystem Services 22:1–10. https://doi.org/10.1016/j.ecoser.2016.09.004

R Core Team (2013) R: A Language and Environment for Statistical Computing. Version 4.0.0. R Foundation for Statistical Computing, Vienna. http://www.R-project.org/. Accessed 5 Dec 2021

Rabenhorst M, Schmehling A, Thompson JA, et al (2015) Reliability of soil color standards. Soil Science Society of America Journal 79:193–199. https://doi.org/10.2136/sssaj2014.10.0401

Rabenhorst MC, Parikh S (2000) Propensity of soils to develop redoximorphic color changes. Soil Science Society of America Journal 64:1904–1910. https://doi.org/10.2136/sssaj2000.6451904x

Rawlins BG, Vane CH, Kim AW, et al (2008) Methods for estimating types of soil organic carbon and their application to surveys of UK urban areas. Soil Use and Management 24:47–59. https://doi.org/10.1111/j.1475-2743.2007.00132.x

Raymond JE, Fernandez IJ, Ohno T, Simon K (2013) Soil drainage class influences on soil carbon in a New England forested watershed. Soil Science Society of America Journal 77:307–317. https://doi.org/10.2136/sssaj2012.0129

Rice TD (1941) Preliminary color standards and color names for soils. US Department of Agriculture, Washington, D.C.

Richardson J, Hole F (1979) Mottling and iron distribution in a Glossoboralf-Haplaquoll hydrosequence on a glacial moraine in northwestern Wisconsin 1. Soil Science Society of America Journal 43:552–558. https://doi.org/10.2136/sssaj1979.03615995004300030024x

Roper WR, Robarge WP, Osmond DL, Heitman JL (2019) Comparing four methods of measuring soil organic matter in North Carolina soils. Soil Science Society of America Journal 83:466–474. https://doi.org/10.2136/sssaj2018.03.0105

Rossi AM, Rabenhorst MC (2016) Pedogenesis and landscape relationships of a Holocene age barrier island. Geoderma 262:71–84. https://doi.org/10.1016/j.geoderma.2015.08.004

Ruck L, Brown CT (2015) Quantitative analysis of Munsell color data from archeological ceramics. Journal of Archaeological Science: Reports 3:549–557. https://doi.org/10.1016/j.jasrep.2015.08.014

Sahoo UK, Singh SL, Gogoi A, et al (2019) Active and passive soil organic carbon pools as affected by different land use types in Mizoram, Northeast India. PLoS One 14:1. https://doi.org/10.1371/journal.pone.0219969

Sánchez-Marañón M, García PA, Huertas R, et al (2011) Influence of natural daylight on soil color description: assessment using a color-appearance model. Soil Science Society of America Journal 75:984–993. https://doi.org/10.2136/sssaj2010.0336

Sanyal S, Amrani F, Dallongeville A, et al (2017) Estimating indoor galaxolide concentrations using predictive models based on objective assessments and data about dwelling characteristics. Inhalation Toxicology 29:611–619. https://doi.org/10.1080/08958378.2018.1432729

Säynäjoki E-S, Korba P, Kalliala E, Nuotio A-K (2018) GHG Emissions reduction through urban planners' improved control over earthworks: a case study in Finland. Sustainability 10:1–1. https://doi.org/10.3390/su10082859

Schelling J (1960) New aspects of soil classification with particular reference to reclaimed hydromorphic soils. Transactions of the 7th International Congress of Soil Science 4:218–224

Schlesinger WH (1990) Evidence from chronosequence studies for a low carbon-storage potential of soils. Nature 348:232–234. https://doi.org/10.1038/348232a0

Schlichting E, Schwertmann U (1973) Pseudogley and gley: Genesis and use of hydromorphic soils. Transactions of Commissions V and VI of the International Society of Soil Science. Verlag Chemie, Weinheim, Germany

Schmidt SA, Ahn C (2019) A comparative review of methods of using soil colors and their patterns for wetland ecology and management. Communications in Soil Science and Plant Analysis 50:1293–1309. https://doi.org/10.1080/00103624.2019.1604737

Schmidt SA, Ahn C (2021a) Predicting forested wetland soil carbon using quantitative color sensor measurements in the region of northern Virginia, USA. Journal of Environmental Management 300:113823. https://doi.org/10.1016/j.jenvman.2021.113823

Schmidt SA, Ahn C (2021b) Analysis of soil color variables and their relationships between two field-based methods and its potential application for wetland soils. Science of The Total Environment 783:147005. https://doi.org/10.1016/j.scitotenv.2021.147005

Schmidt SA, Ahn C (2022) Characterization of redoximorphic features of forested wetland soils by simple hydro-physicochemical attributes in Northern Virginia, USA. Wetlands Ecology and Management 30:295–312. https://doi.org/10.1007/s11273-021-09855-z

Schober P, Boer C, Schwarte LA (2018) Correlation coefficients: Appropriate use and interpretation. Anesthesia & Analgesia 126:1763–1768. https://doi.org/10.1213/ANE.0000000000002864

Schoeneberger PJ, Wysocki DA, Benham EC, Soil Survey Staff (2012) Field Book for Describing and Sampling Soils, version 3.0. USDA–NRCS, National Soil Survey Center, Lincoln, NE.

https://www.nrcs.usda.gov/Internet/FSE_DOCUMENTS/nrcs142p2_052523.pdf. Accessed 17 Dec 2018

Schoenholtz SH, Miegroet HV, Burger JA (2000) A review of chemical and physical properties as indicators of forest soil quality: challenges and opportunities. Forest Ecology and Management 138:335–356. https://doi.org/10.1016/S0378-1127(00)00423-0

Schulze DG, Nagel JL, Scoyoc GEV, et al (1993) Significance of organic matter in determining soil colors. In: Bigham JM, Ciolkosz EJ (eds) Soil Color. John Wiley & Sons, Ltd, pp 71–90. https://doi.org/10.2136/sssaspecpub31.c5

Schwertmann U (1993) Relations between iron oxides, soil color, and soil formation. In: Bigham JM, Ciolkosz EJ (eds) Soil Color. John Wiley & Sons, Ltd, pp 51–69. https://doi.org/10.2136/sssaspecpub31.c4

Schwertmann U, Fanning D (1976) Iron-manganese concretions in hydrosequences of Soils in Loess in Bavaria 1. Soil Science Society of America Journal 40:731–738. https://doi.org/10.2136/sssaj1976.03615995004000050054x

Schwertmann U, Lentze W (1966) Bodenfarbe und Eisenoxidform. Zeitschrift für Pflanzenernährung, Düngung, Bodenkunde 115:209–214. https://doi.org/10.1002/jpln.19661150307

Schwertmann U, Taylor RM (1989) Iron oxides. In: Dixon JB, Weed SB (eds) Minerals in Soil Environments. John Wiley & Sons, Ltd, pp 379–438. https://doi.org/10.2136/sssabookser1.2ed.c8

Shields JA, St. Arnaud RJ, Paul EA, Clayton JS (1966) Measurement of soil color. Canadian Journal of Soil Science 46:83–90. https://doi.org/10.4141/cjss66-012

Silva PG, Roquero E, Rodriguez-Pascua M, et al (2013) Development of a numerical system and field-survey charts for earthquake environmental effects based on the Munsell Soil Color Charts. In: Seismic Hazard, Critical Facilities and Slow Active Faults. INQUA Focus Group on Paleoseismology and Active Tectonics

Simon FT, Frost JA (1987) A new method for the conversion of CIE colorimetric data to munsell notations. Color Research and Application 12:256–260. https://doi.org/10.1002/col.5080120506

Simonson GH, Boersma L (1972) Soil Morphology and Water Table Relations: II. Correlation Between Annual Water Table Fluctuations and Profile Features 1.

Soil Science Society of America Journal 36:649–653. https://doi.org/10.2136/sssaj1972.03615995003600040041x

Simonson RW (1993) Soil color standards and terms for field use—history of their development. In: Bigham JM, Ciolkosz EJ (eds) Soil Color. Soil Science Society of America 31:1–20. https://doi.org/10.2136/sssaspecpub31.c1

Simonson RW (1989) Historical Highlights of Soil Survey and Soil Classification with Emphasis on the United States, 1899-1970. International Soil Reference and Information Centre (ISRIC), Wageningen, The Netherlands. https://www.isric.org/sites/default/files/ISRIC_TechPap18.pdf. Accessed 5 June 2020

Six J, Conant RT, Paul EA, Paustian K (2002) Stabilization mechanisms of soil organic matter: Implications for C-saturation of soils. Plant and Soil 241:155–176. https://doi.org/10.1023/A:1016125726789

Spieles DJ (2005) Vegetation development in created, restored, and enhanced mitigation wetland banks of the United States. Wetlands 25:51–63. https://doi.org/10.1672/0277-5212(2005)025[0051:VDICRA]2.0.CO;2

Stiglitz RY, Mikhailova E, Post C, et al (2016a) Evaluation of an inexpensive sensor to measure soil color. Computers and Electronics in Agriculture 121:141–148. https://doi.org/10.1016/j.compag.2015.11.014

Stiglitz RY, Mikhailova E, Post C, et al (2017a) Using an inexpensive color sensor for rapid assessment of soil organic carbon. Geoderma 286:98–103. https://doi.org/10.1016/j.geoderma.2016.10.027

Stiglitz RY, Mikhailova E, Post C, et al (2016b) Teaching soil color determination using an inexpensive color sensor. Natural Sciences Education 45:1. https://doi.org/10.4195/nse2016.03.0005

Stiglitz RY, Mikhailova E, Post C, et al (2017b) Soil color sensor data collection using a GPS-enabled smartphone application. Geoderma 296:108–114. https://doi.org/10.1016/j.geoderma.2017.02.018

Stiglitz RY, Mikhailova EA, Sharp JL, et al (2018) Predicting soil organic carbon and total nitrogen at the farm scale using quantitative color sensor measurements. Agronomy 8:212. https://doi.org/10.3390/agronomy8100212

Stitt JM, Svancara LK, Vierling LA, Vierling KT (2019) Smartphone LIDAR can measure tree cavity dimensions for wildlife studies. Wildlife Society Bulletin 43:159–166. https://doi.org/10.1002/wsb.949

Stolt MH, Genthner MH, Daniels WL, et al (2000) Comparison of soil and other environmental conditions in constructed and adjacent palustrine reference wetlands. Wetlands 20:671–683. https://doi.org/10.1672/0277-5212(2000)020[0671:COSAOE]2.0.CO;2

Summers D, Lewis M, Ostendorf B, Chittleborough D (2011) Visible near-infrared reflectance spectroscopy as a predictive indicator of soil properties. Ecological Indicators 11:123–131. https://doi.org/10.1016/j.ecolind.2009.05.001

Tassinari C, Lagacherie P, Bouzigues R, Legros J (2002) Estimating soil water saturation from morphological soil indicators in a pedologically contrasted Mediterranean region. Geoderma 108:225–235. https://doi.org/10.1016/S0016-7061(02)00132-5

Teacher AGF, Griffiths DJ, Hodgson DJ, Inger R (2013) Smartphones in ecology and evolution: a guide for the app-rehensive. Ecology and Evolution 3:5268–5278. https://doi.org/10.1002/ece3.888

Thompson JA, Bell JC (1996) Color index for identifying hydric conditions for seasonally saturated mollisols in Minnesota. Soil Science Society of America Journal 60:1979–1988. https://doi.org/10.2136/sssaj1996.03615995006000060051x

Tiner RW (2017) Wetland indicators: a guide to wetland identification, delineation, classification, and mapping, Second edition. Taylor & Francis, Boca Raton. http://www.ncwetlands.org/wp-content/uploads/Tiner-2017-Wetland-indicators.pdf. Accessed 12 Oct 2018

Torn MS, Trumbore SE, Chadwick OA, et al (1997) Mineral control of soil organic carbon storage and turnover. Nature 389:170–173. https://doi.org/10.1038/38260

Torrent J, Barrón V (1993) Laboratory measurement of soil color: Theory and practice. In: Bigham JM, Ciolkosz EJ (eds) Soil Color. Soil Science Society of America, pp 21–33. https://doi.org/10.2136/sssaspecpub31.c2

Torrent J, Schwertmann U, Fechter H, Alferez F (1983) Quantitative relationships between soil color and hematite content. Soil Science 136:354–358

Turk JK, Young RA (2020) Field conditions and the accuracy of visually determined Munsell soil color. Soil Science Society of America Journal 84:163–169. https://doi.org/10.1002/saj2.20023

U.S. Army Corps of Engineers (2018) Performance Standards and Monitoring Protocol for Nontidal Wetland Mitigation Banks. www.nab.usace.army.mil/Portals/63/docs/Regulatory/Mitigation/4-3-18-IRT-NT-Wetland-Buffer-Monitoring-Protocol-Bank.pdf?ver=2018-07-05-155015-800. Accessed 19 Oct 2018

US EPA (2021) Watershed Index Online (WSIO) Indicator Data for EPA Region 3, Version 2.3. https://www.epa.gov/system/files/other-files/2021-12/20211112-wsio-indicator-data-v2.3-epa-region03_0.xlsx. Accessed 15 Jan 2022

U.S. Fish and Wildlife Service (2010) Elizabeth Hartwell Mason Neck and Featherstone National Wildlife Refuges: Draft Comprehensive Conservation Plan and the Environmental Assessment. https://www.fws.gov/northeast/planning/MasonNeck_Featherstone/draftccp/Entire_Document.pdf Accessed 18 June 2020

USDA–NRCS (2018) Field Indicators of Hydric Soils in the United States, Version 8.2. USDA–NRCS, in cooperation with the National Technical Committee for Hydric Soils., Washington, D.C. https://www.nrcs.usda.gov/Internet/FSE_DOCUMENTS/nrcs142p2_053171.pdf. Accessed 21 Nov 2018

USDA–NRCS Soil Survey Staff (2020) Web Soil Survey. Version 3.4.0 http://websoilsurvey.nrcs.usda.gov/app/WebSoilSurvey.aspx. Accessed 2 Apr 2022

Valeeva AA, Aleksandrova AB, Koposov GF (2016) Color estimation of forest-steppe soils by digital photography under laboratory conditions. Eurasian Soil Science 49:1033–1037. https://doi.org/10.1134/S1064229316090131

Van Aken H (2006) Munsell Conversion. Version 6.5.9. http://wallkillcolor.com/index2.htm. Accessed 21 Dec 2018

Van Huyssteen C, Ellis F, Lambrechts J (1997) The relationship between subsoil colour and degree of wetness in a suite of soils in the Grabouw district, Western Cape II. Predicting duration of water saturation and evaluation of colour definitions for colour-defined horizons. South African Journal of Plant and Soil 14:154–157. http://hdl.handle.net/10019.1/9595. Accessed 19 Dec 2018

Veneman P, Spokas L, Lindbo D (1998) Soil moisture and redoximorphic features: a historical perspective. In: Rabenhorst MC, Bell JC, McDaniel PA (eds) Quantifying Soil Hydromorphology. Soil Science Society of America, Madison, WI, pp 1–23. https://doi.org/10.2136/sssaspecpub54.c1

Vepraskas MJ (2015) Redoximorphic features for identifying aquic conditions. North Carolina University, Raleigh, NC. https://content.ces.ncsu.edu/redoximorphic-features-for-identifying-aquic-conditions.pdf. Accessed 17 Dec 2018

Vepraskas MJ (2000) Morphological features of seasonally reduced soils. In: Vepraskas MJ, Richardson JL, Vepraskas M, Craft CB (eds) Wetland soils: Genesis, Hydrology, Landscapes, and Classification. CRC Press, pp 163–183

Vepraskas MJ, Caldwell PV (2008) Interpreting morphological features in wetland soils with a hydrologic model. CATENA 73:153–165. https://doi.org/10.1016/j.catena.2007.07.005

Vepraskas MJ, Craft CB, Richardson JL (2015) Wetland Soils: Genesis, Hydrology, Landscapes, and Classification, Second Edition. Taylor & Francis Group, Baton Rouge, US. https://doi.org/10.1201/b18996

Vepraskas MJ, He X, Lindbo DL, Skaggs RW (2004) Calibrating hydric soil field indicators to long-term wetland hydrology. Soil Science Society of America Journal 68:1461–1469. https://doi.org/10.2136/sssaj2004.1461

Vepraskas MJ, Lindbo DL (2012) Redoximorphic features as related to soil hydrology and hydric soils. In: Lin H (ed) Hydropedology. Academic Press, Boston, US, pp 143–172. http://dx.doi.org/10.1016/B978-0-12-386941-8.00005-8

Vepraskas MJ, Lindbo DL, Stolt MH (2018) Redoximorphic features. In: Stoops G, Marcelino V, Mees F (eds) Interpretation of Micromorphological Features of Soils and Regoliths (Second Edition). Elsevier, Amsterdam, pp 425–445. https://doi.org/10.1016/B978-0-444-63522-8.00015-2

Vepraskas MJ, Richardson JL, Tandarich JP (2006) Dynamics of redoximorphic feature formation under controlled ponding in a created riverine wetland. Wetlands 26:486–496. https://doi.org/10.1672/0277-5212(2006)26[486:DORFFU]2.0.CO;2

Vepraskas MJ, Vaughan KL (2016) Morphological features of hydric and reduced soils. In: Vepraskas MJ, Craft CB (eds) Wetland Soils: Genesis, Hydrology, Landscapes, and Classification. CRC Press, Boca Raton, pp 189–217

Villa JA, Bernal B (2018) Carbon sequestration in wetlands, from science to practice: An overview of the biogeochemical process, measurement methods, and policy framework. Ecological Engineering 114:115–128. https://doi.org/10.1016/j.ecoleng.2017.06.037

Villa JA, Mitsch WJ (2015) Carbon sequestration in different wetland plant communities in the Big Cypress Swamp region of southwest Florida. International Journal of Biodiversity Science, Ecosystem Services and Management 11:17–28. https://doi.org/10.1080/21513732.2014.973909

Virginia Department of Environmental Quality (2019) Chesapeake Bay TMDL Phase III Watershed Implementation Plan. Virginia Department of Environmental Quality

Viscarra Rossel RA, Cattle SR, Ortega A, Fouad Y (2009) In situ measurements of soil colour, mineral composition and clay content by vis–NIR spectroscopy. Geoderma 150:253–266. https://doi.org/10.1016/j.geoderma.2009.01.025

Viscarra Rossel RA, Fouad Y, Walter C (2008) Using a digital camera to measure soil organic carbon and iron contents. Biosystems Engineering 100:149–159. https://doi.org/10.1016/j.biosystemseng.2008.02.007

Viscarra Rossel RA, Minasny B, Roudier P, McBratney AB (2006) Colour space models for soil science. Geoderma 133:320–337. https://doi.org/10.1016/j.geoderma.2005.07.017

Vogel S, Märker M (2011) Characterization of the pre-AD 79 Roman paleosol south of Pompeii (Italy): Correlation between soil parameter values and paleo-topography. Geoderma 160:548–558. https://doi.org/10.1016/j.geoderma.2010.11.003

Votteler TH, Muir TA (1996) Wetland protection legislation. National Water Summary on Wetland Resources 57–64. https://water.usgs.gov/nwsum/WSP2425/legislation.html. Accessed 8 Jan 2019

Wals AEJ, Brody M, Dillon J, Stevenson RB (2014) Convergence between science and environmental education. Science 344:583–584. https://doi.org/10.1126/science.1250515

Wang H, Piazza SC, Sharp LA, et al (2017) Determining the spatial variability of wetland soil bulk density, organic matter, and the conversion factor between organic matter and organic carbon across Coastal Louisiana, USA. Journal of Coastal Research 33:507–517. https://doi.org/10.2112/JCOASTRES-D-16-00014.1

Webster MA, Mollon JD (1997) Adaptation and the color statistics of natural images. Vision Research 37:3283–3298. https://doi.org/10.1016/S0042-6989(97)00125-9

Werner JS, Walraven J (1982) Effect of chromatic adaptation on the achromatic locus: The role of contrast, luminance and background color. Vision Research 22:929–943. https://doi.org/10.1016/0042-6989(82)90029-3

Wetland Studies and Solutions Inc. (2020) Julie J. Metz Wetland Bank. https://www.wetlands.com/julie-metz. Accessed 2 Feb 2022

Wheeler DB, Thompson JA, Bell JC (1999) Laboratory comparison of soil redox conditions between red soils and brown soils in Minnesota, USA. Wetlands 19:607–616. https://doi.org/10.1007/BF03161698

Whiting GJ, Chanton JP (2001) Greenhouse carbon balance of wetlands: Methane emission versus carbon sequestration. Tellus B 53:521–528. https://doi.org/10.1034/j.1600-0889.2001.530501.x

Wills SA, Burras CL, Sandor JA (2007) Prediction of soil organic carbon content using field and laboratory measurements of soil color. Soil Science Society of America Journal 71:380–388. https://doi.org/10.2136/sssaj2005.0384

Wissmar RC, Timm RK, Logsdon MG (2004) Effects of changing forest and impervious land covers on discharge characteristics of watersheds. Environmental Management 34:91–98. https://doi.org/10.1007/s00267-004-0224-5

Wolf KL, Ahn C, Noe GB (2011) Development of soil properties and nitrogen cycling in created wetlands. Wetlands 31:699–712. https://doi.org/10.1007/s13157-011-0185-4

Wu C-Y, Jacobson AR, Laba M, Baveye PC (2009) Accounting for surface roughness effects in the near-infrared reflectance sensing of soils. Geoderma 152:171–180. https://doi.org/10.1016/j.geoderma.2009.06.002

Xie H, Zhang Y, Zeng X, He Y (2020) Sustainable land use and management research: a scientometric review. Landscape Ecology 35:2381–2411. https://doi.org/10.1007/s10980-020-01002-y

Xue Z, Hou G, Zhang Z, et al (2019) Quantifying the cooling-effects of urban and peri-urban wetlands using remote sensing data: Case study of cities of Northeast China. Landscape and Urban Planning 182:92–100. https://doi.org/10.1016/j.landurbplan.2018.10.015

Yang S, Fang X, Li J, et al (2001) Transformation functions of soil color and climate. Science In China Series D-Earth Sciences 44:218–226. https://doi.org/10.1007/BF02911990

Yonekura Y, Ohta S, Kiyono Y, et al (2010) Changes in soil carbon stock after deforestation and subsequent establishment of “Imperata” grassland in the Asian humid tropics. Plant and Soil 329:495–507. https://doi.org/10.1007/s11104-009-0175-y

Yu J, Wang Y, Li Y, et al (2012) Soil organic carbon storage changes in coastal wetlands of the modern Yellow River Delta from 2000 to 2009. Biogeosciences 9:2325–2331. https://doi.org/10.5194/bg-9-2325-2012

# BIOGRAPHY

Stephanie Ann Schmidt grew up in Wheaton, IL and graduated from Wheaton Warrenville South High School in 2011. Though she entered Michigan State University with the intent to major in chemistry and mathematics, she eventually added on a major in environmental science and management due to her desire to gain knowledge more applicable to a career in environmental stewardship. While taking a gap year in Dubuque, Iowa serving as a Green Iowa Americorps member, she prudently decided to apply to George Mason University's Environmental Science and Public Policy Ph.D. program and began working on her PhD degree in the fall of 2016. She has family all over the US, with her parents still residing in Wheaton, her older sister living in Chicago, IL, and her brother, sister-in-law, and nephew live in Fruita, CO. While she has yet to put down roots in the Washington, D.C. region, she is happy to call it home for the start of her career.